MONTHLY MEAN CLIMATOLOGIES OF TEMPERATURE AND SALINITY IN THE WESTERN NORTH ATLANTIC

Yuri Geshelin, Jinyu Sheng, and Richard J. Greatbatch

Ocean Sciences Division
Maritimes Region
Fisheries and Oceans Canada

Bedford Institute of Oceanography
P.O. Box 1006
Dartmouth, Nova Scotia
Canada B2Y 4A2

1999

Canadian Data Report of Hydrography and Ocean Sciences 153

Fisheries and Oceans / Pêches et Océans

Canada

Canadian Data Report of
Hydrography and Ocean Sciences 153

1999

MONTHLY MEAN CLIMATOLOGIES OF TEMPERATURE AND SALINITY IN THE WESTERN NORTH ATLANTIC

by

Yuri Geshelin[1], Jinyu Sheng[1] and Richard J. Greatbatch[1]

Ocean Sciences Division
Maritimes Region
Department of Fisheries and Oceans
Bedford Institute of Oceanography
P.O. Box 1006
Dartmouth, Nova Scotia
Canada B2Y 4A2

[1]Department of Oceanography, Dalhousie University, Halifax, Nova Scotia, Canada, B3H 4J1

Cat. No. Fs 97-16/153E ISSN 0711-6721

Correct citation for this publication:

Geshelin, Y., J. Sheng and R. J. Greatbatch. 1999. Monthly mean climatologies of temperature and salinity in the western North Atlantic. Can. Tech. Rep. Hydrogr. Ocean. Sci. 153: vi + 62 pp.

Contents

TABLE CAPTIONS

FIGURE CAPTIONS

ABSTRACT

Geshelin, Y., J. Sheng, and R. J. Greatbatch. 1999. Monthly mean climatologies of temperature and salinity in the western North Atlantic. Can. Data Rep. Hydrogr. Ocean Sci. 153: vi + 62 pp.

Monthly-mean gridded fields of in-situ temperature and salinity in the western North Atlantic Ocean were obtained by interpolating hydrographic observations onto a 1/6 degree by 1/6 degree grid. The hydrographic data at the 32 standard vertical levels were extracted from a database compiled by the US National Oceanographic Data Center (NODC, 1998). The gridded fields were produced using the modified Barnes' algorithm with a time- and space-dependent weight function. For each calendar month, the hydrographic data from three consecutive months were used in the analysis. The major axis of the search area at each grid point is roughly aligned with the local bathymetry. The decorrelation scale increases with water depth to take advantage of the many more hydrographic observations available on the shelf than in deep waters.

RÉSUMÉ

Geshelin, Y., J. Sheng, and R. J. Greatbatch. 1999. Monthly mean climatologies of temperature and salinity in the western North Atlantic. Can. Data Rep. Hydrogr. Ocean Sci. 153: vi + 62 pp.

Nous avons obtenu la moyenne mensuelle aux points de grille des champs de température et de salinité *in situ*, dans l'ouest de l'Atlantique Nord, en interpolant les observations hydrographiques sur une grille de 1/6 par 1/6 de degré. Les données hydrographiques aux 32 niveaux verticaux standards ont été extraites d'une base de données compilée par le US National Oceanographic Data Center (NODC, 1998). Nous avons établi les champs aux points de grille en modifiant l'algorithme de Barnes à l'aide d'une fonction de pondération dépendante dans l'espace et dans le temps. Pour chaque mois civil, nous avons utilisé, pour fin d'analyse, les données hydrographiques de trois mois consécutifs. L'axe principal de la zone de recherche, à chaque point de grille, est grossièrement aligné en fonction de la bathymétrie locale. L'échelle de décorrélation augmente avec la profondeur de l'eau pour tirer parti du nombre beaucoup plus grand d'observations hydrographiques disponibles sur le plateau par rapport aux observations disponibles en eaux profondes.

INTRODUCTION

The work described in this report is the first stage of a study in which estimates of the observed hydrography will be used in conjunction with a numerical model to estimate the monthly and seasonal circulation in the western North Atlantic Ocean. The model requires temperature and salinity data as the model inputs. The region to be studied is shown in Figure 1.

One of the main hydrographic features in the western North Atlantic Ocean is the strong temperature and salinity fronts associated with three main current systems: the Gulf Stream, the North Atlantic Current and the Labrador Current. The horizontal sea surface temperature and salinity gradients in some areas are comparable with the maximum gradients observed in the World Ocean beyond the shelf break. This poses special requirements for generating monthly climatological fields to be used as model input. On one hand, the gridded fields should represent the mean state of the ocean in the past, meaning that the irregularly sampled hydrographic data must be smoothed in both time and space to eliminate extremes associated with rare events. On the other hand, the hydrography should not be smoothed too heavily in order to resolve reasonably well the temperature and salinity gradients associated with the three main current systems over this region.

The main purpose of this report is to generate 1/6 degree by 1/6 degree monthly-mean gridded fields of temperature and salinity for the western North Atlantic Ocean that meet the above requirements. This is meant to improve the existing climatologies in terms of better representation of mesoscale features such as stationary Gulf Stream meanders and estuary buoyancy fronts. For example, the widely used 1 degree by 1 degree Levitus climatologies (Levitus and Boyer, 1994; Levitus et. al, 1994) are rather too smooth for our applications. Other climatologies such as those generated by deYoung et al. (1994), Reynaud et al. (1995) and Tang and Wang (1996) have finer resolution but cover only smaller areas of the western North Atlantic Ocean. Umoh and Greatbatch (1997) generated the seasonal and annual climatologies with 1/6 degree by 1/6 degree resolution for the whole North Atlantic, but did not generate the monthly fields. Monthly fields were also not produced by deYoung et al. (1994), Reynaud et al. (1995) or Tang and Wang (1996).

The hydrographic data used in this report are the standard level in-situ temperature and salinity data extracted from the World Ocean Database 1998 compiled by the US National Oceanographic Data Center (NODC, 1998). The objective analysis technique known as Barnes' algorithm (Barnes, 1964) is used. The iterative Barnes' algorithm is a successive-correction method that is widely used in the mesoscale analysis of radar and satellite observations.

Section 2 describes the objective analysis technique. Section 3 discusses the bathymetry data used in the objective analysis. Section 4 is a summary. It is followed by the contour plots of monthly mean in-situ temperature and salinity fields at eight selected standard levels.

DATA ANALYSIS

NODC Hydrographic Data

The hydrographic data used in this report have been quality-checked at NODC, with questionable observations flagged. Consequently, no further quality check was performed in this report. Note that the following steps were taken in extracting the data from the NODC database: (1) only the data not flagged by NODC were used; and (2) any data with temperature less than -2°C or salinity less than 15 part per thousand (psu) were excluded. Obviously, the temperature threshold of -2°C was used to reject any unrealistic temperature observations. The salinity threshold of 15 psu was mainly used to exclude any observations from lakes and rivers.

The hydrographic data at 32 standard vertical levels (Table 1) were extracted from the NODC database for the study area of 35°N to 66°N and 76° to 30°W. The extracted data were grouped by month and standard level. The number of observations for each month at each standard level is given in Table 2. As seen from the table, the number of sea surface temperature observations in summer months is about 4 times more than those of the sea surface salinity. The annual mean value of that ratio averaged over all levels is about 2.6. In addition to the geographical position, each observation also contains the time of the measurement in Julian day which was used to construct the time-dependent weight function used in the objective analysis (see below).

The Modified Barnes' Algorithm

At each standard level, 12 monthly mean gridded in-situ temperature and salinity fields were produced using the modified Barnes' algorithm (Barnes, 1964). Barnes' algorithm is iterative. It estimates the value of the field at a grid point as a weighted sum of the surrounding observations. As the number of iterations increases, the interpolated values approach the observations. The point at which to stop iterating is somewhat subjective: it depends on the believability of the fitted fields, taking into account the spatial distribution of observations and their expected signal-to-noise ratio. The results presented in this report were obtained with three iterations.

The weight assigned to each observation in the original Barnes' algorithm depends only on the spatial distance between the grid and observation points. In this report, we followed Reynaud et al. (1995) and others to specify the weight function to be time- and space-dependent as described below.

At each grid point $\mathbf{r}_i$, the interpolated field at the jth iteration $f_A^j(\mathbf{r}_i)$ is given as:

$$f_A^j(\mathbf{r}_i) = f_A^{j-1}(\mathbf{r}_i) + \sum_{k=1}^{K_i} W_{ik} \left[f_O(\mathbf{r}_k) - f_A^{j-1}(\mathbf{r}_k) \right] \qquad (1)$$

for $j \geq 1$. The subscripts A and O in Eq. (1) denote analyzed and observed fields respectively, $\mathbf{r}_k$ is the position vector of the kth observation, K_i is the number of observations inside the search area for the ith grid point, and W_{ik} is the weight function of the kth observation at the ith grid point defined as

$$W_{ik} = \frac{w_{ik}}{\sum_{k=1}^{K_i} w_{ik}} \tag{2}$$

with

$$w_{ik} = \exp\left[-\frac{4\left(d_{ik} + R_{ij}\delta_{ik}\right)^2}{R_{ij}^2} - \frac{4\left(t_O - t_A\right)^2}{T^2}\right] \tag{3}$$

where R_{ij} is the decorrelation scale at each iteration for the ith grid point, d_{ik} is the distance between the ith grid point and the kth observation, δ_{ik} is a parameter controlling the orientation of the search area with regard to the local features of the bottom relief (Reynaud et al., 1995), T is twice the e-folding time of the temporal weight function, and t_O and t_A are the time of the kth observation and of mid-month of the interpolated field respectively.

A step function for δ_{ik} was proposed originally by Reynaud et al. (1995). In this report, we modified their step function by defining δ_{ik} as

$$\delta_{ik} = 0.5\left[1 + \tanh\frac{|H_i - H_k| - \Delta_i}{0.2\Delta_i}\right] \tag{4}$$

where H_i and H_k are water depths (in meters) at the ith grid point and the kth hydrographic observation, and Δ_i was given as

$$\Delta_i = 800 - 500\exp\left[-\left(\frac{H_i}{1000}\right)^2\right] \tag{5}$$

Note that δ_{ik} is near zero over the areas with gentle bottom slopes (i.e., $|H_i - H_k \approx 0$). As a result, the weight function W_{ik} is near isotropic over these areas.

The decorrelation scale R_{ij} in Eq. (3) was defined as

$$R_{ij} = D_j\Gamma_i \tag{6}$$

where D_j is only a function of the iteration number. The values of D_j for the first three iterations were chosen to be 1200, 500, and 250 km, respectively. The value of Γ_i, on the other hand, depends only on the water depth at each grid point:

$$\Gamma_i = 0.6 + 0.4\tanh\frac{H_i - 800}{400} \tag{7}$$

except for the following areas with horizontal dimension of about 100 km by 100 km: (1) off Cape Hatteras (centered at 37°N and 74.5°W); (2) northwest part of the Labrador Sea (centered at 59°N and 62.5°W); and (3) off the southeast coast of Greenland (centered at 60.5°N and 47°W). In these areas, the values of Γ_i smoothly fall from unity in the center to those computed from (7) on the boundaries. Formula (7) yields the values of Γ_i, which range from 0.2 for water depths less than 100 m to 1 for water depths greater than 1000 m.

Note that the main purpose of the Γ_i-function is to allow a smaller decorrelation scale to be used in the shallower regions, based on the fact that there are more hydrographic observations in the shelf region than in the offshore deep water region. Exceptions to this general rule, however, occur over the above-mentioned three shelf areas, where water depths are relatively shallow but hydrographic observations are rather scarce.

Ideally, the in-situ temperature and salinity climatologies in each month should be gridded from the hydrographic observations made in that month. Poor data coverage over many areas, particularly in winter months, however, makes the gridded fields interpolated from the hydrography in a single month very noisy. We decided therefore to use the hydrographic data during three consecutive months from previous month to the next month to generate the monthly mean climatologies. The term $(t_O - t_A)$ in Eq. (3) measures the number of Julian days of the kth hydrographic observation relative to the mid-month of the interpolated field. The value of T in Eq. (1) was chosen to be 75 days in this report.

As shown in Eq. (1), we also need to initialize the interpolated field at the kth location of the observations, i.e., we must specify $f_A^0(\mathbf{r}_k)$. There are many ways to define the initial field. In this report, the initial values at all the locations of the observations were set to zero, i.e., $f_A^0(\mathbf{r}_k) = 0$. For $j > 0$, the analyzed field at the observation points $f_A^j(\mathbf{r}_k)$ is generated from the gridded field $f_A^j(\mathbf{r}_i)$ using bilinear interpolation.

BATHYMETRY DATA

The bathymetry data were used in the objective analysis for two specific purposes: (1) to determine the shape of the weight function through δ_{ik}; and (2) to define the decorrelation scale R_{ij} at each grid point through Γ_i.

To get the 1/6 degree by 1/6 degree bathymetry data, we interpolated the 5-minute gridded elevation/bathymetry of the Earth surface known as ETOPO5 compiled by the US National Geophysical Data Center, National Oceanic and Atmospheric Administration (NOAA, 1988) onto the model grid. Since spurious seamounts and anomalous depths were found over the shelf region in this dataset, as the first step of the interpolation procedure, we substituted the ETOPO5 dataset with

the sounding data compiled by the Bedford Institute of Oceanography (BIO) for the eastern Canadian shelf seas that consists of the Newfoundland Shelf, Gulf of St. Lawrence, Scotian Shelf and Gulf of Maine.

As mentioned above, relatively more hydrographic observations in the shelf region allow us to use smaller values of the decorrelation scale R_{ij} to resolve the finer-scale hydrographic features over these areas. We have, however, identified three shelf areas where larger R_{ij} is required due to the poor data coverage. In addition, the areas over the small-scale offshore seamounts, such as New England, also require larger R_{ij} appropriate to the deep ocean, since hydrographic observations over these areas are also scarce in comparison with observations at similar depths on the shelf. To cope with the problem, we defined a polygon that aligns roughly along the shelf break (the dashed line in Figure 1). We smoothed the 1/6 degree by 1/6 degree gridded bathymetry with different smoothing parameters applied to the grid points inside and outside the polygon. The water depths outside the polygon were smoothed 4 times with a 5×5 point filter (a simple arithmetic mean was taken); inside the polygon the analogous 3×3 point filter was applied only once. Smoothing parameters were chosen to ensure that the bathymetry varies smoothly in the transition zone across the polygon's boundary. Figure 1 shows the polygon and the resulting contour lines of bathymetry in the western North Atlantic Ocean.

SUMMARY AND BRIEF DISCUSSION

We generated 1/6 degree by 1/6 degree monthly climatologies for the western North Atlantic Ocean using the modified Barnes' algorithm (Barnes, 1964). To produce the gridded fields with better representation of mesoscale hydrographic features over the eastern Canadian shelf, we followed Reynaud et al. (1995) and others to use the space-dependent weight function, allowing the major axis of the search area to align roughly with the bathymetry. Since there are generally more hydrographic observations in the shelf regions than in the offshore deep waters, we used smaller values of the decorrelation scale R_{ij} in the shallower water regions, allowing us to better resolve the smaller-scale hydrographic features.

The data coverage over many areas is relatively poor, particularly in winter months. As a result, we used the hydrography during three consecutive months to generate the high resolution climatologies in each month. A time-dependent weighting is incorporated into the Barnes' algorithm with the e-folding time set to 37.5 days.

Before presenting gridded monthly temperature and salinity climatologies at eight selected standard levels, we discuss briefly the spatial and temporal variations in the sea surface fields. Figures 2a and b show differences in sea surface temperature (SST) and salinity (SSS) between August

and February. The August-February difference is conventionally used to represent the annual variability of SST. It can be see from Figure 2 that the significant annual variability in the gridded sea surface hydrography occurs in the western part of the study area, consistent with previous studies (Levitus and Boyer, 1994; Levitus et. al, 1994; Tang and Wang, 1996; Umoh and Greatbatch, 1997). Based on the seasonal fields gridded from hydrography data over four months, Umoh and Greatbatch (1997) estimated the annual variations in SST and SSS over the study area to be about 14°C and 2 psu, respectively. According to their results, the maximum annual variation of SST occurs in the Newfoundland shelf area, which is consistent with our findings. However, the *maximum* August - February SST difference is much higher in our study. It reaches 18°C off the US coast (Figure 2a). The difference between our results and Umoh and Greatbatch (1997) is well expected since we calculated the difference from the monthly climatology rather than from the seasonal-mean fields.

The August-February difference of SSS reaches local maxima in the areas of river runoff, Ungava Bay (60°N, 67°W), the Labrador shelf and the Gulf of St. Lawrence. In those areas, the difference in SSS between August and February is about 5-7 psu (see Figure 2b). Note that the salinity difference between January and May is the most profound (Figure 2c), with the largest variability of SSS of about 13 psu over the Ungava Bay.

In the south-western part of the study area the SST seasonal cycle is fairly pronounced. In February, the tongue of 20°C water barely extends to the north from 35°N. In August it reaches 45°N. However, there is no such distinct change in the salinity structure. Associated with that tongue is a notable feature of the vertical structure: starting from 75 m and deeper, this water mass is colder in the summer than in winter months. This holds true down to the 900 m level, where the summer - winter temperature difference vanishes.

Umoh and Greatbatch (1997) demonstrated that the seasonal signal in temperature and salinity decays at 500 m. This is also consistent with our findings. Overall, the water temperature decreases with depth, while salinity increases. There is one significant exception to this tendency: the subzero water mass on the Labrador Shelf where temperature increases with depth in winter.

The strongest horizontal gradients in SST and SSS are associated with the Gulf Stream and river runoff. With the present grid resolution they reach significant values of 1.5°C per 10 km and 0.25 psu per 10 km (Figure 3).

HOW TO ACCESS THE MONTHLY CLIMATOLOGY

The gridded monthly climatology of temperature and salinity on the western North Atlantic can be obtained through our anonymous ftp site "*skye.phys.ocean.dal.ca*". When prompted for a user

name type *"anonymous"*. Type your e-mail address for a password. After receiving *"Guest login ok"* type *"cd users/CANDIE"*. Then type *"bin"* and *"get TS-WNA.tar"*. For further information please contact Jinyu Sheng by email at Jinyu.Sheng@Dal.Ca or by telephone at (902) 494-2718.

ACKNOWLEDGMENTS

The authors wish to thank Dr. Dan Wright for his suggestions and comments. The MATLAB program for generating the bathymetry data was provided by Dr. Youyu Lu. The original FORTRAN program for gridding the hydrographic data was provided by Dr. Michael Dowd. This work was funded by NSERC, AES and MARTEC under the Industrial Research Chair Program.

REFERENCES

Barnes, S. L., 1964: A technique for maximizing details in numerical weather map analysis. *Journal of Applied Meteorology*, **3**, 396-409.

deYoung, B., F. Perry and R. J. Greatbatch, 1994: Objective analysis of hydrographic data in the Northwest Atlantic. Canadian Technical Report of Hydrography and Ocean Sciences, No.130. 95 pp.

Levitus, S. and T. P. Boyer, 1994:. World Ocean Atlas 1994, Volume 4: Temperature. NOAA Atlas NESDIS 4, 129 pp.

Levitus, S., R. Burgett, and T. P. Boyer, 1994: World Ocean Atlas 1994, Volume 3: Salinity. NOAA Atlas NESDIS 3, 111 pp.

NOAA, National Geophysical Data Center, Data Announcement 88-MGG-02, 1988: Digital relief of the Surface of the Earth. Boulder, Colorado.

NODC, National Oceanographic Data Center, 1998: World Ocean Database 1998.

Reynaud, T. H., A. J. Weaver and R. J. Greatbatch, 1995: Summer mean circulation of the northwestern Atlantic Ocean. *Journal of Geophysical Research*, **100**, 779-816.

Tang, C. L. and C. K. Wang, 1996: A gridded data set of temperature and salinity for the northwest Atlantic Ocean. Bedford Institute of Oceanography, 45 pp.

Umoh, J. U. and and R. J. Greatbatch, 1997: Annual and seasonal mean fields of temperature and salinity in the North Atlantic. Department of Oceanography, Dalhousie University, 321 pp.

Table 1. Standard levels and depths (in m).

Depth	Level	Depth	Level	Depth	Level	Depth	Level
0	1	150	9	800	17	1750	25
10	2	200	10	900	18	2000	26
20	3	250	11	1000	19	2500	27
30	4	300	12	1100	20	3000	28
50	5	400	13	1200	21	3500	29
75	6	500	14	1300	22	4000	30
100	7	600	15	1400	23	4500	31
125	8	700	16	1500	24	5000	32

Table 2a. Number of in-situ temperature observations at each standard level for each month.

Depth	Jan	Feb	Mar	Apr	May	Jun	Jul	Aug	Sep	Oct	Nov	Dec
0	56103	65453	82499	90970	108951	118806	122655	118857	99076	90977	86950	54230
10	53554	61709	76622	87655	105530	115248	117952	114976	96492	86687	81986	52258
20	53673	61689	76096	87333	105217	114359	117628	114649	96039	87042	82627	52562
30	52407	60256	74191	85416	102598	111176	114802	111020	92913	85090	81393	51578
50	50294	57678	71284	81902	97464	104782	107963	102171	85951	80320	77854	49483
75	46661	52361	63485	73450	85927	93896	95116	89607	73973	70042	69377	45567
100	43875	48852	58325	66694	77606	86421	86888	80547	66279	64119	63933	42378
125	39987	44182	52625	59829	68722	78136	76354	70996	57831	57296	57873	38538
150	33015	36720	43792	48857	55774	63188	58328	56715	45888	46787	47223	31591
200	29906	32895	39445	42514	48656	55759	51014	49922	40685	40643	41514	28563
250	17438	20293	24595	27195	31466	30750	28614	28993	24922	24797	23608	17237
300	15486	17909	21883	23787	27811	27192	24398	25045	22345	22407	20606	15242
400	15486	17909	21883	23787	27811	27192	24398	25045	22345	22407	20606	15242
500	8911	9477	11949	15116	15870	16186	13483	15252	12608	12763	12431	9180
600	7106	7145	9265	12020	13068	12627	10076	11737	9354	9904	9790	7429
700	6424	6207	8322	10493	11777	11248	8562	9809	7875	8635	8623	6525
800	3381	3782	4305	6309	6698	6942	5354	6196	4317	4857	4559	3622
900	4043	4795	5615	8830	8661	9174	7852	8065	5411	6447	5707	4144
1000	3693	4242	4793	7377	7255	7828	6542	6809	4562	5459	4729	3520
1100	3229	3792	4420	6341	5957	7125	5780	6209	3957	5108	4401	3452
1200	2724	3100	3543	5198	5175	5988	4592	5096	3236	4065	3778	2802
1300	2308	2766	3095	4577	4820	5254	4134	4856	3033	3531	3216	2411
1400	2540	2906	3473	4907	4859	5290	4405	4799	2997	3530	3405	2680
1500	1965	2264	2550	3871	4184	4263	3345	3770	2346	2616	2557	1901
1750	560	635	1029	1835	1843	2031	1474	1342	838	912	704	466
2000	2312	2914	3291	4826	4505	4681	4906	5124	3005	3592	3152	2723
2500	342	484	926	1873	1690	1650	1649	1624	946	894	591	339
3000	242	306	674	1494	1414	1361	1317	1175	697	626	421	231
3500	188	216	474	1067	952	814	894	887	488	497	317	171
4000	141	157	339	857	844	629	641	595	392	334	255	138
4500	93	122	265	606	620	405	332	336	265	233	155	79
5000	27	79	90	279	343	215	129	230	80	113	85	29

Table 2b. Number of salinity observations at each standard level for each month.

Depth	Jan	Feb	Mar	Apr	May	Jun	Jul	Aug	Sep	Oct	Nov	Dec
0	10267	12615	17710	23613	26558	27681	32655	31142	22140	19347	17937	9101
10	8936	10520	13447	22393	24470	24966	28999	29259	20620	17303	14504	8100
20	9105	10707	13481	22275	24642	24923	29628	30475	20739	18276	15116	8213
30	8871	10319	13196	21869	24193	24281	29098	29541	19916	18331	14884	8044
50	8342	9716	12798	20956	22785	22725	27295	26041	18372	17194	13970	7542
75	7370	8410	10190	18126	19644	19849	22758	22571	15087	14665	11923	6637
100	6898	7695	9091	16136	17585	17956	20068	19211	13649	12819	11012	6198
125	6588	7132	8512	14828	15596	16280	17566	17051	12183	11607	10177	5913
150	6128	6811	7778	13744	14874	15627	16518	16285	11776	10873	9538	5493
200	5309	5710	6506	10875	12081	12409	12972	13300	9403	8564	7671	4657
250	5244	5895	6616	11172	11206	11564	11344	11730	8538	7945	7187	4788
300	4448	5274	5571	9064	9024	9397	8774	9477	7000	6751	5922	4105
400	4448	5274	5571	9064	9024	9397	8774	9477	7000	6751	5922	4105
500	3984	4965	5293	7945	7853	8601	7675	8435	6232	6092	5344	3765
600	3091	3836	4009	6271	6374	6784	5896	6463	4333	4704	4097	2991
700	2502	3091	3295	5147	5481	5625	4518	4926	3204	3742	3229	2325
800	2358	2743	3015	4759	5010	5093	4044	4471	2863	3278	2933	2059
900	3494	4181	4954	7989	7702	7987	7237	7497	4676	5466	4784	3533
1000	3237	3757	4258	6852	6639	6857	6106	6502	4066	4728	4138	3104
1100	2826	3360	3965	5801	5296	6244	5372	5966	3483	4421	3806	3038
1200	2451	2794	3198	4749	4651	5224	4254	4896	2859	3513	3303	2465
1300	2078	2498	2801	4237	4288	4708	3812	4626	2675	3155	2790	2131
1400	2305	2650	3165	4500	4342	4894	4101	4623	2672	3176	2958	2395
1500	1761	2044	2307	3599	3783	3949	3084	3565	2103	2399	2227	1663
1750	498	533	860	1665	1610	1850	1363	1278	747	818	583	401
2000	2153	2696	3075	4613	4170	4495	4718	4949	2811	3279	2796	2429
2500	313	430	840	1824	1645	1612	1615	1588	880	792	530	318
3000	213	268	625	1446	1375	1333	1296	1151	647	552	373	206
3500	172	188	441	1037	920	794	872	868	447	435	292	152
4000	130	128	333	842	810	602	617	584	356	285	231	121
4500	88	97	255	593	582	385	317	333	249	199	142	72
5000	23	69	85	272	317	201	129	241	69	89	74	20

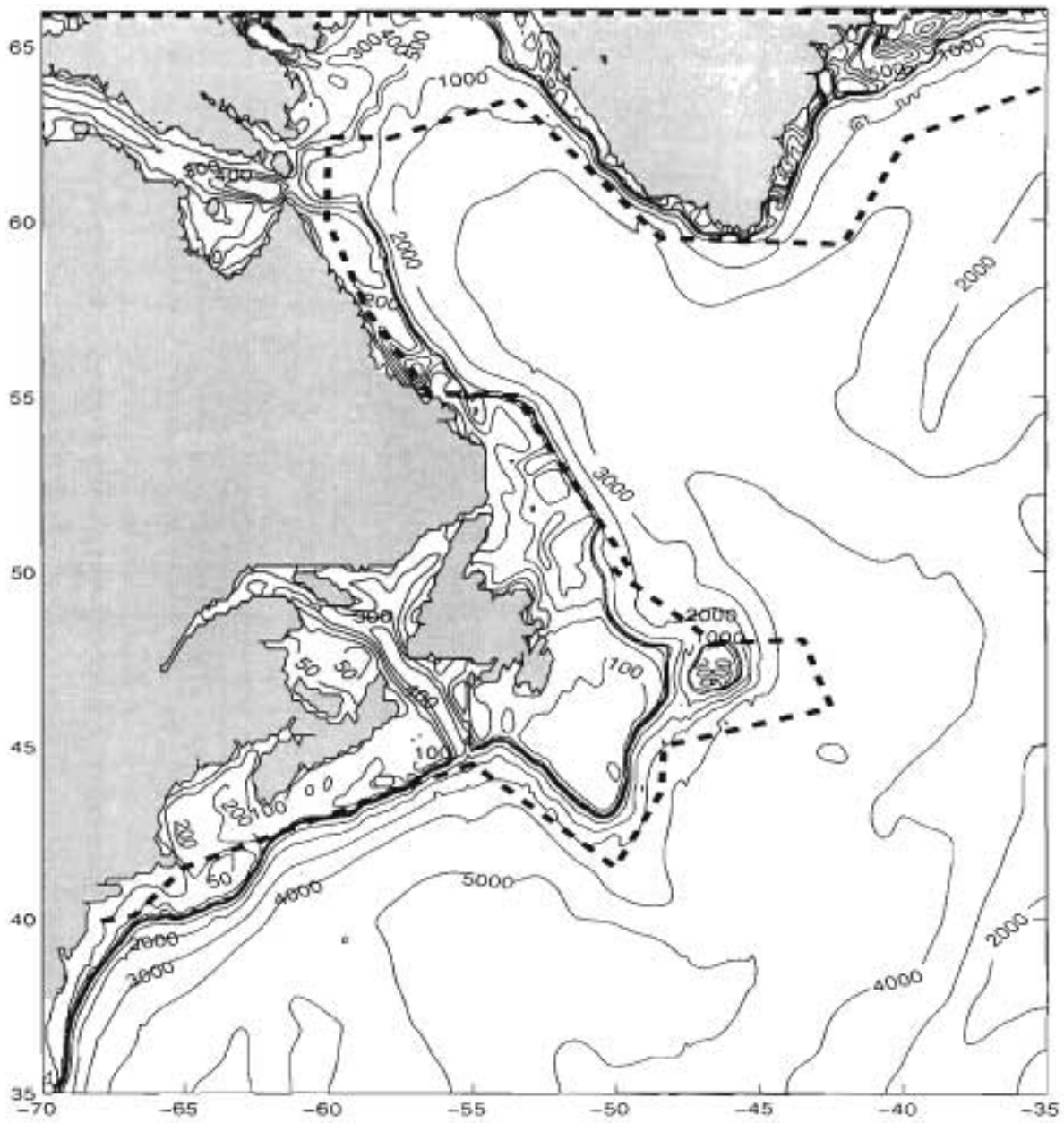

Figure 1. The selected contours of smoothed bathymetry (thin solid lines) and the contour of the polygon (dashed line) used to apply two different sets of bathymetry smoothing parameters in the western North Atlantic Ocean.

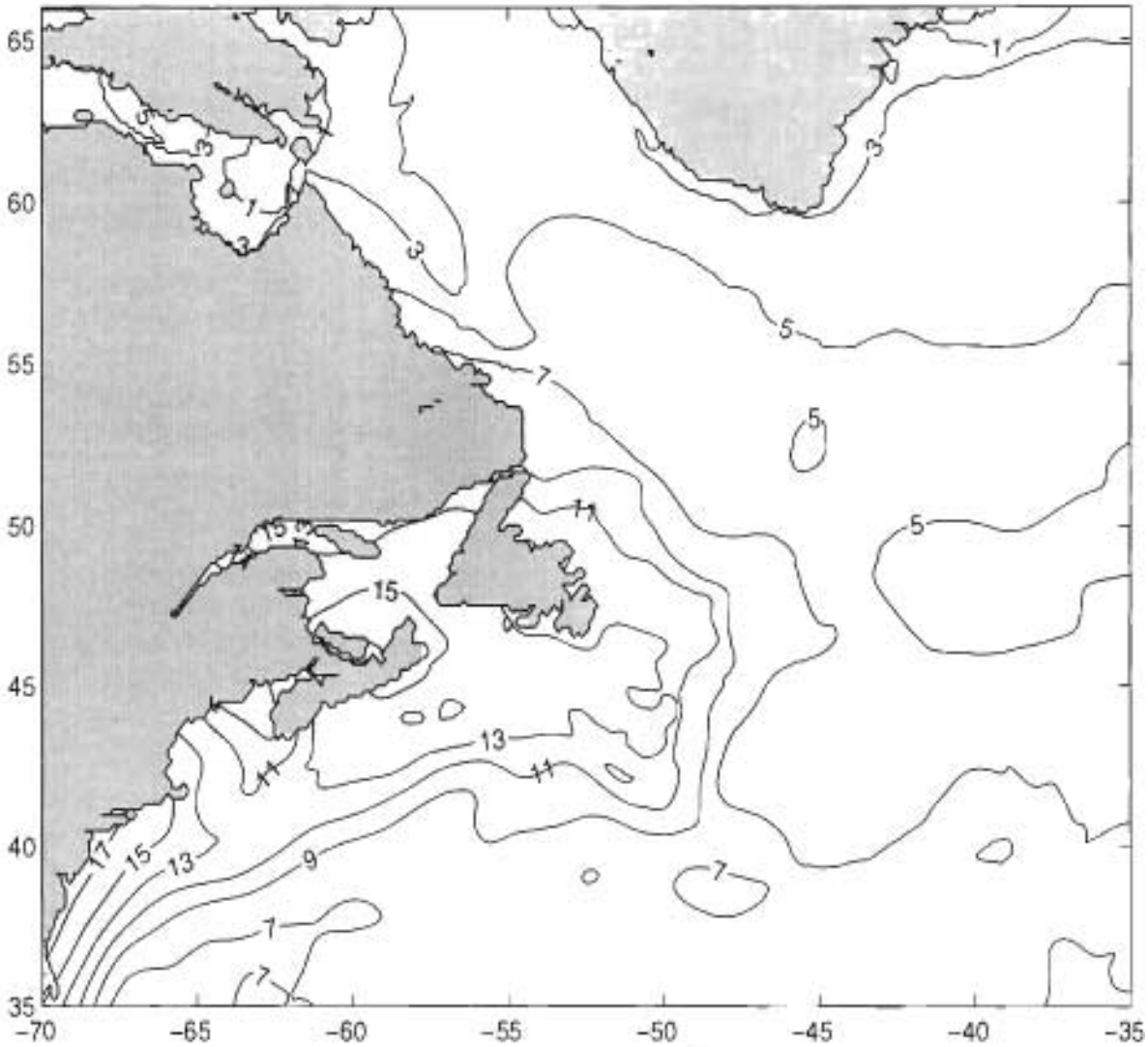

Figure 2a. Sea surface temperature difference (°C) between August and February.

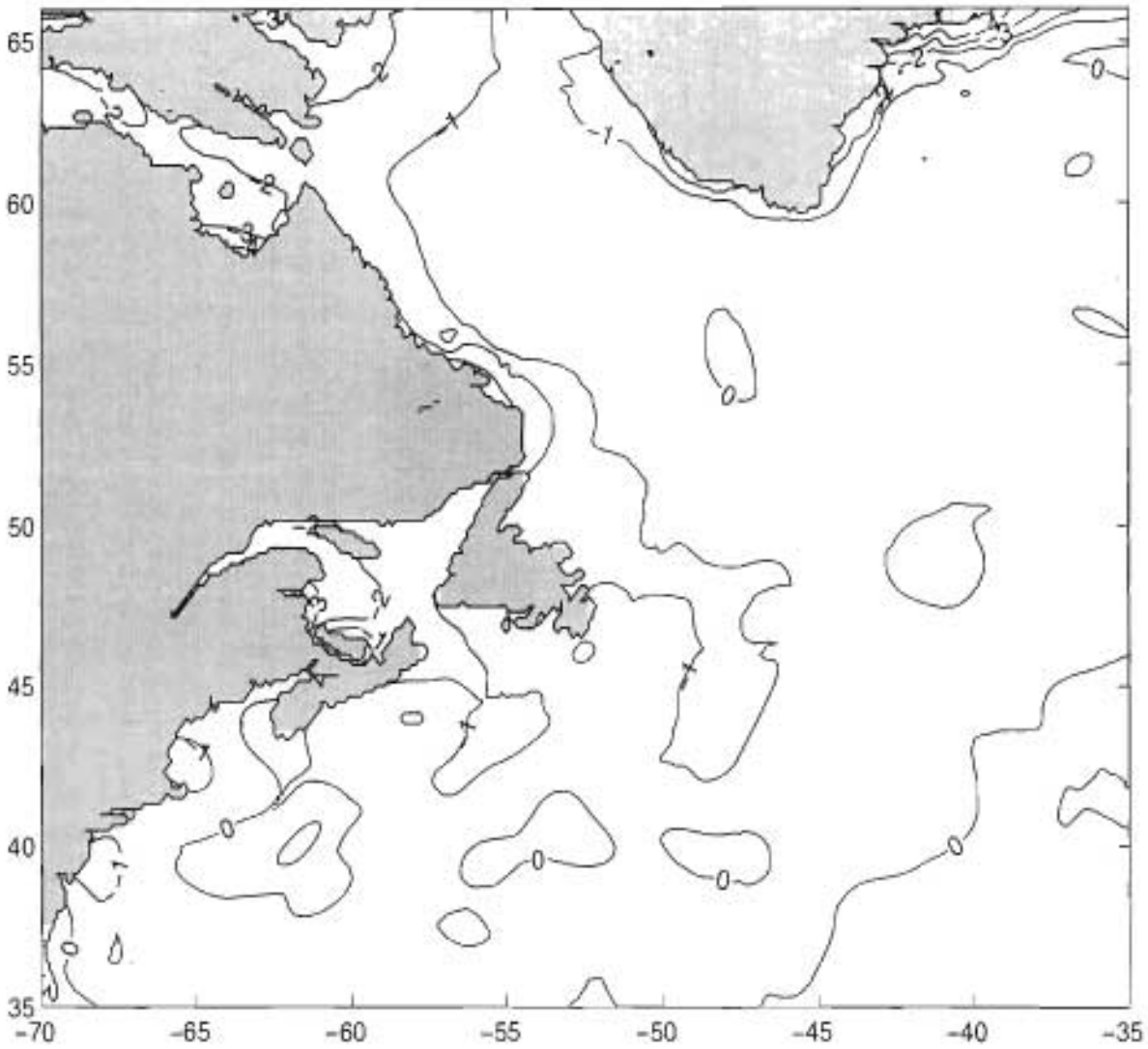

Figure 2b. Sea surface salinity difference (psu) between August and February .

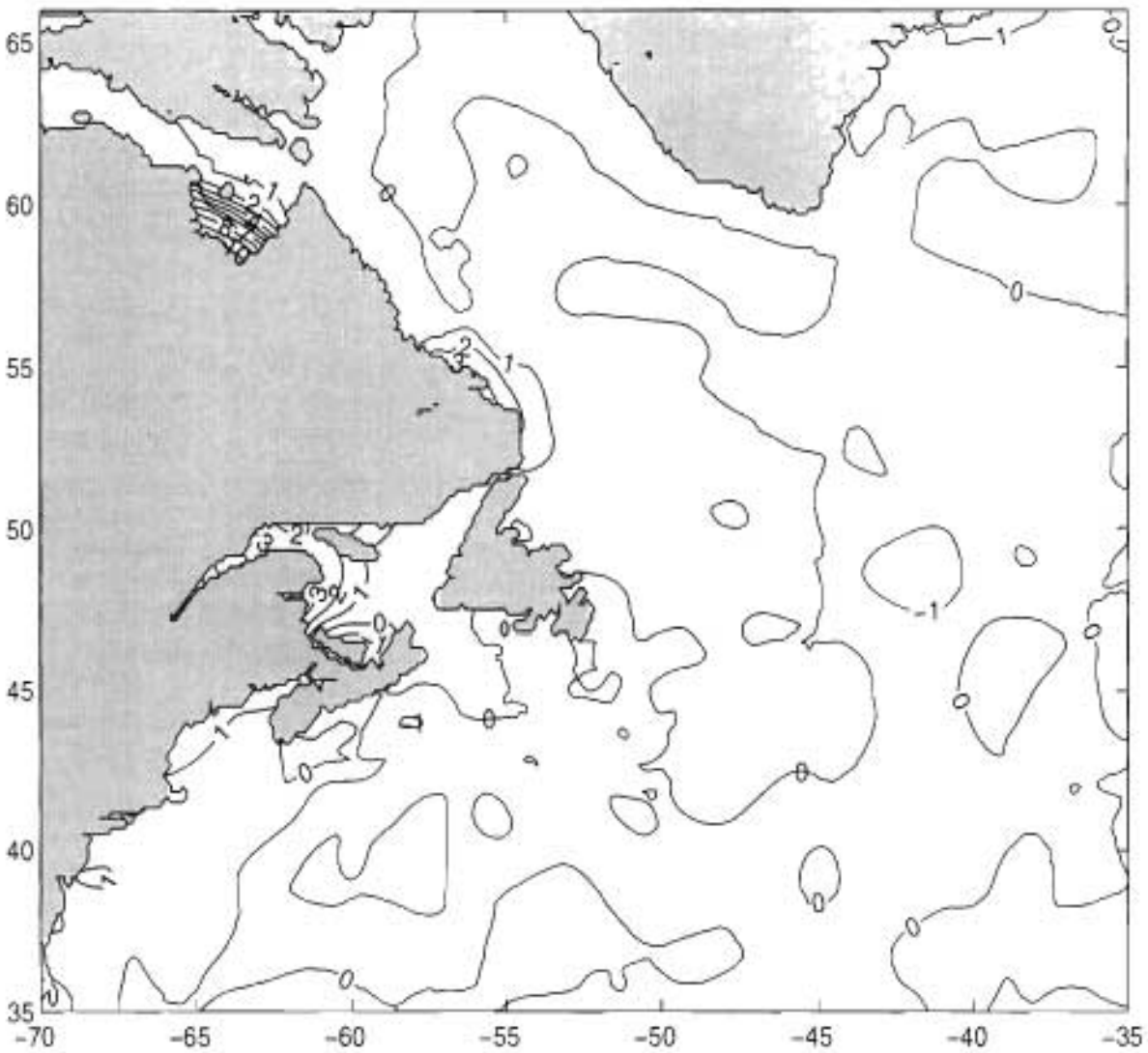

Figure 2c. Sea surface salinity difference (psu) between May and January.

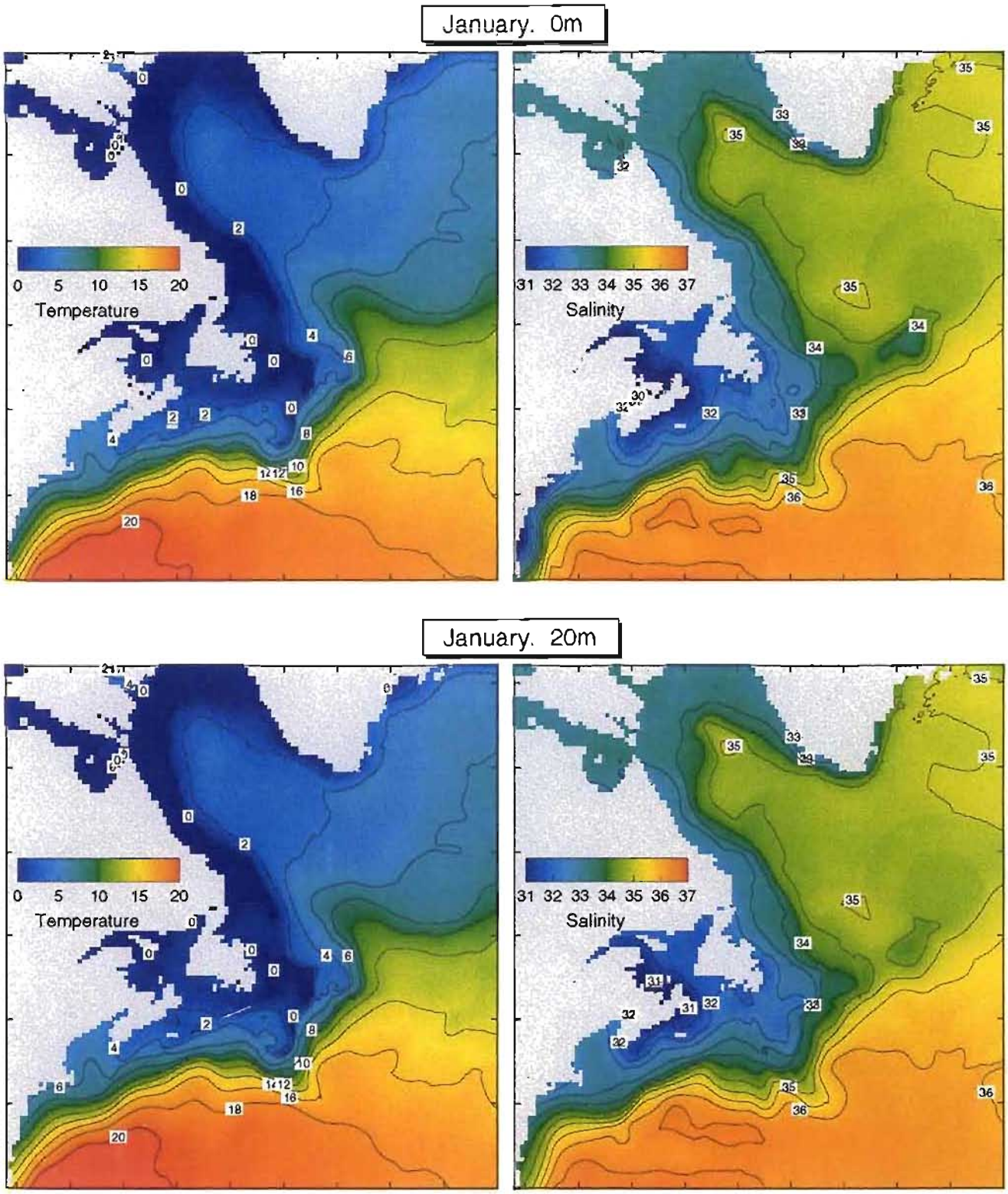

Figure 3a. Monthly mean in-situ temperature (°C) and salinity (psu) in January at 0 and 20 m.

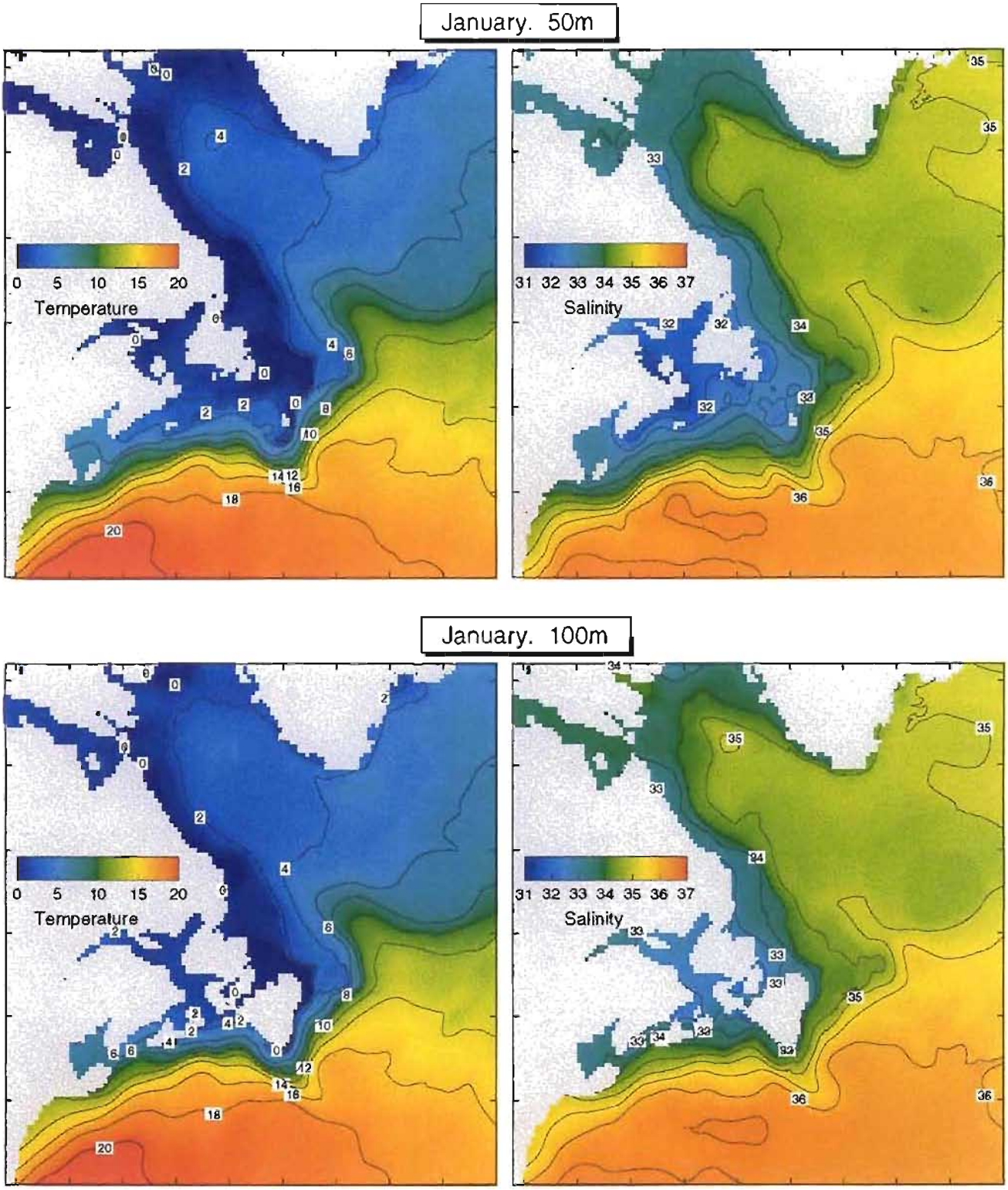

Figure 3b. Monthly mean in-situ temperature (°C) and salinity (psu) in January at 50 and 100 m.

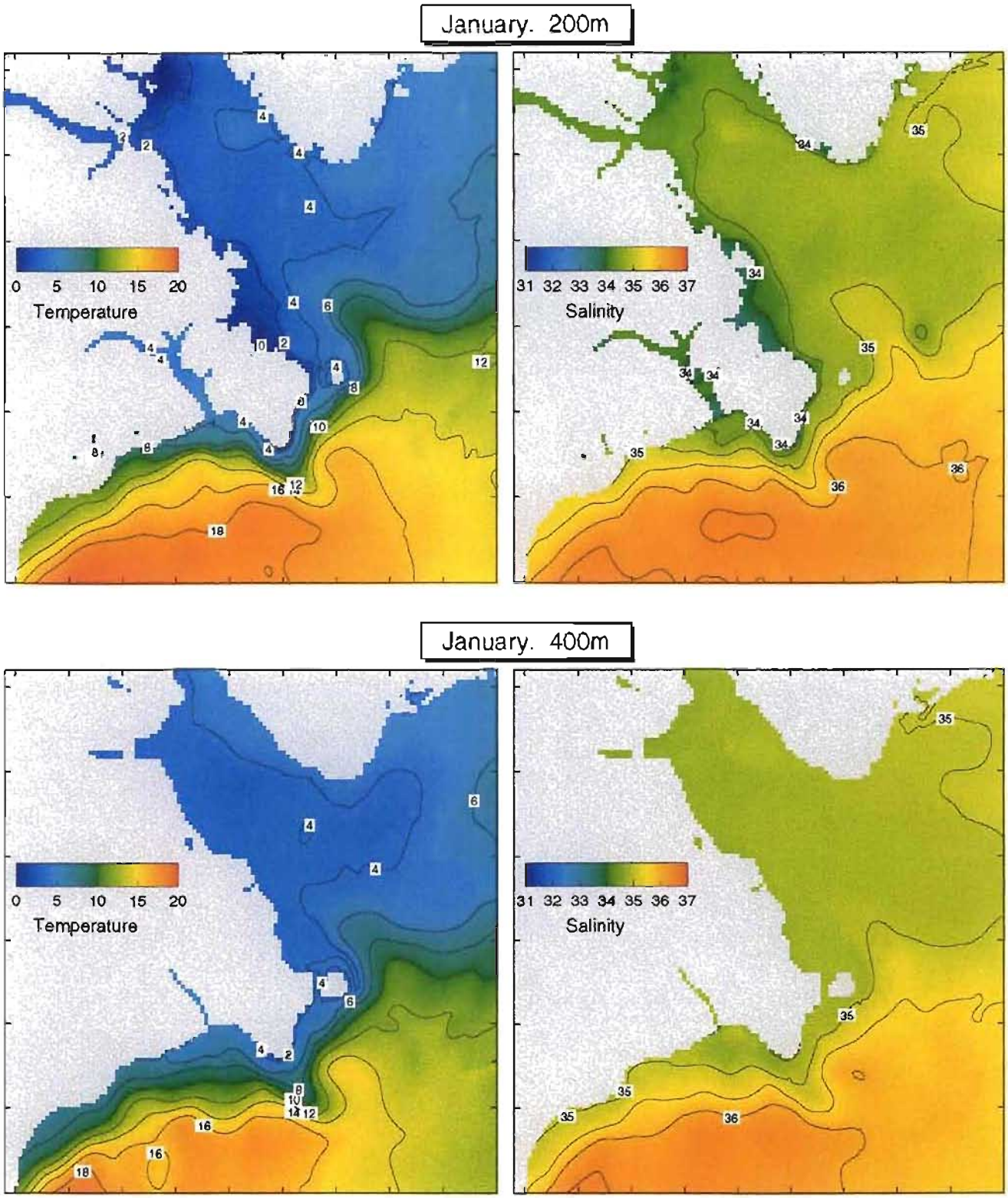

Figure 3c. Monthly mean in-situ temperature (°C) and salinity (psu) in January at 200 and 400 m.

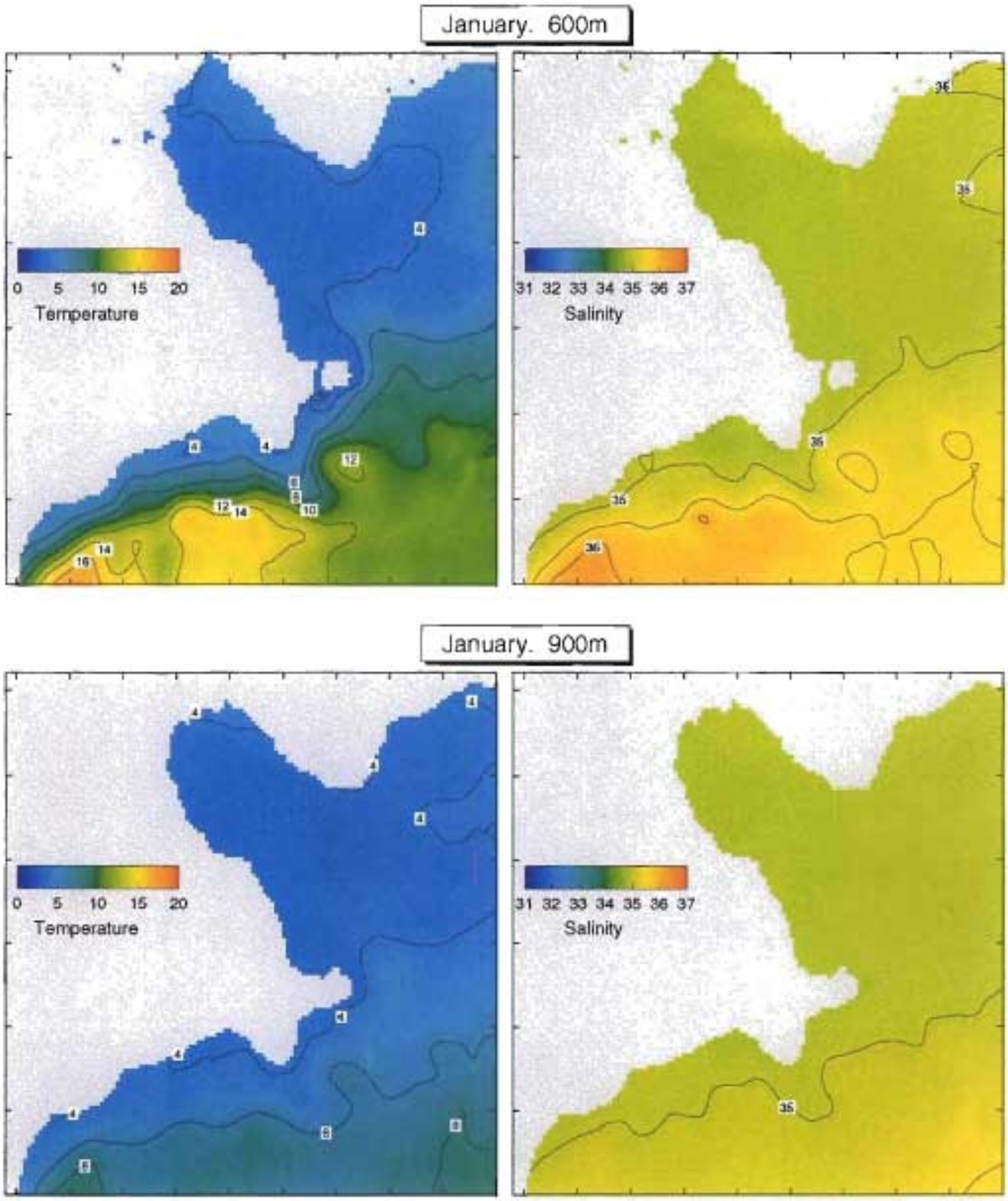

Figure 3d. Monthly mean in-situ temperature (°C) and salinity (psu) in January at 600 and 900 m.

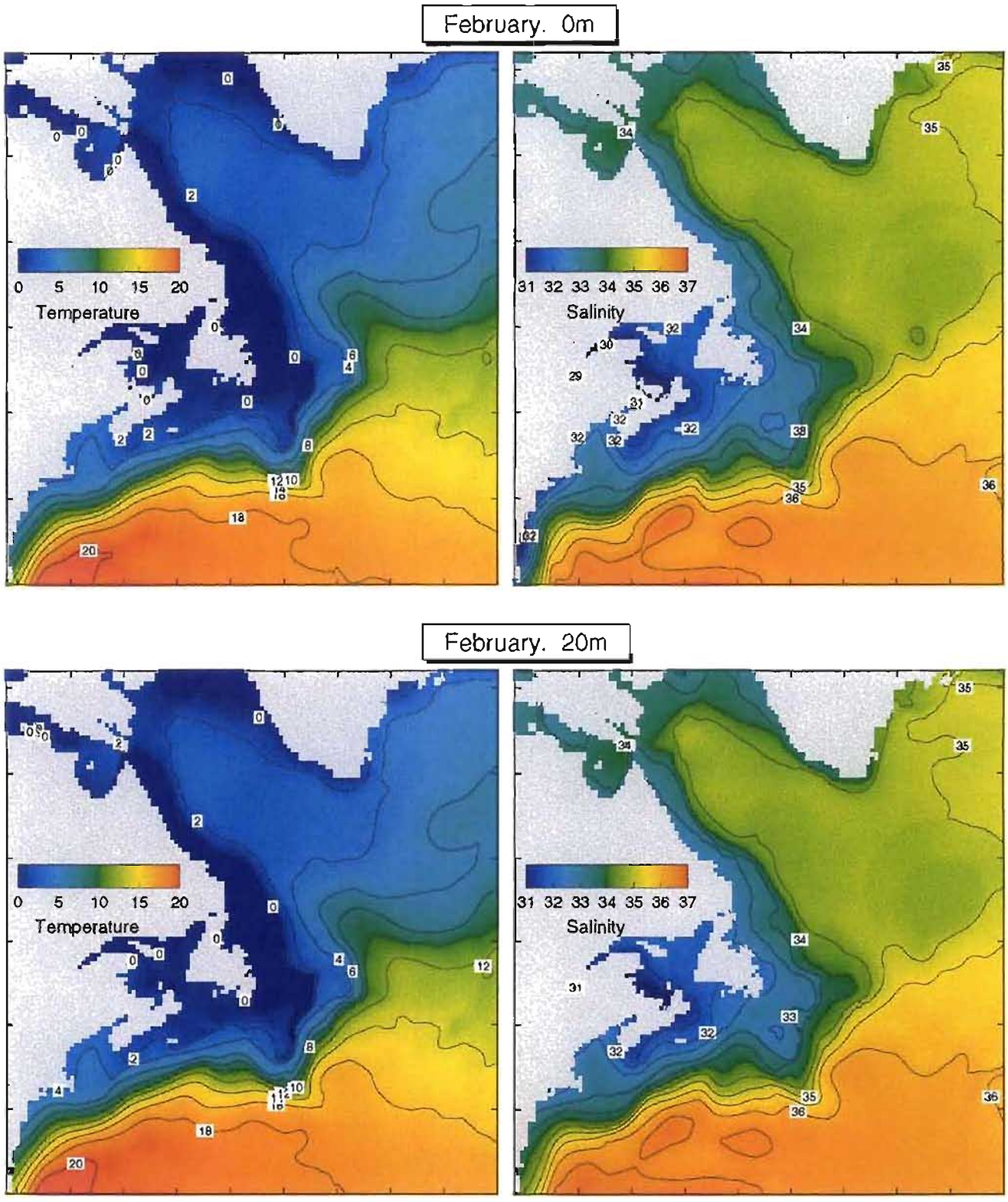

Figure 4a. Monthly mean in-situ temperature (°C) and salinity (psu) in February at 0 and 20 m.

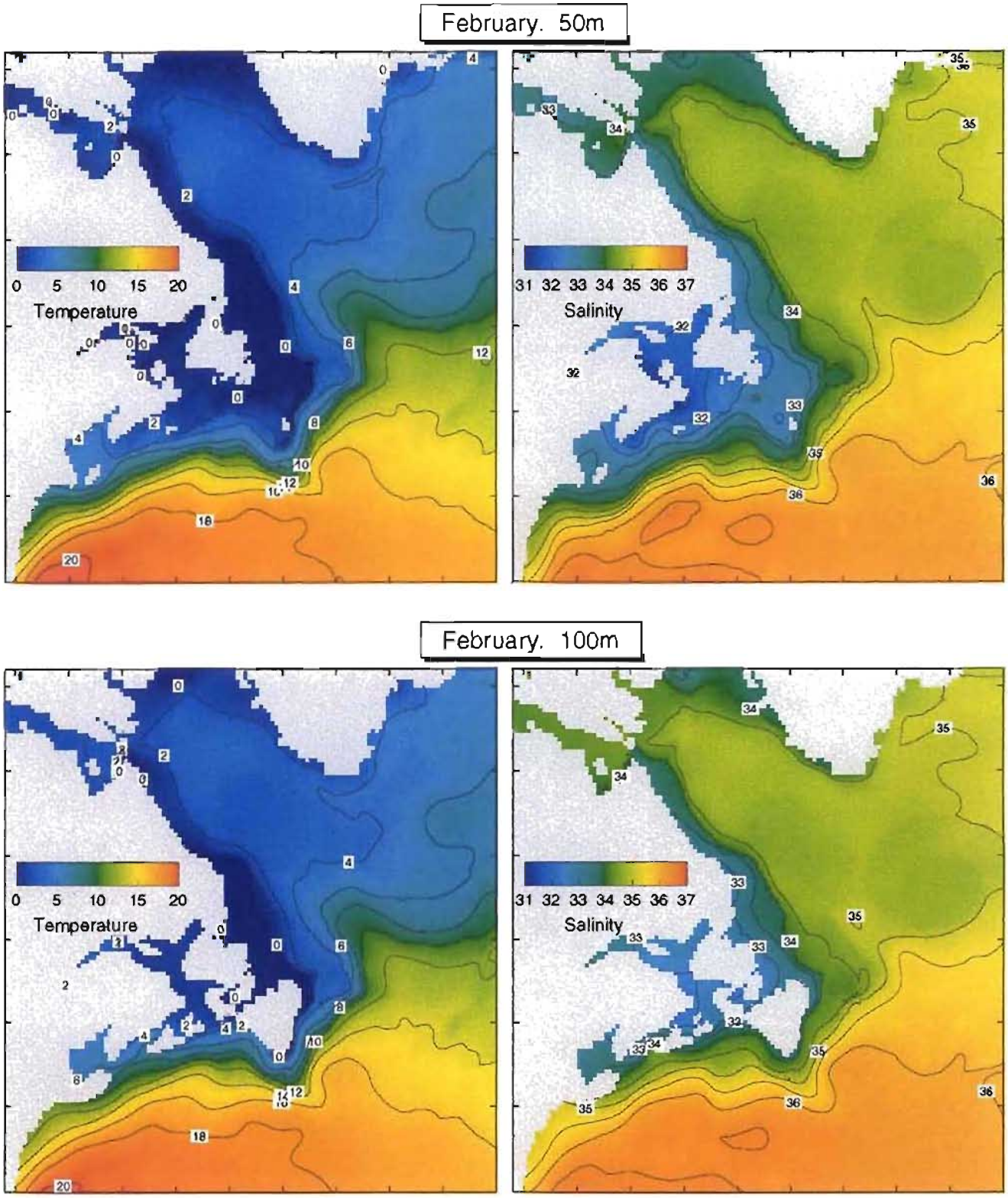

Figure 4b. Monthly mean in-situ temperature (^{o}C) and salinity (psu) in February at 50 and 100 m.

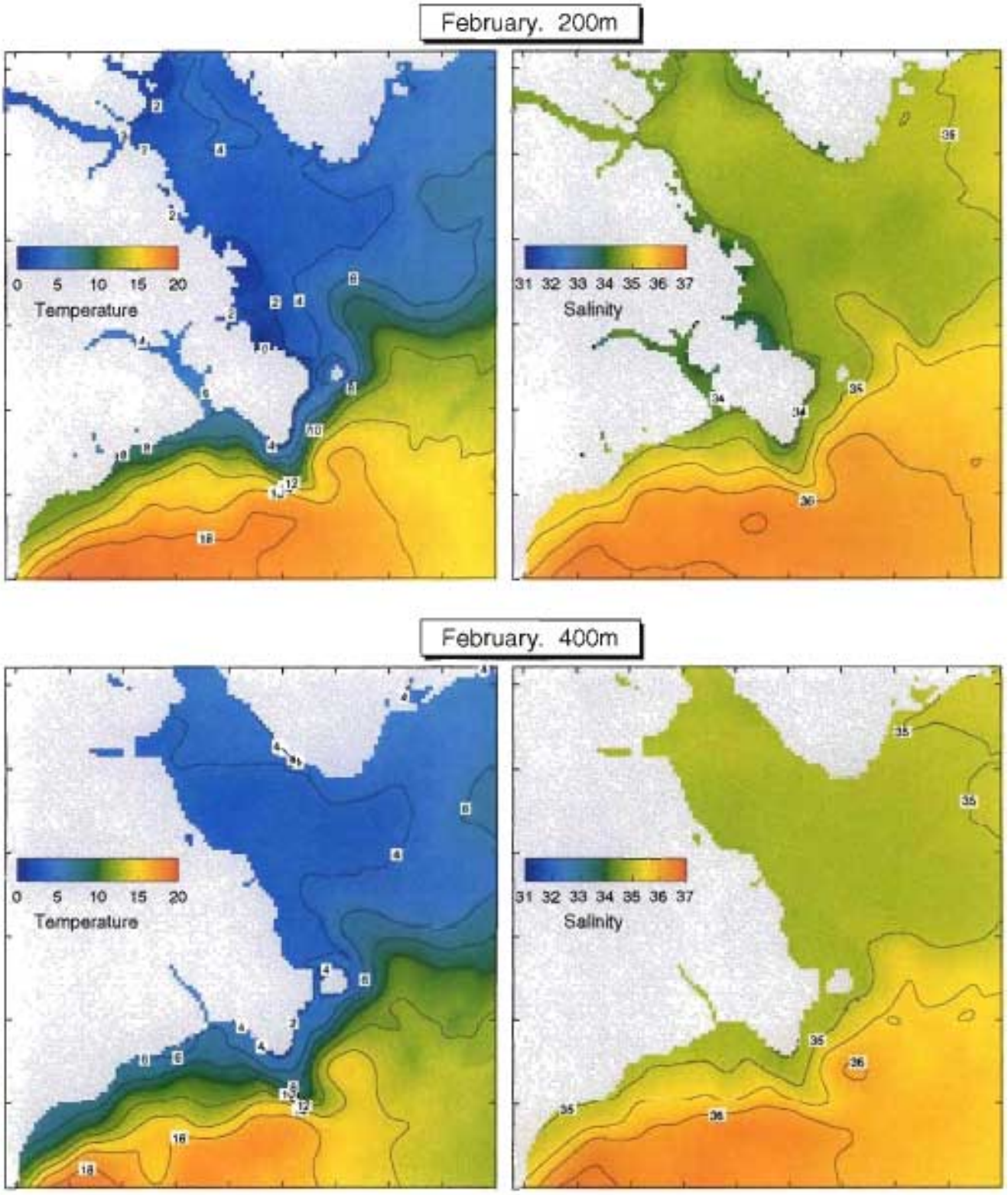

Figure 4c. Monthly mean in-situ temperature (°C) and salinity (psu) in February at 200 and 400 m.

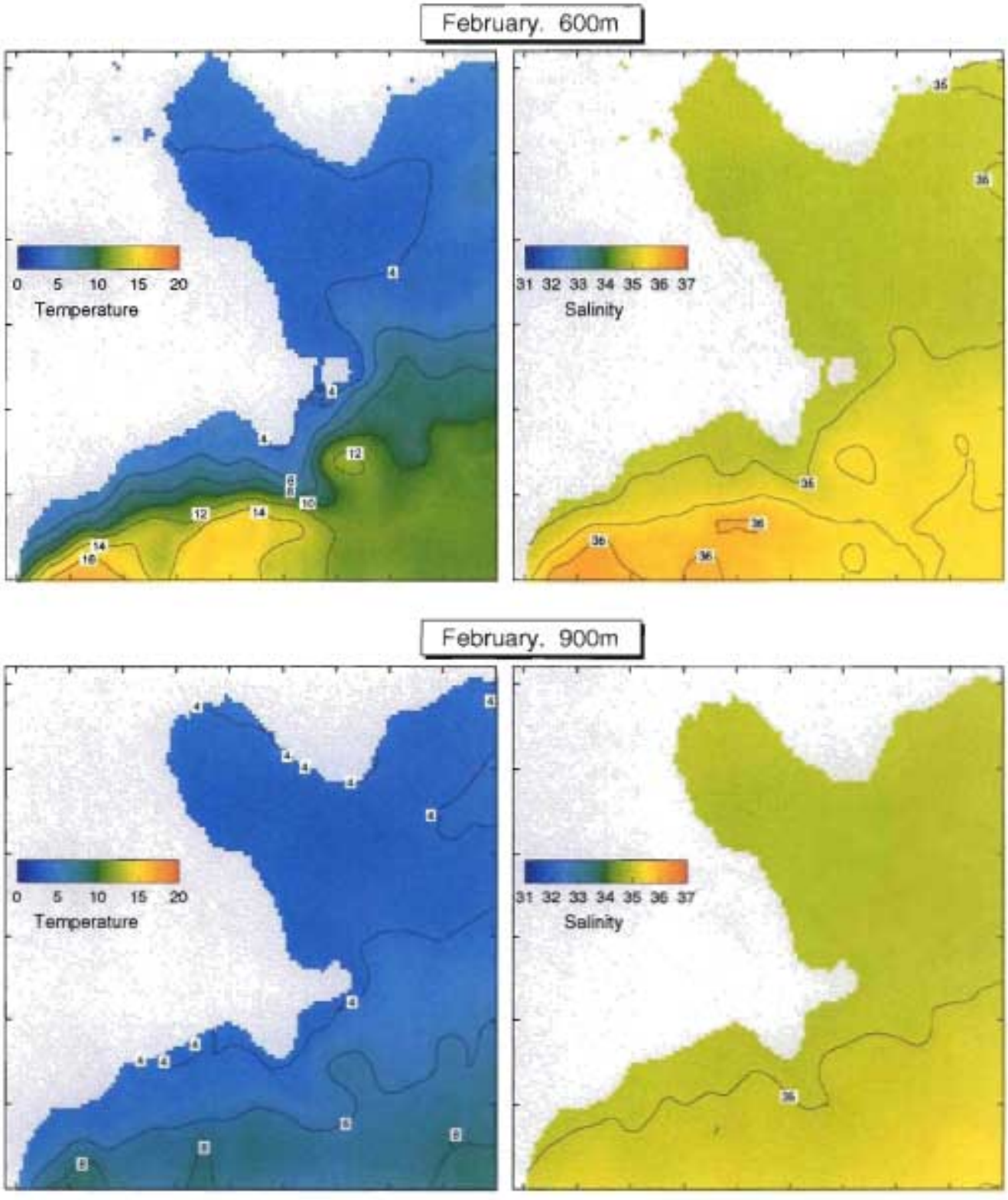

Figure 4d. Monthly mean in-situ temperature (°C) and salinity (psu) in February at 600 and 900 m.

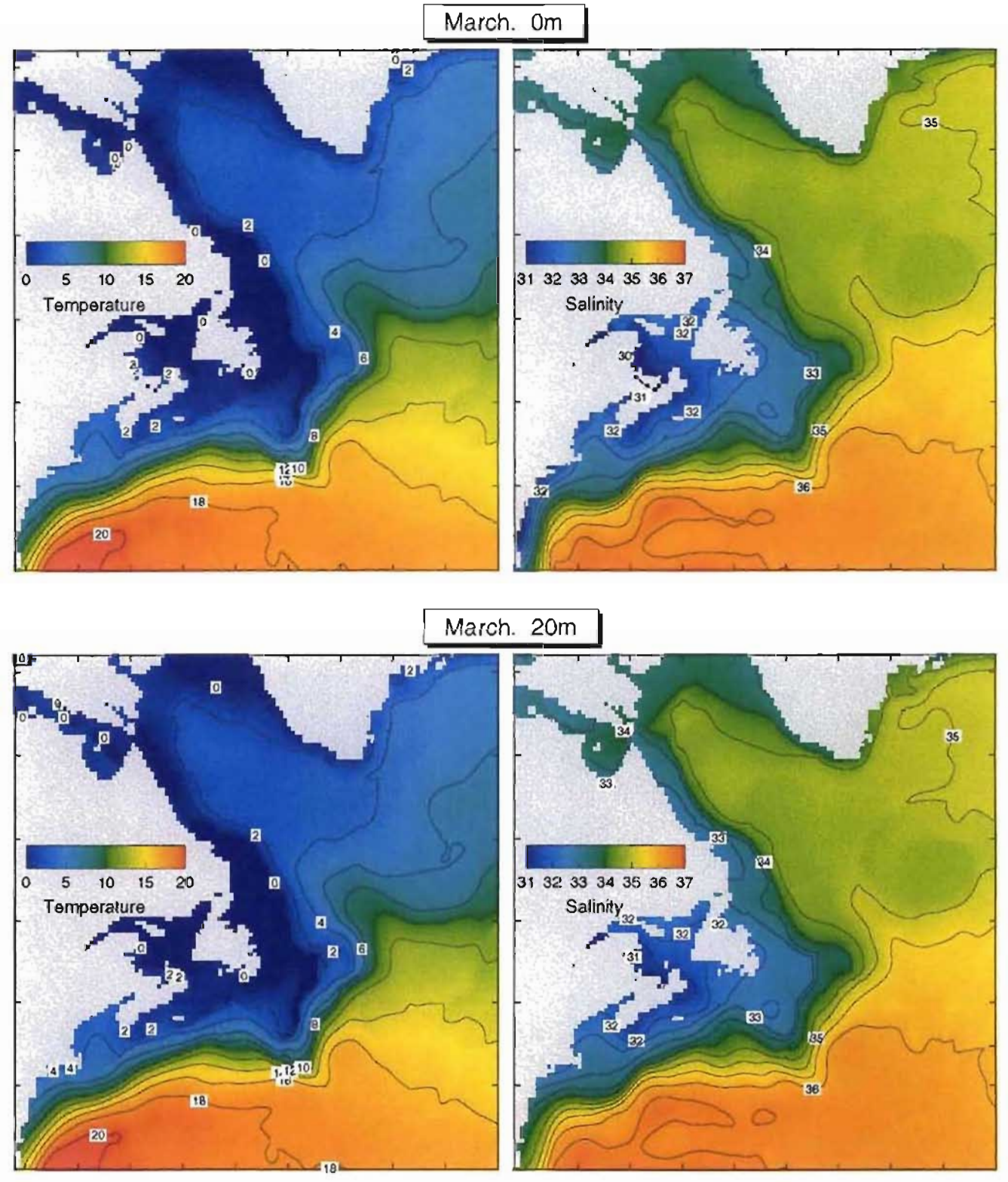

Figure 5a. Monthly mean in-situ temperature (°C) and salinity (psu) in March at 0 and 20 m.

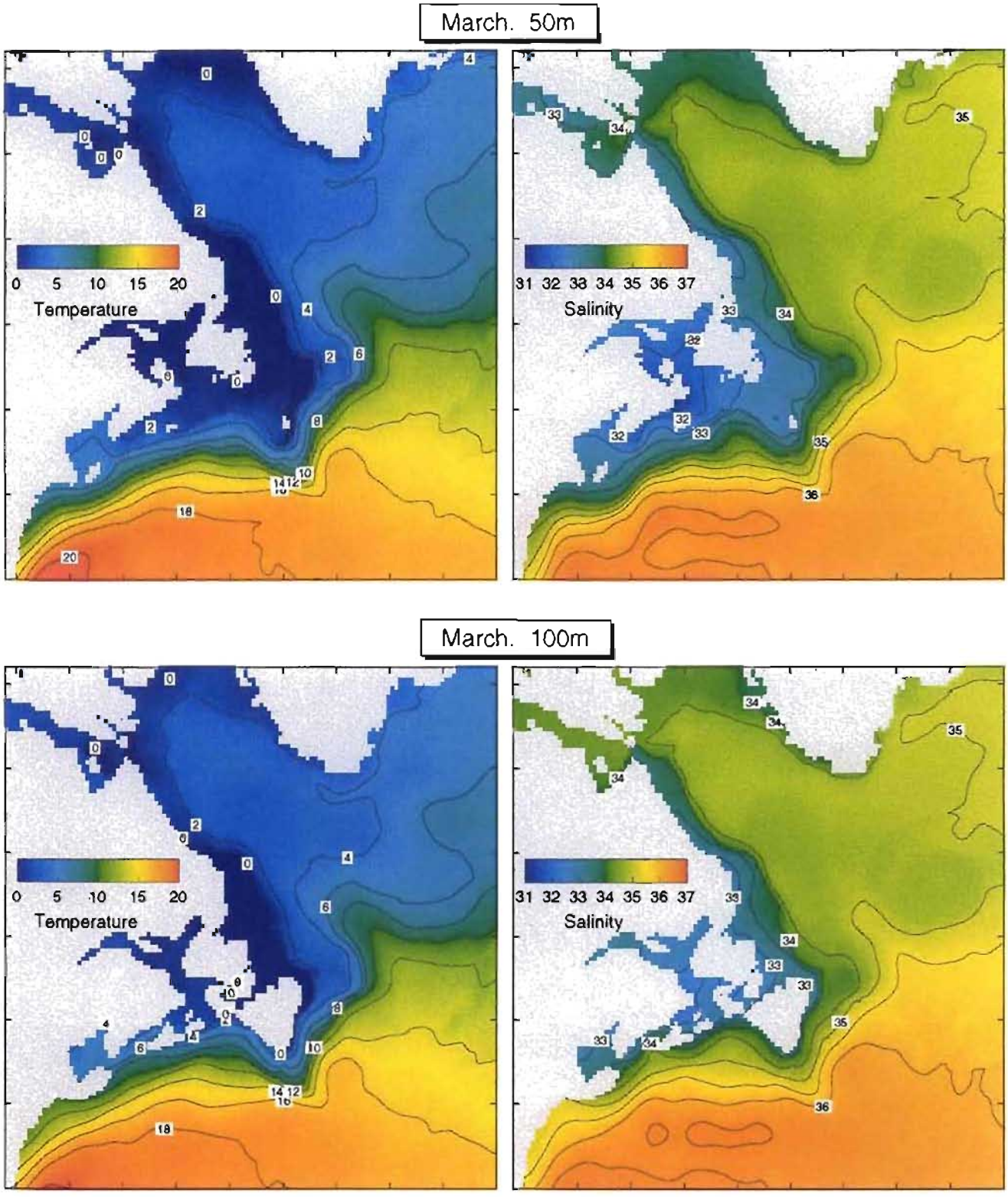

Figure 5b. Monthly mean in-situ temperature (°C) and salinity (psu) in March at 50 and 100 m.

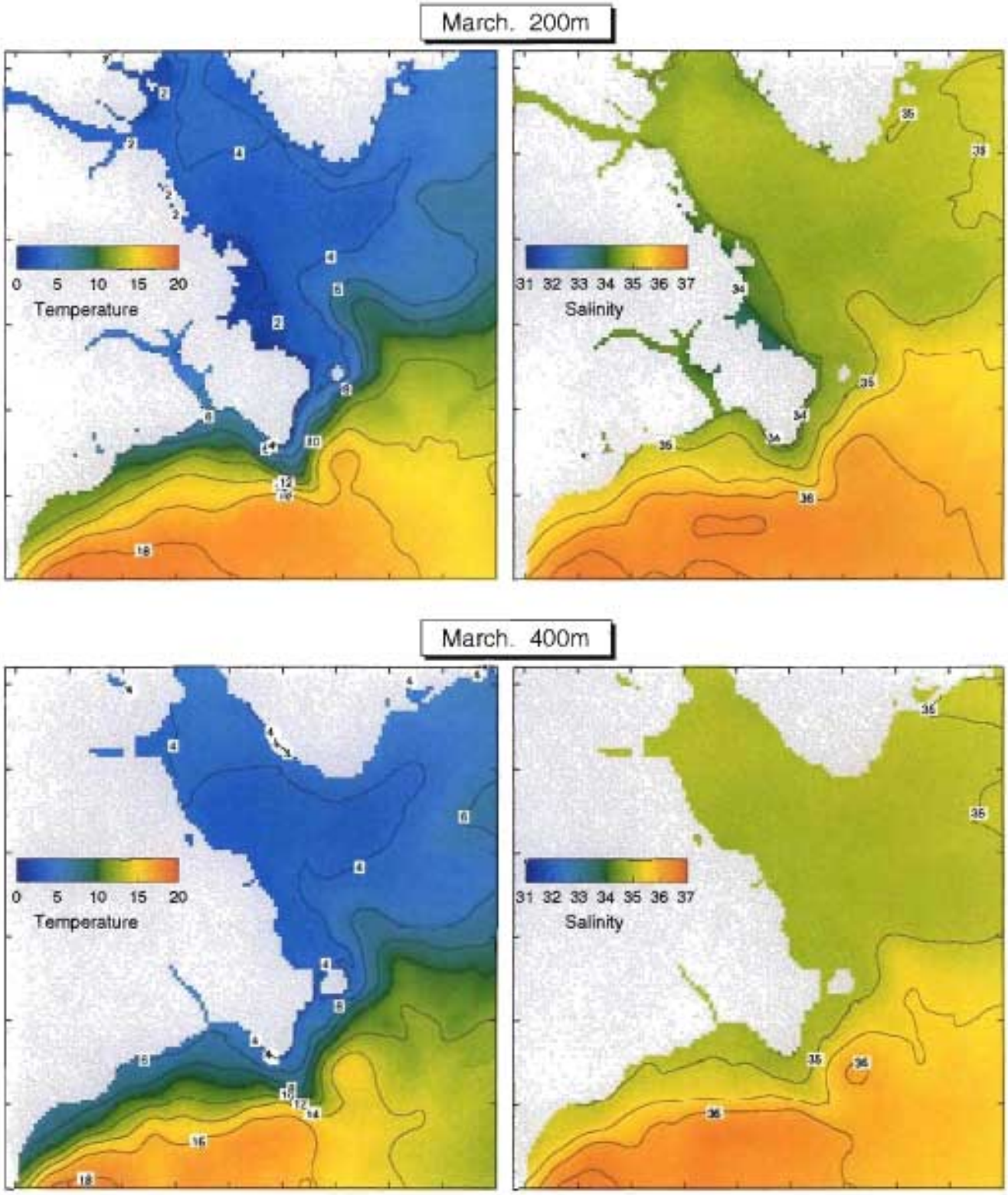

Figure 5c. Monthly mean in-situ temperature (°C) and salinity (psu) in March at 200 and 400 m.

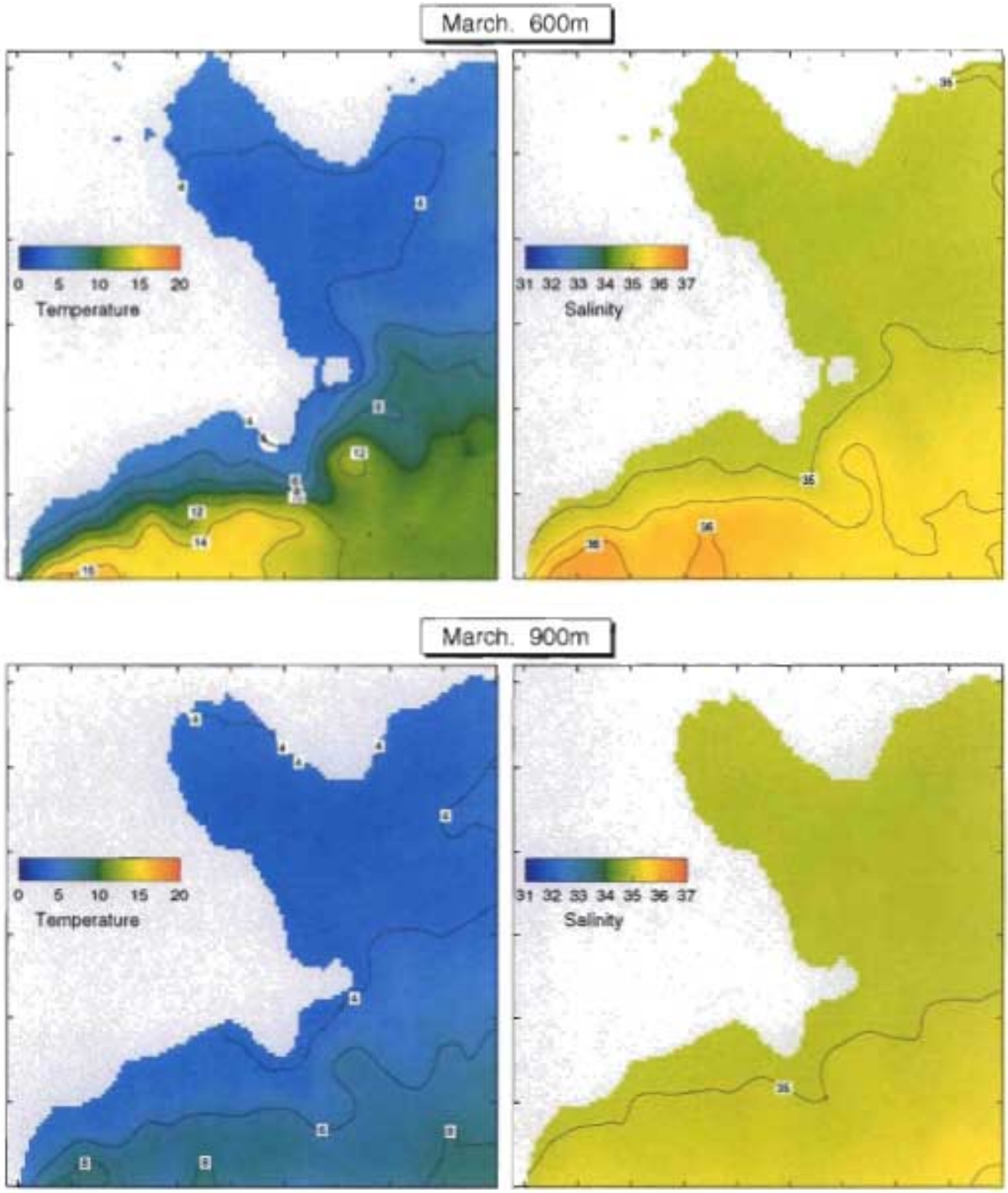

Figure 5d. Monthly mean in-situ temperature (°C) and salinity (psu) in March at 600 and 900 m.

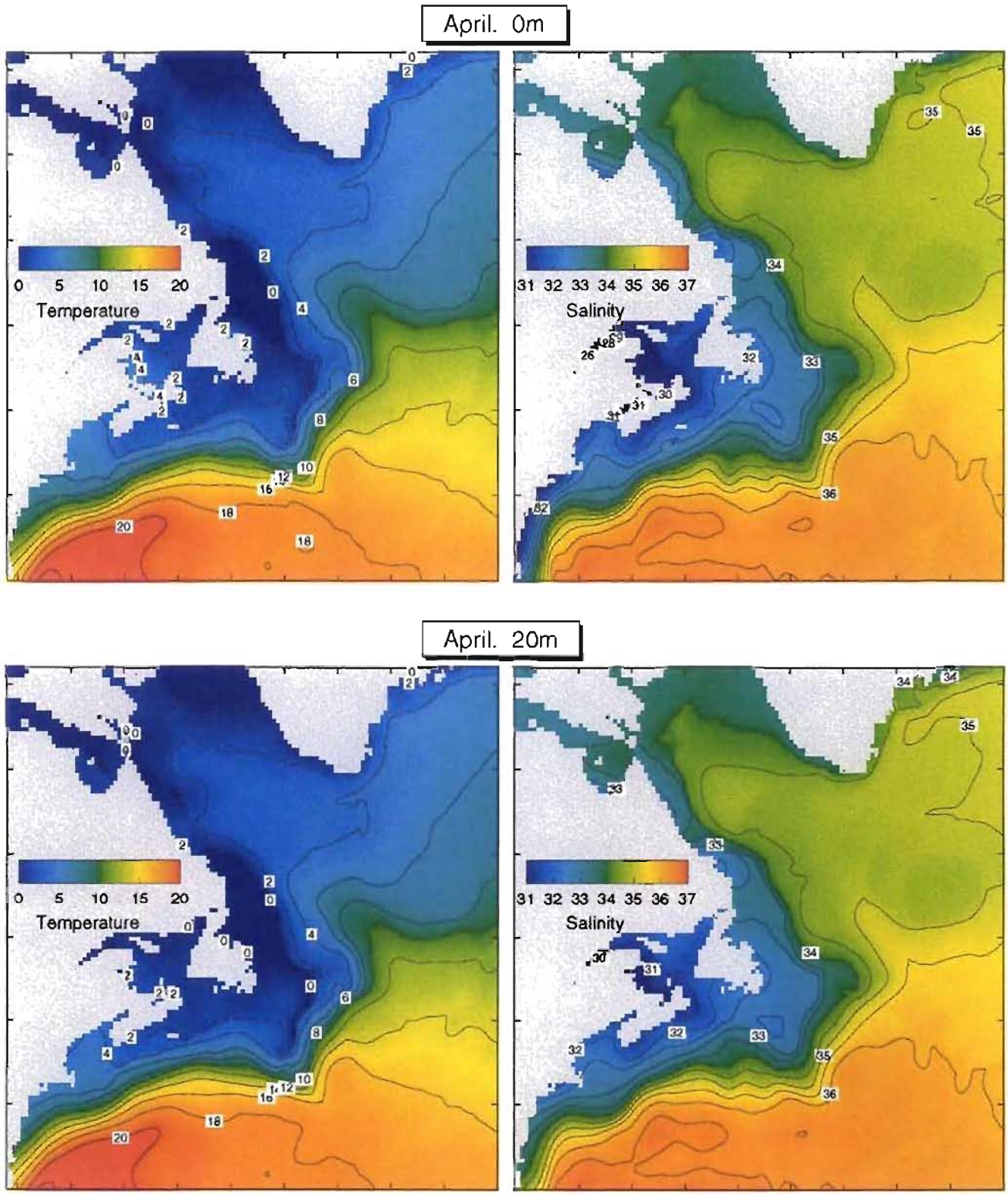

Figure 6a. Monthly mean in-situ temperature (°C) and salinity (psu) in April at 0 and 20 m.

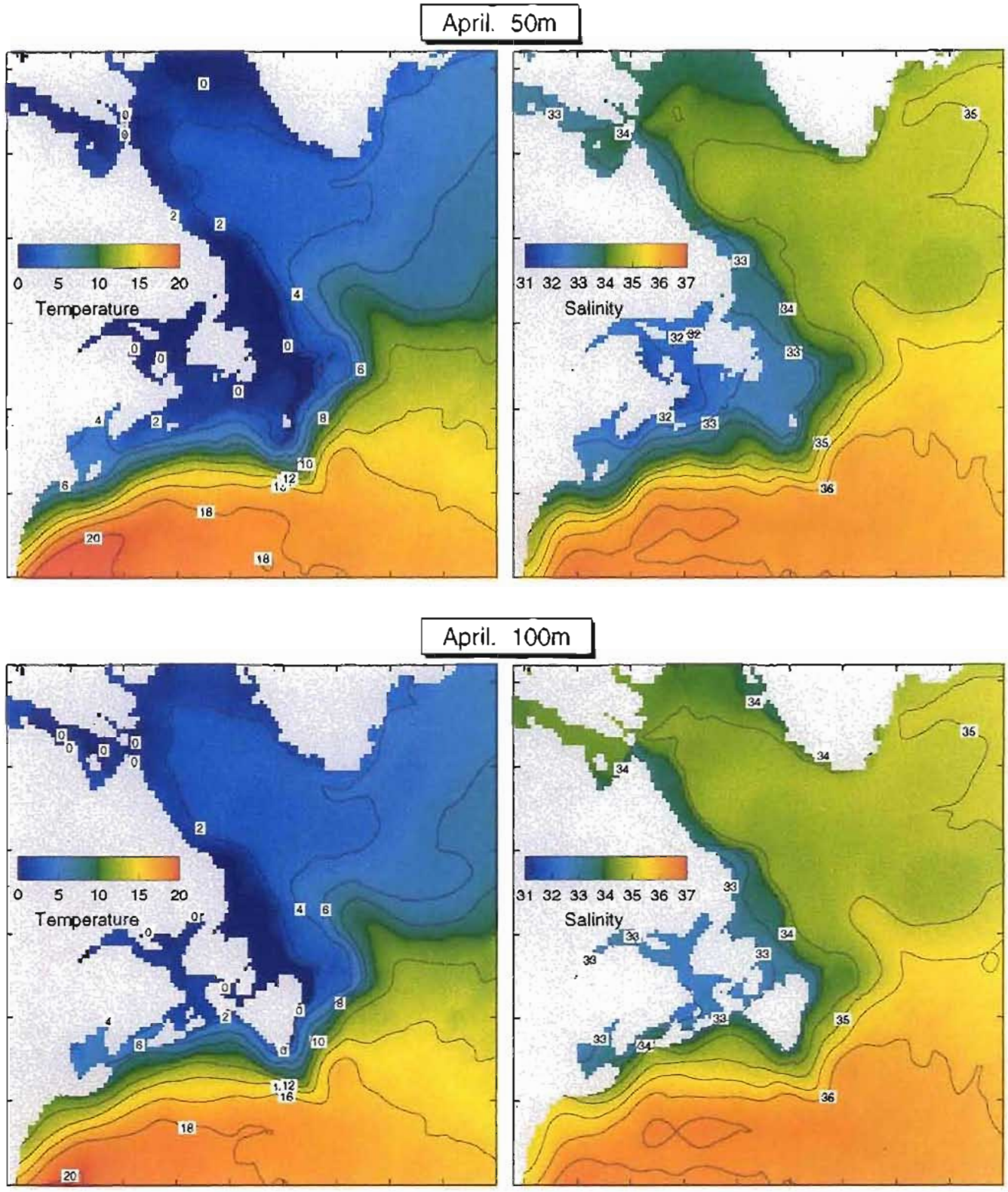

Figure 6b. Monthly mean in-situ temperature (°C) and salinity (psu) in April at 50 and 100 m.

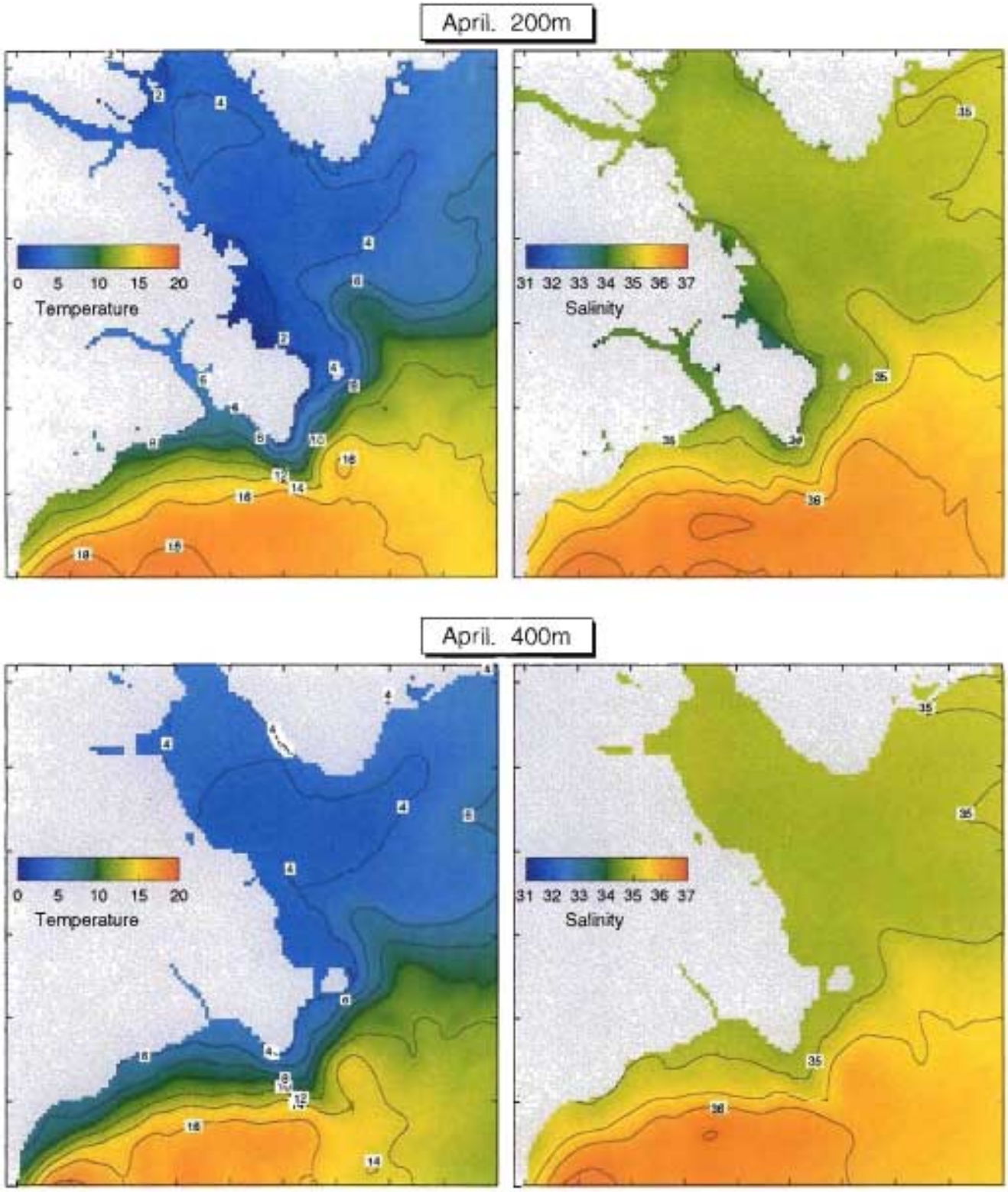

Figure 6c. Monthly mean in-situ temperature (°C) and salinity (psu) in April at 200 and 400 m.

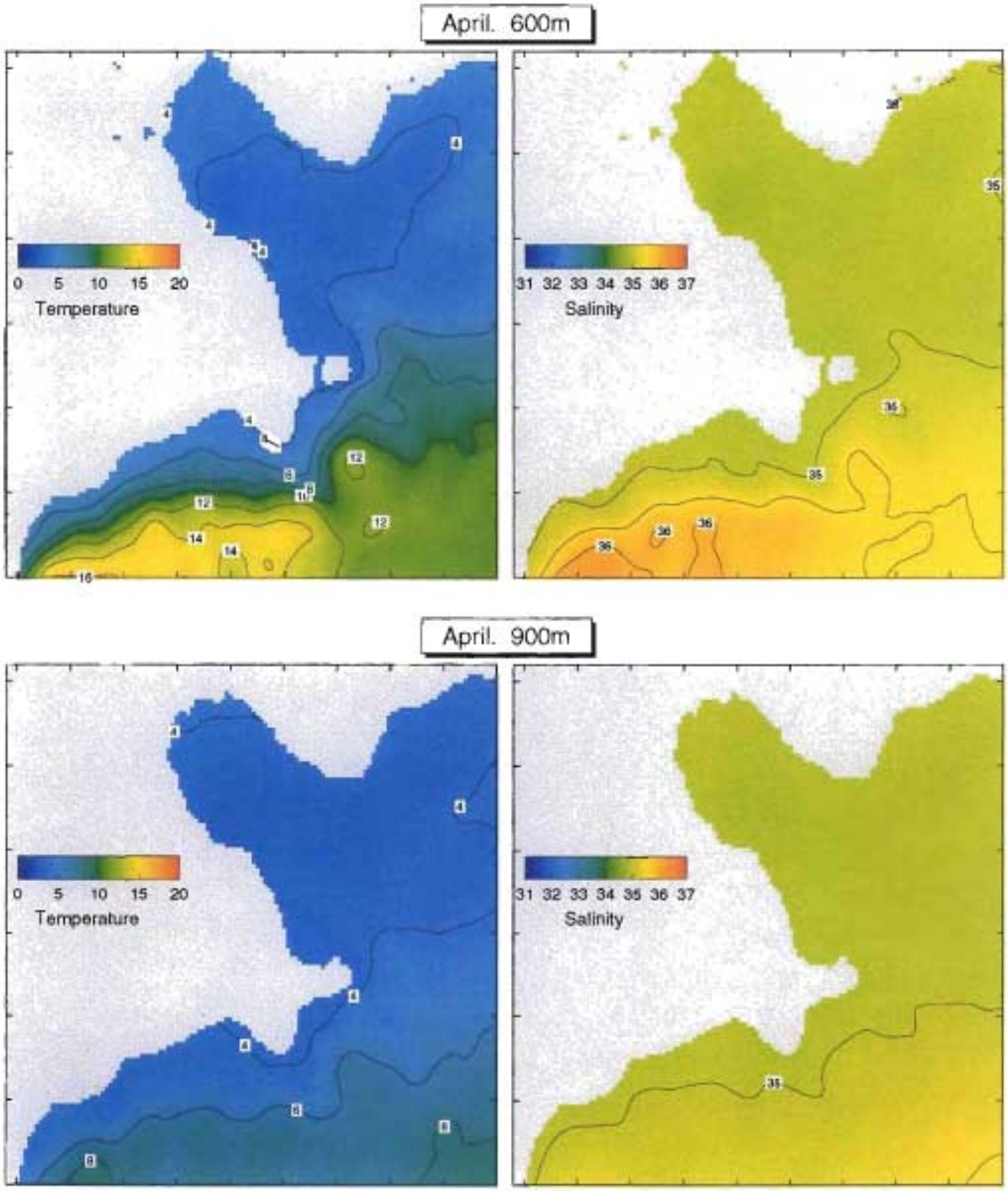

Figure 6d. Monthly mean in-situ temperature (°C) and salinity (psu) in April at 600 and 900 m.

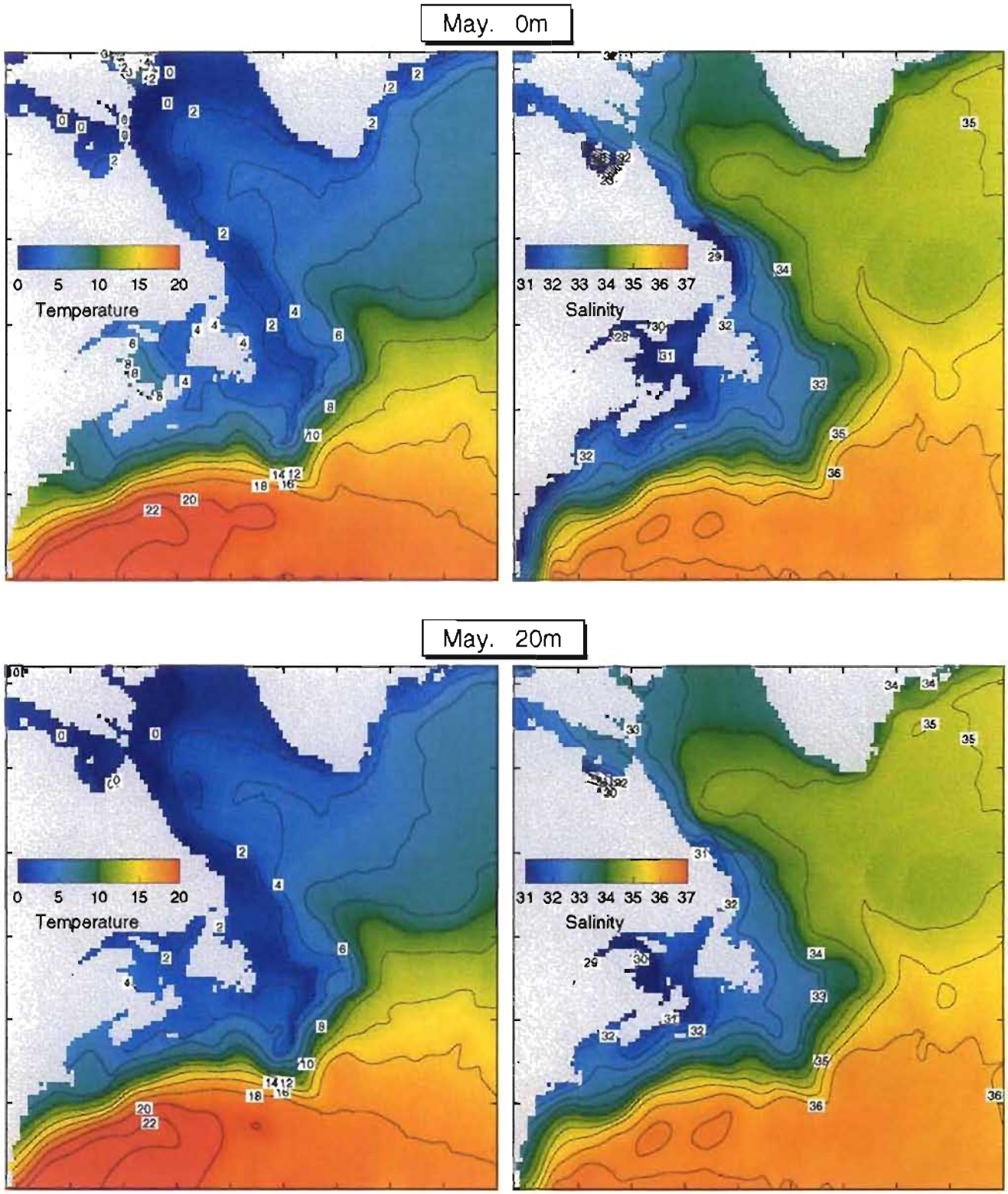

Figure 7a. Monthly mean in-situ temperature (°C) and salinity (psu) in May at 0 and 20 m.

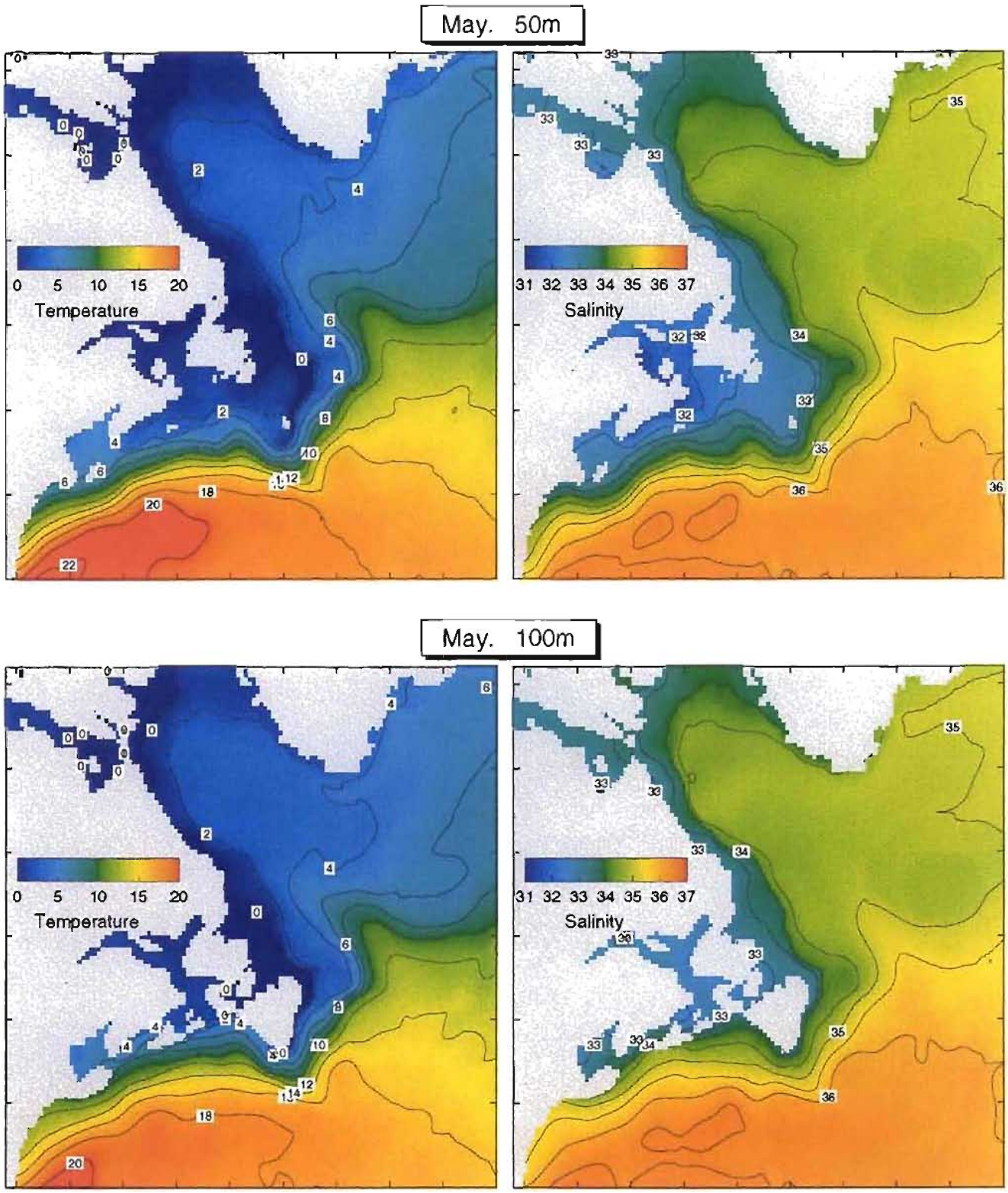

Figure 7b. Monthly mean in-situ temperature (°C) and salinity (psu) in May at 50 and 100 m.

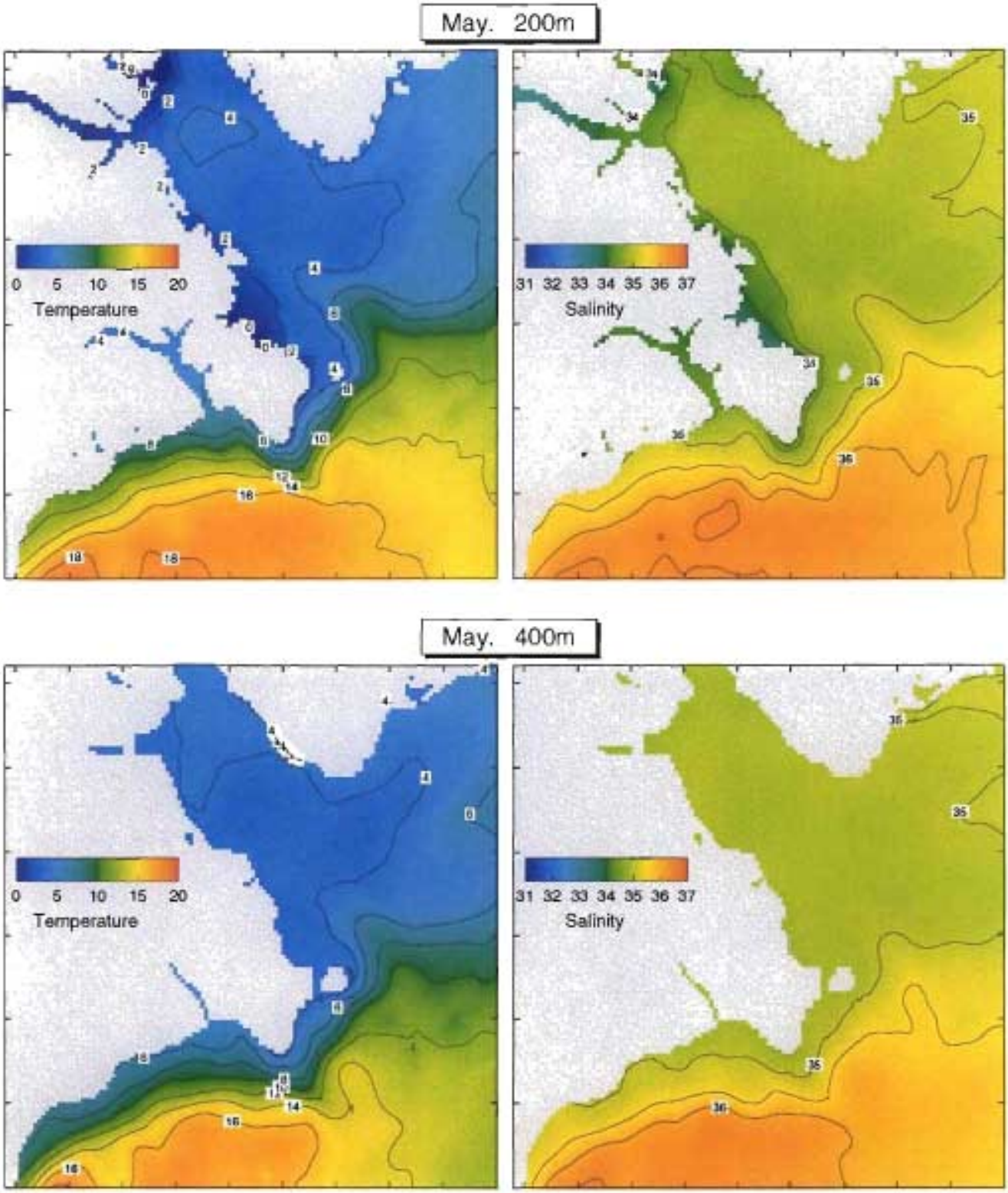

Figure 7c. Monthly mean in-situ temperature (°C) and salinity (psu) in May at 200 and 400 m.

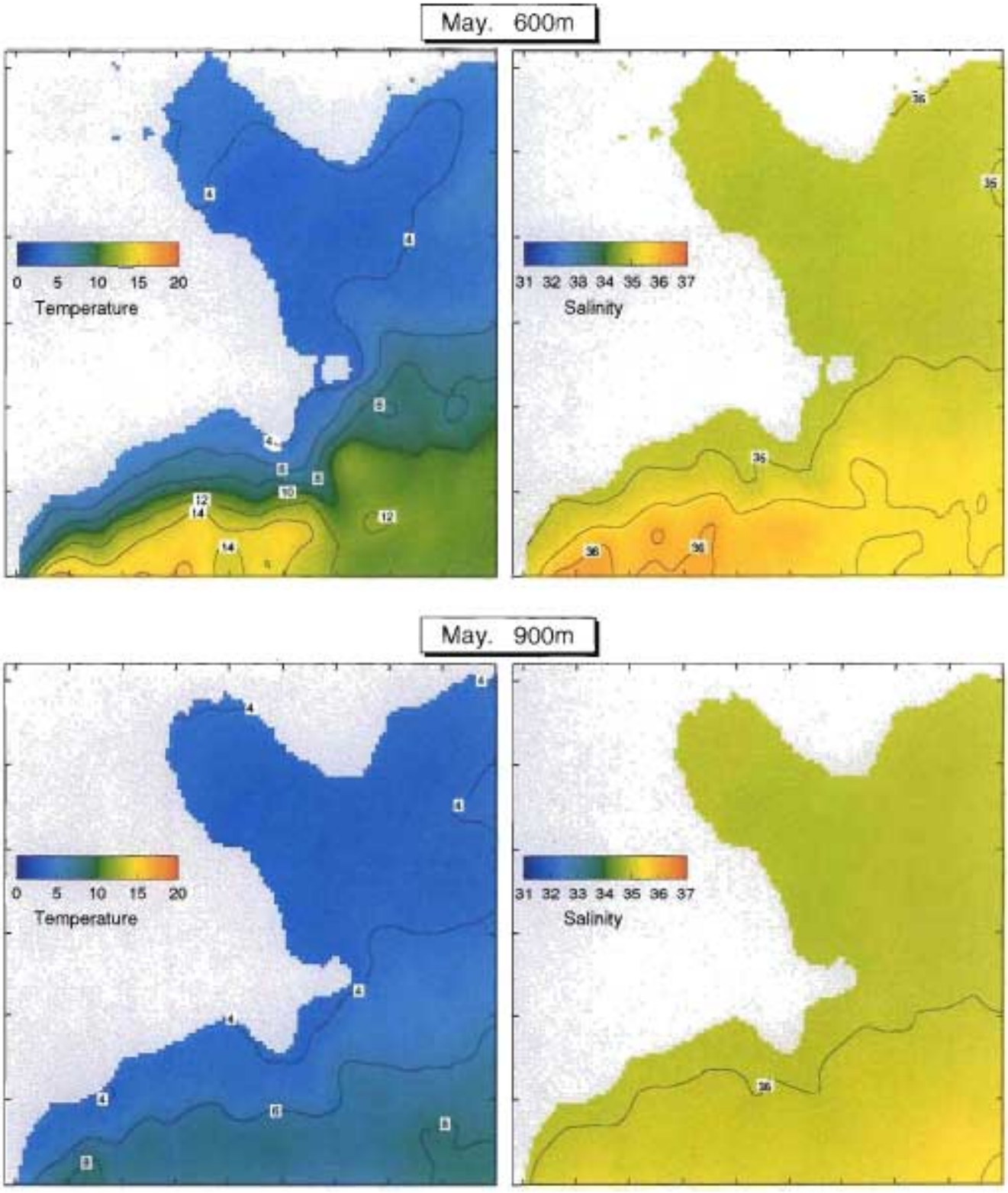

Figure 7d. Monthly mean in-situ temperature (°C) and salinity (psu) in May at 600 and 900 m.

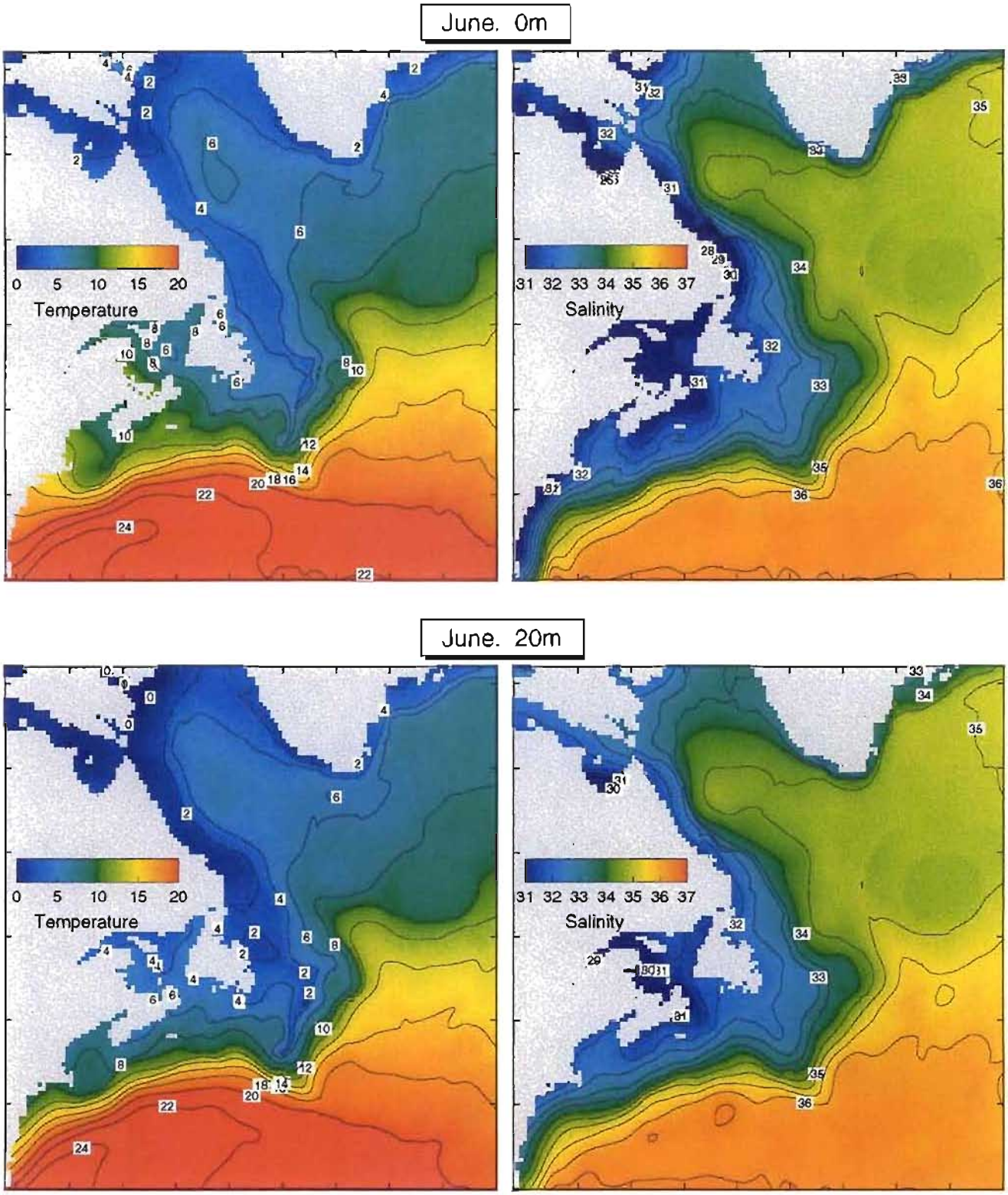

Figure 8a. Monthly mean in-situ temperature (°C) and salinity (psu) in June at 0 and 20 m.

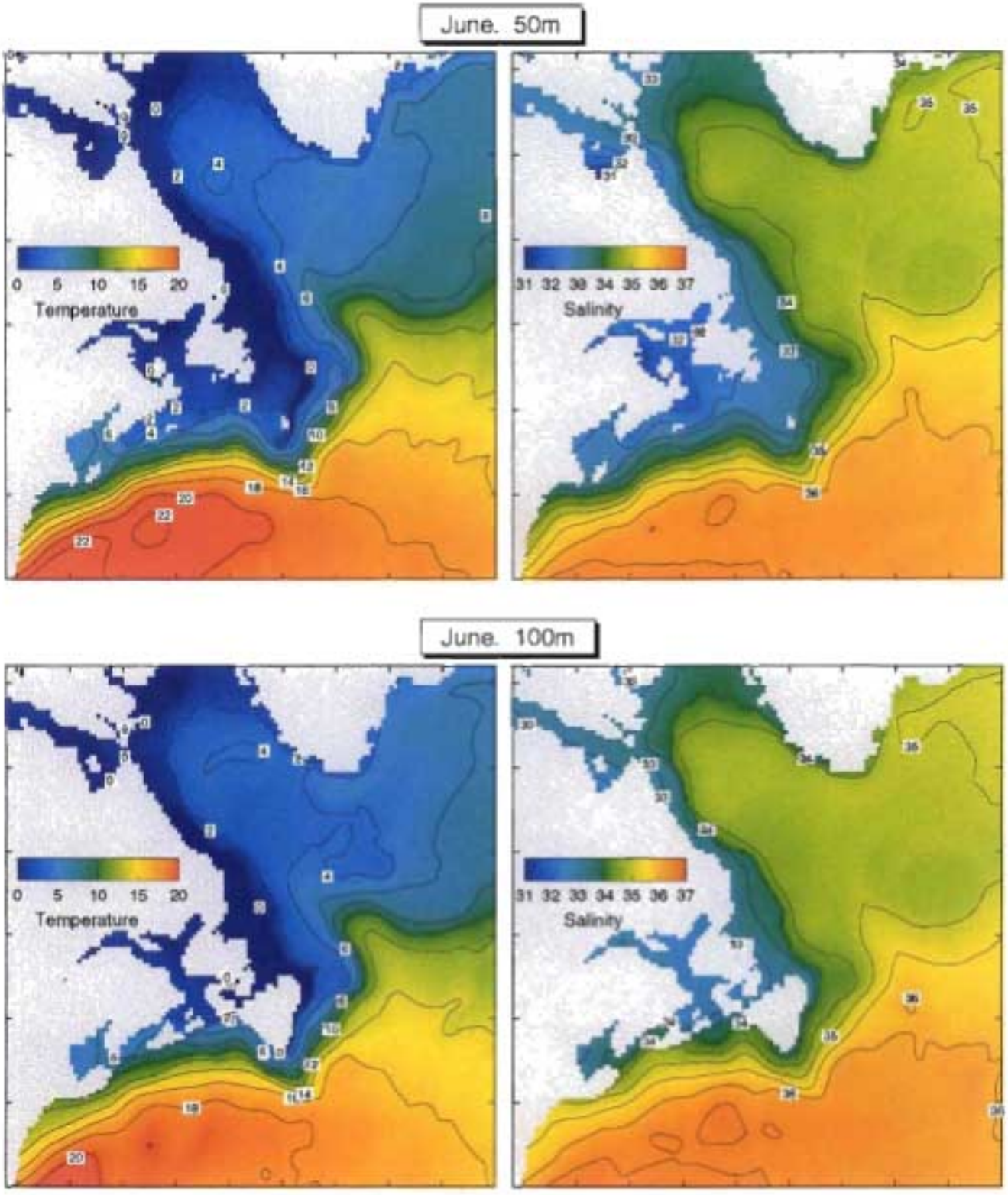

Figure 8b. Monthly mean in-situ temperature (°C) and salinity (psu) in June at 50 and 100 m.

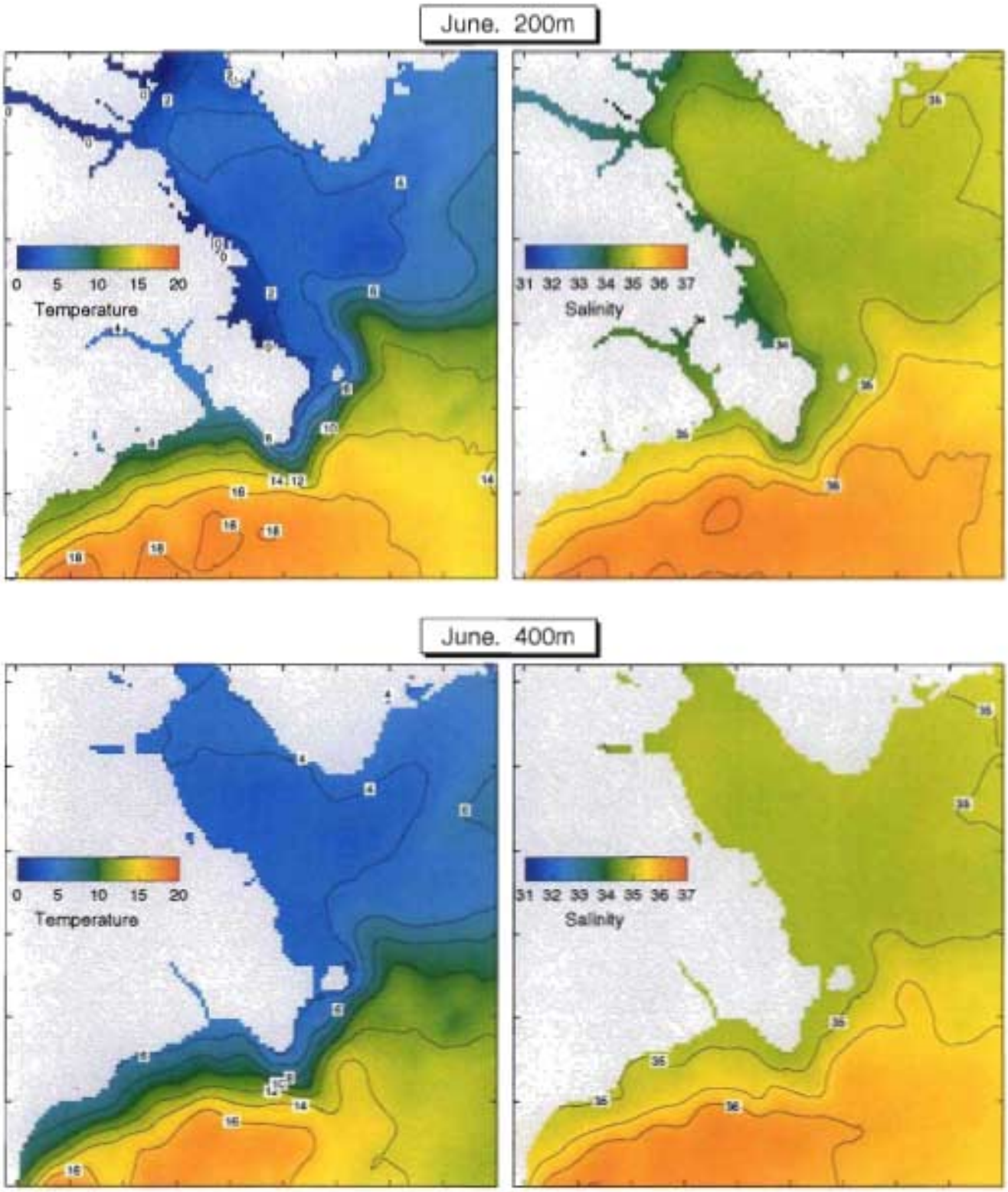

Figure 8c. Monthly mean in-situ temperature (°C) and salinity (psu) in June at 200 and 400 m.

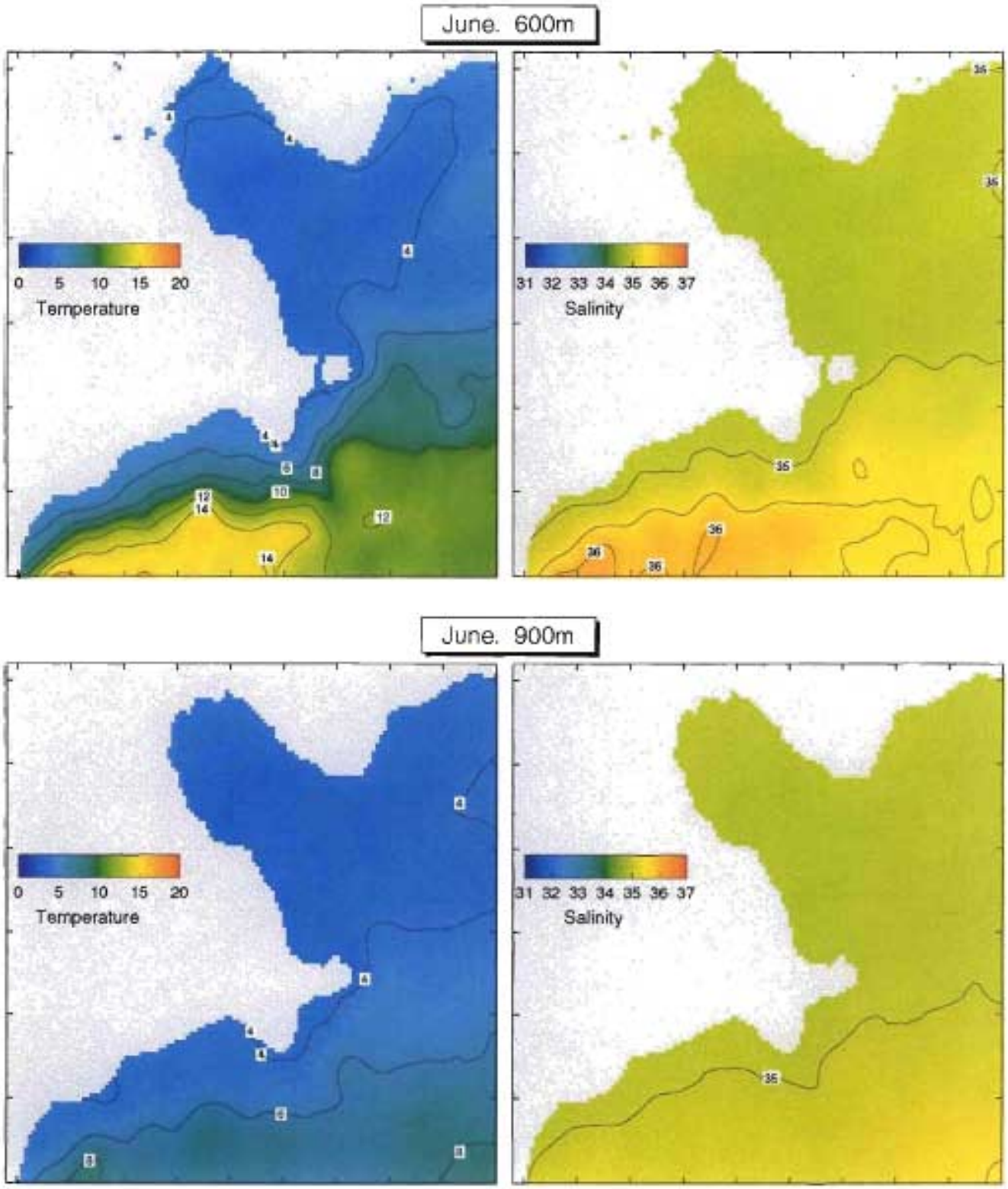

Figure 8d. Monthly mean in-situ temperature (°C) and salinity (psu) in June at 600 and 900 m.

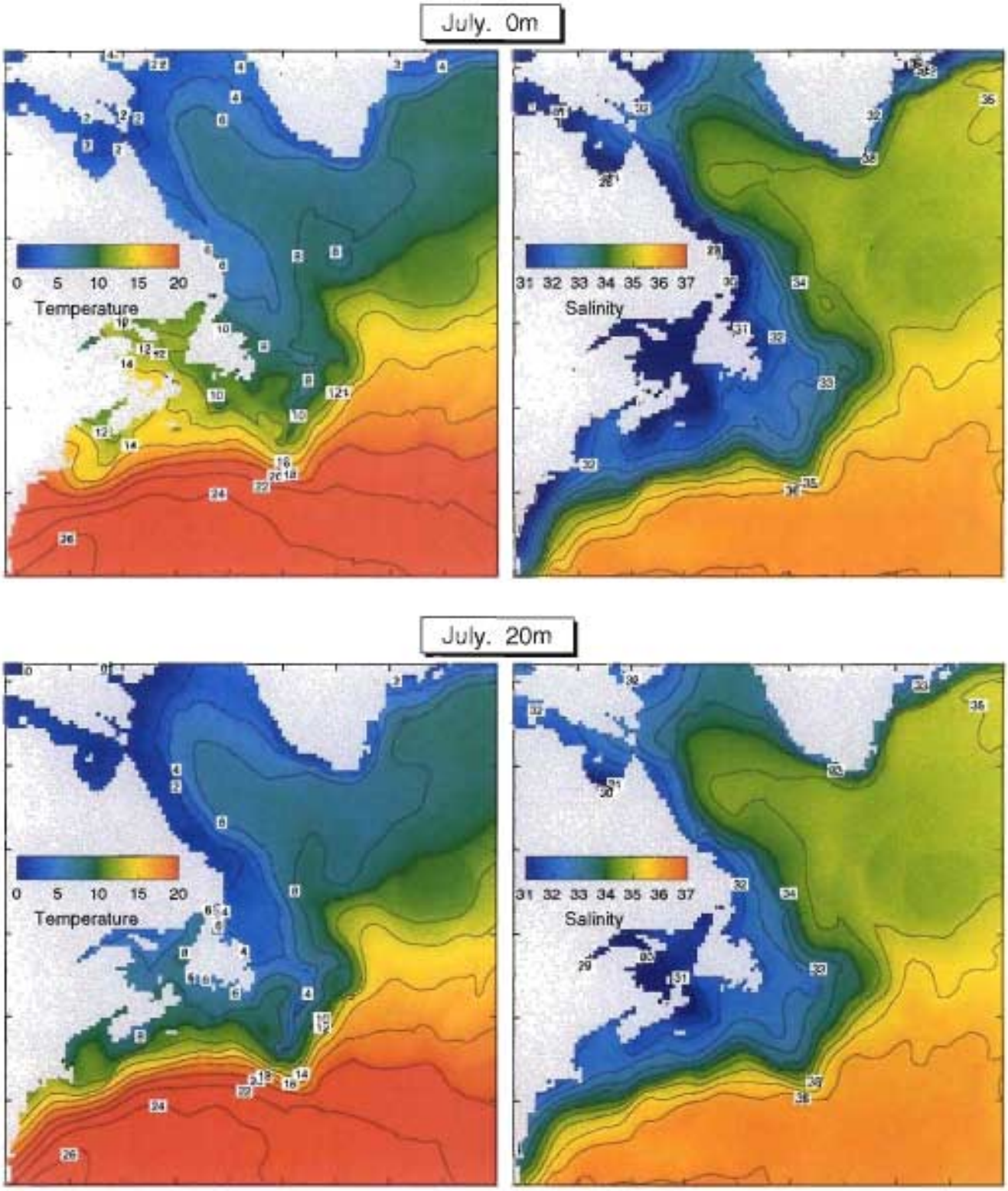

Figure 9a. Monthly mean in-situ temperature (°C) and salinity (psu) in July at 0 and 20 m.

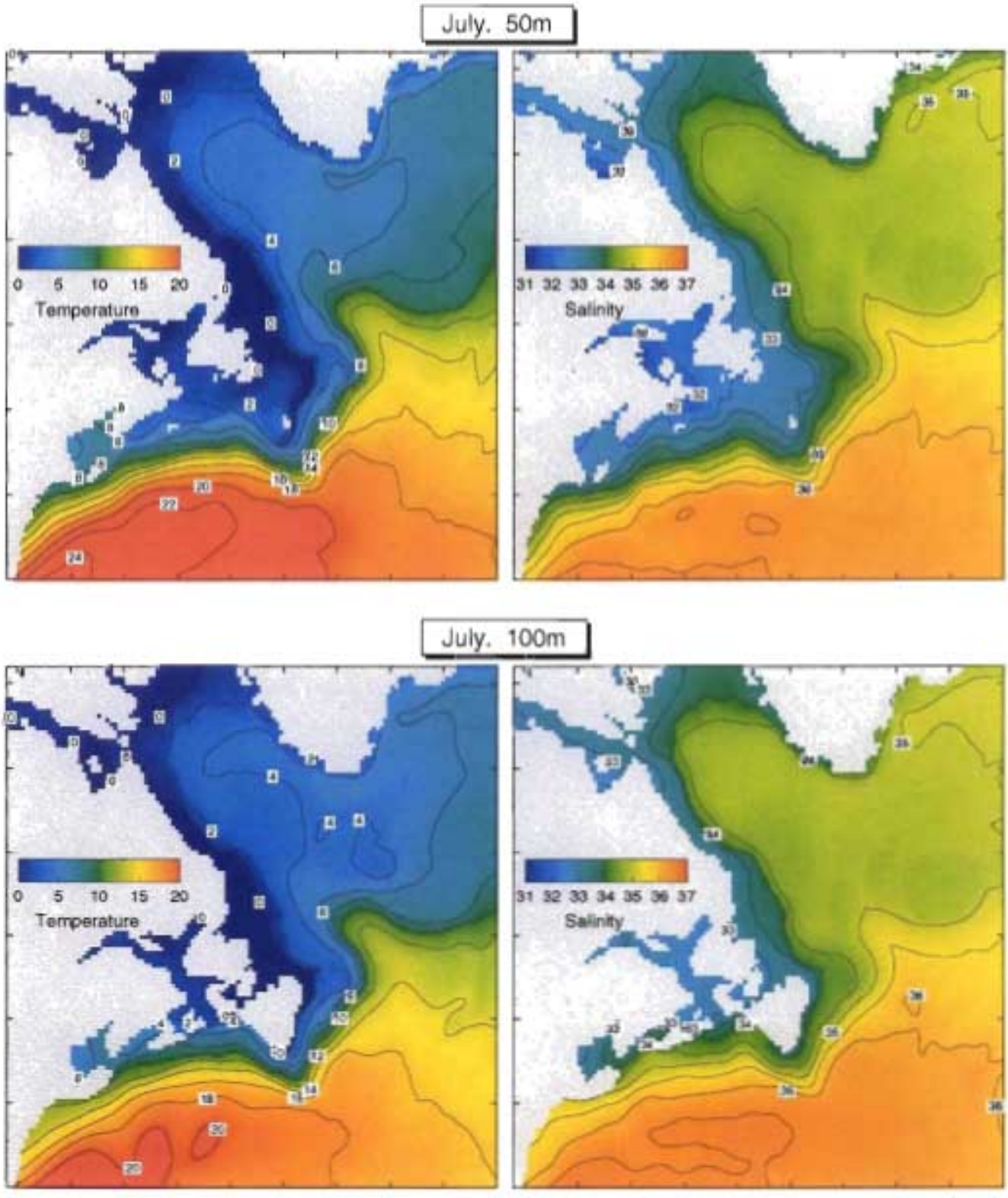

Figure 9b. Monthly mean in-situ temperature (°C) and salinity (psu) in July at 50 and 100 m.

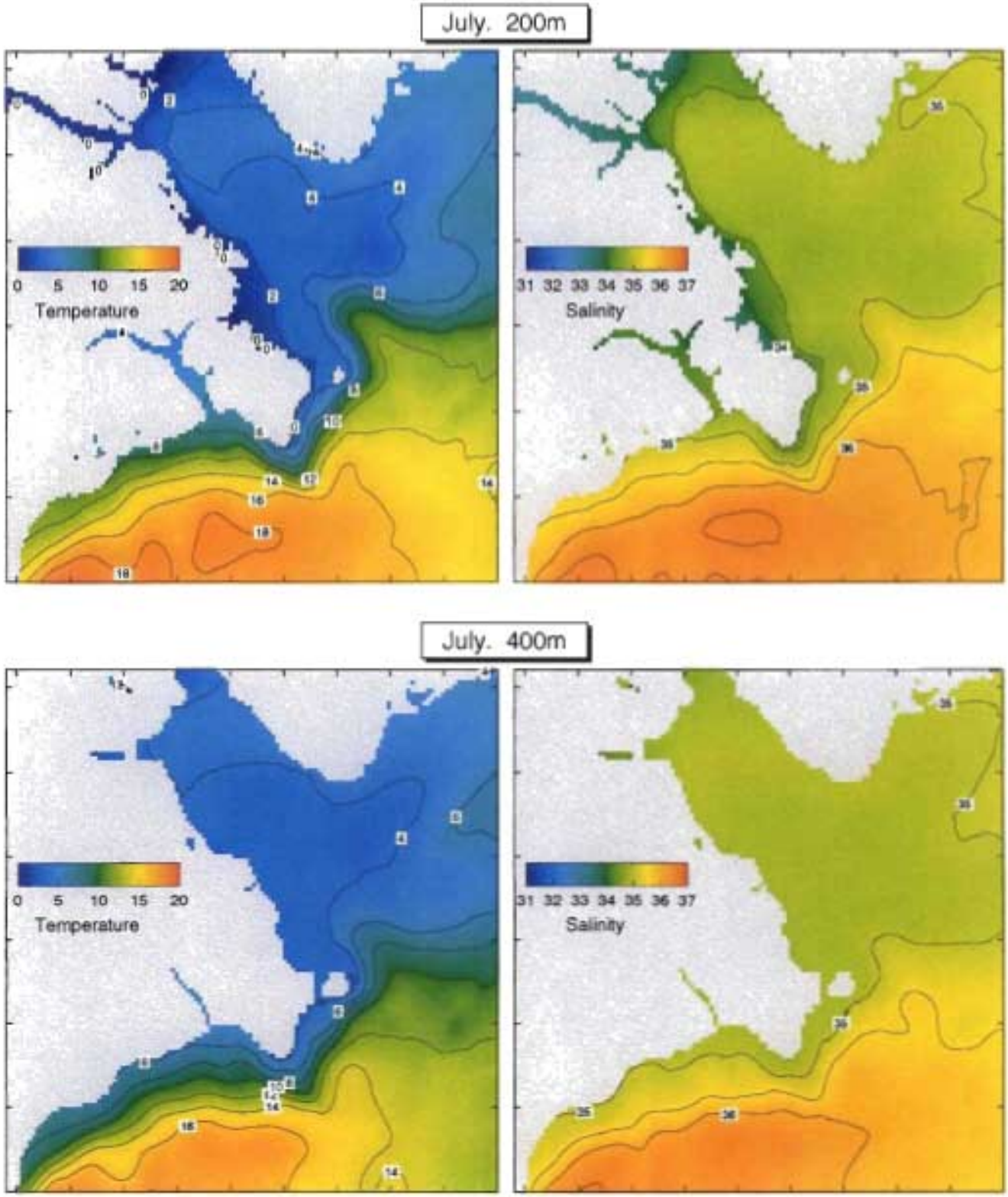

Figure 9c. Monthly mean in-situ temperature (°C) and salinity (psu) in July at 200 and 400 m.

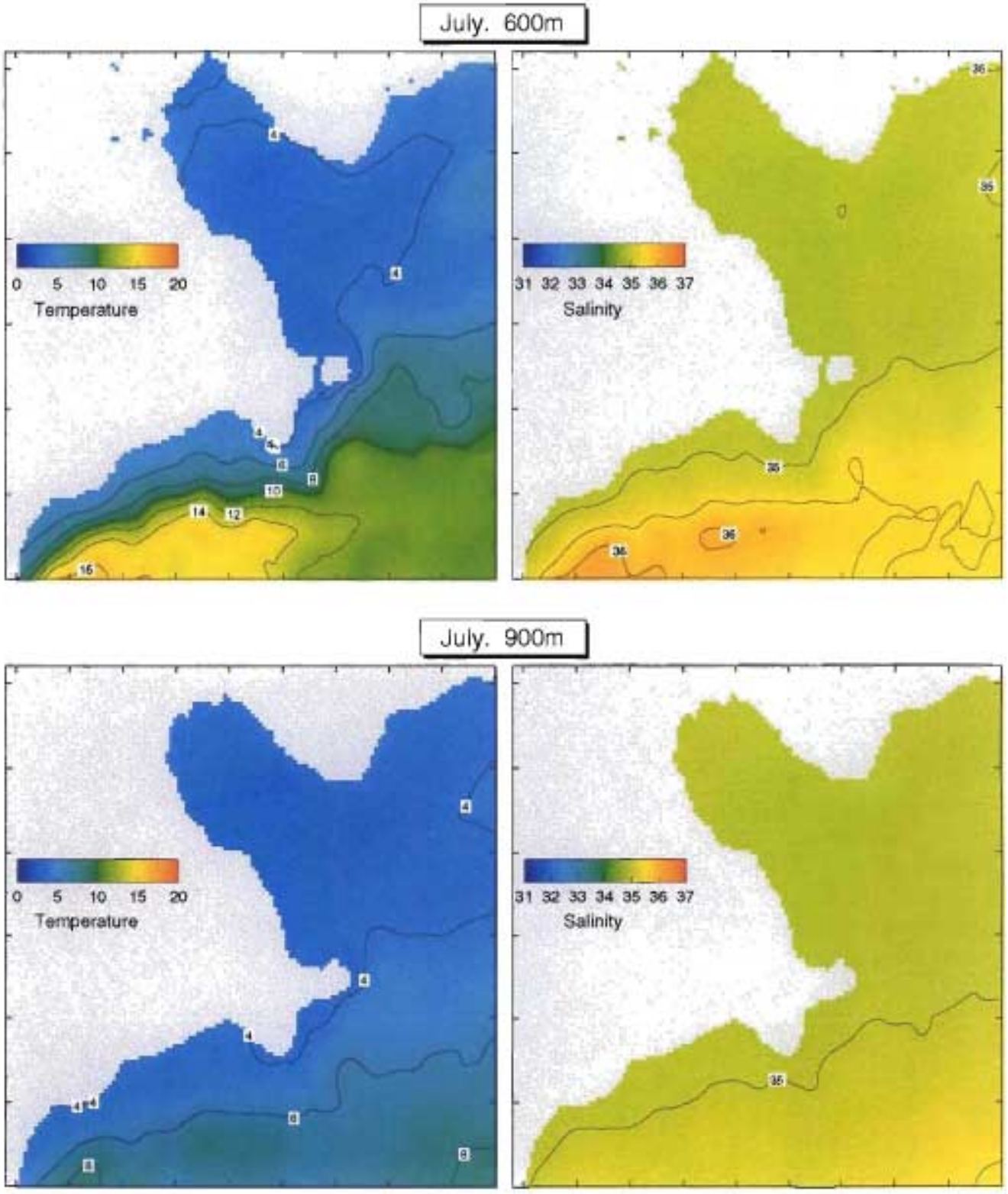

Figure 9d. Monthly mean in-situ temperature (^{o}C) and salinity (psu) in July at 600 and 900 m.

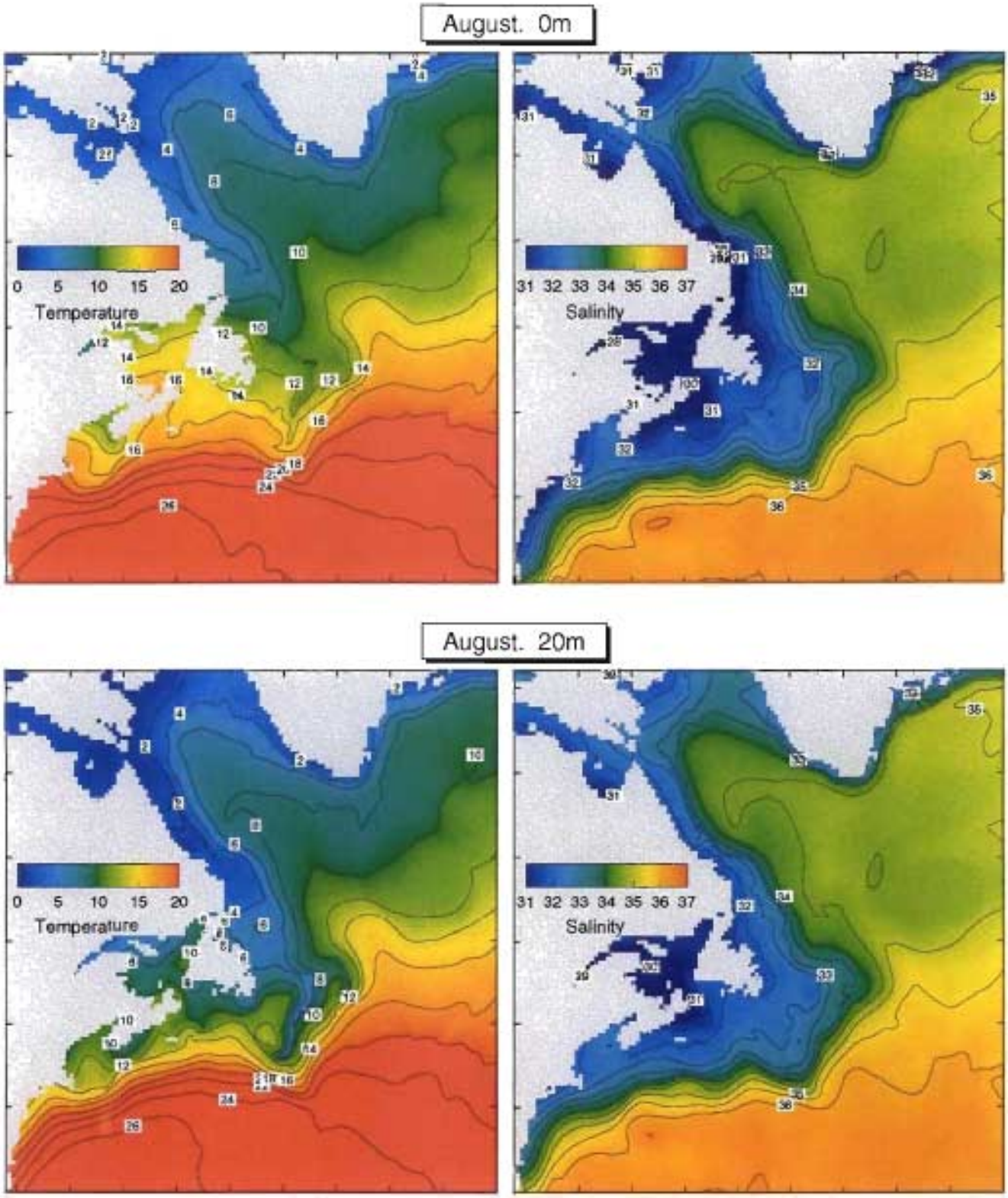

Figure 10a. Monthly mean in-situ temperature (°C) and salinity (psu) in August at 0 and 20 m.

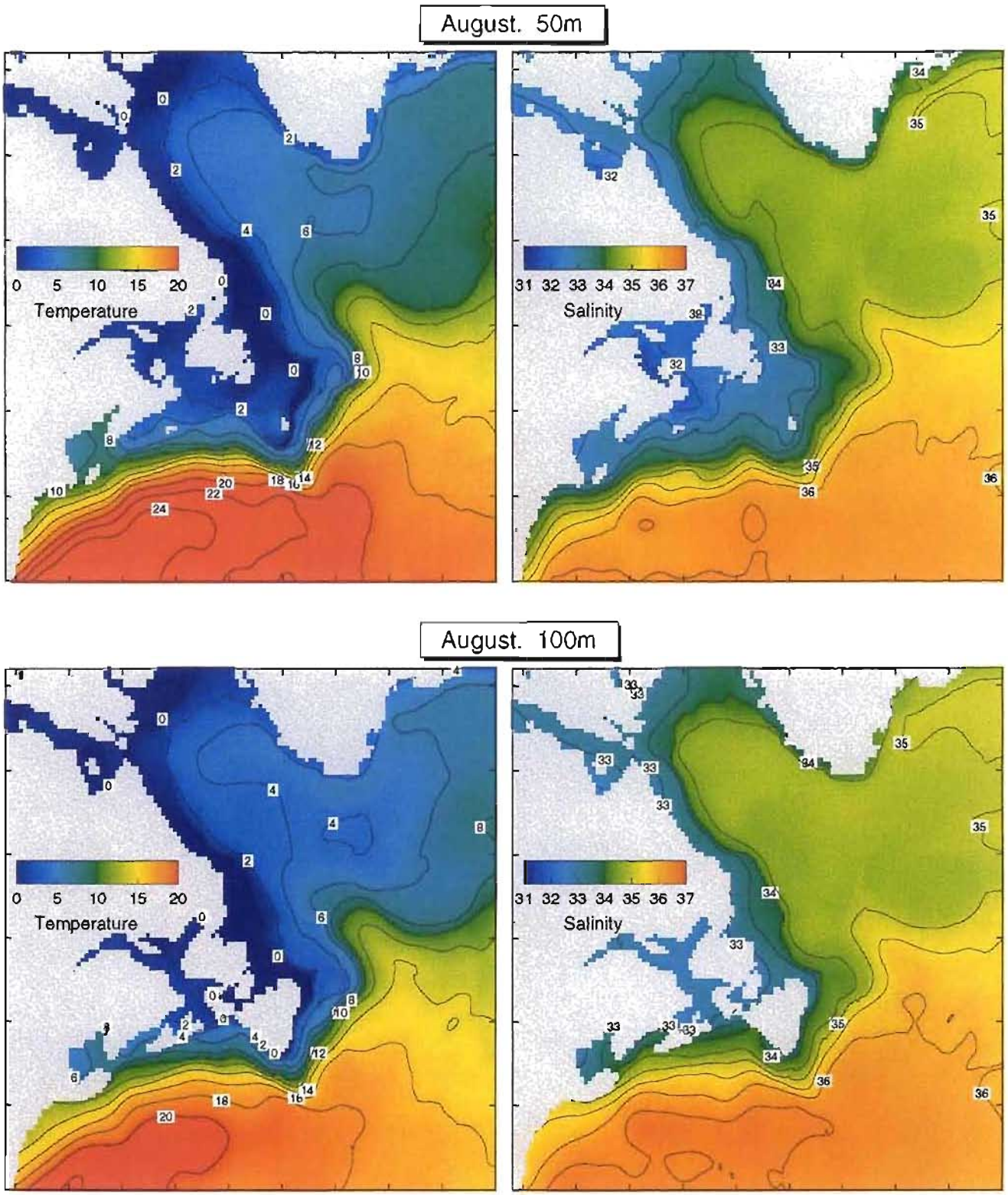

Figure 10b. Monthly mean in-situ temperature (°C) and salinity (psu) in August at 50 and 100 m.

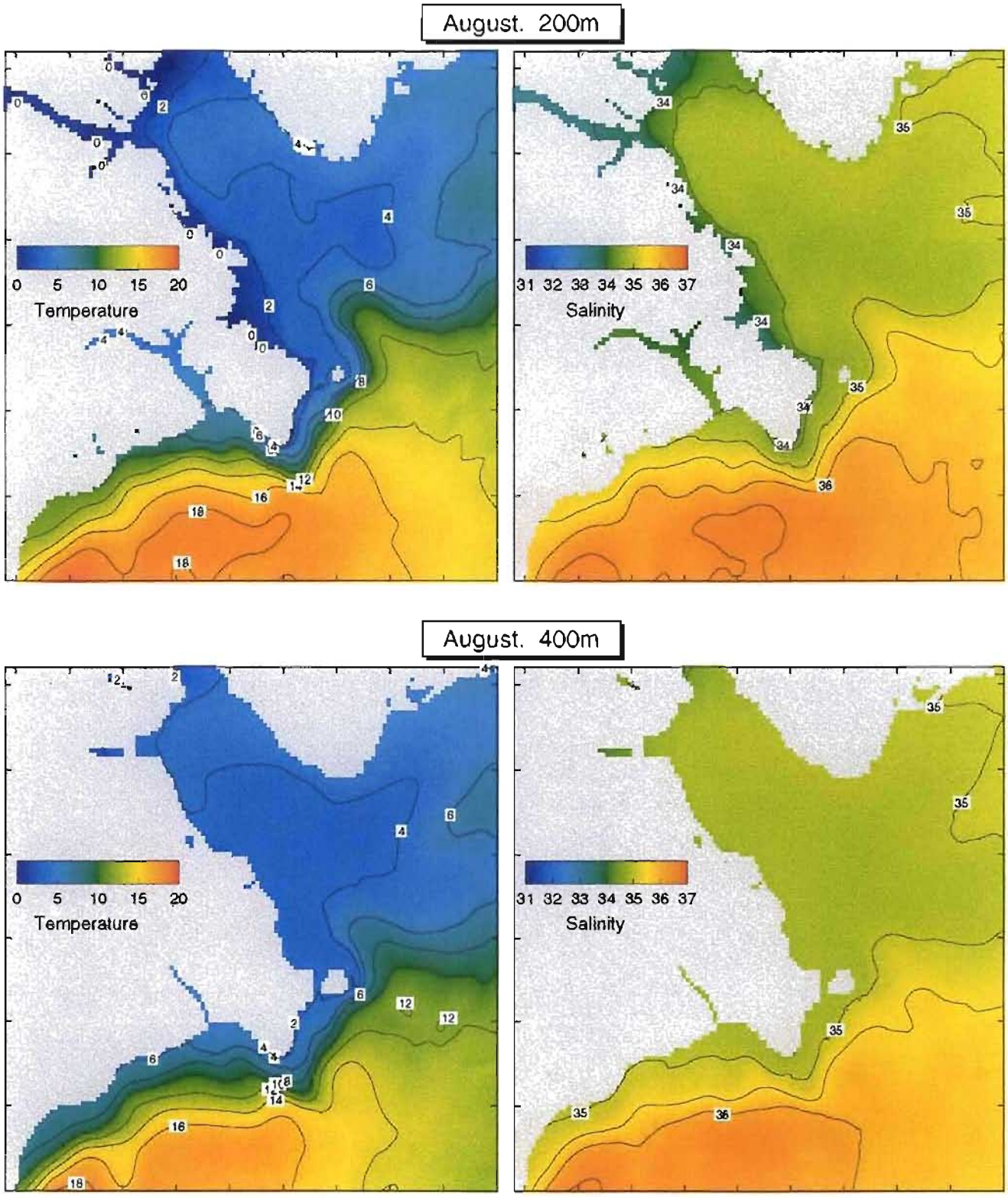

Figure 10c. Monthly mean in-situ temperature (°C) and salinity (psu) in August at 200 and 400 m.

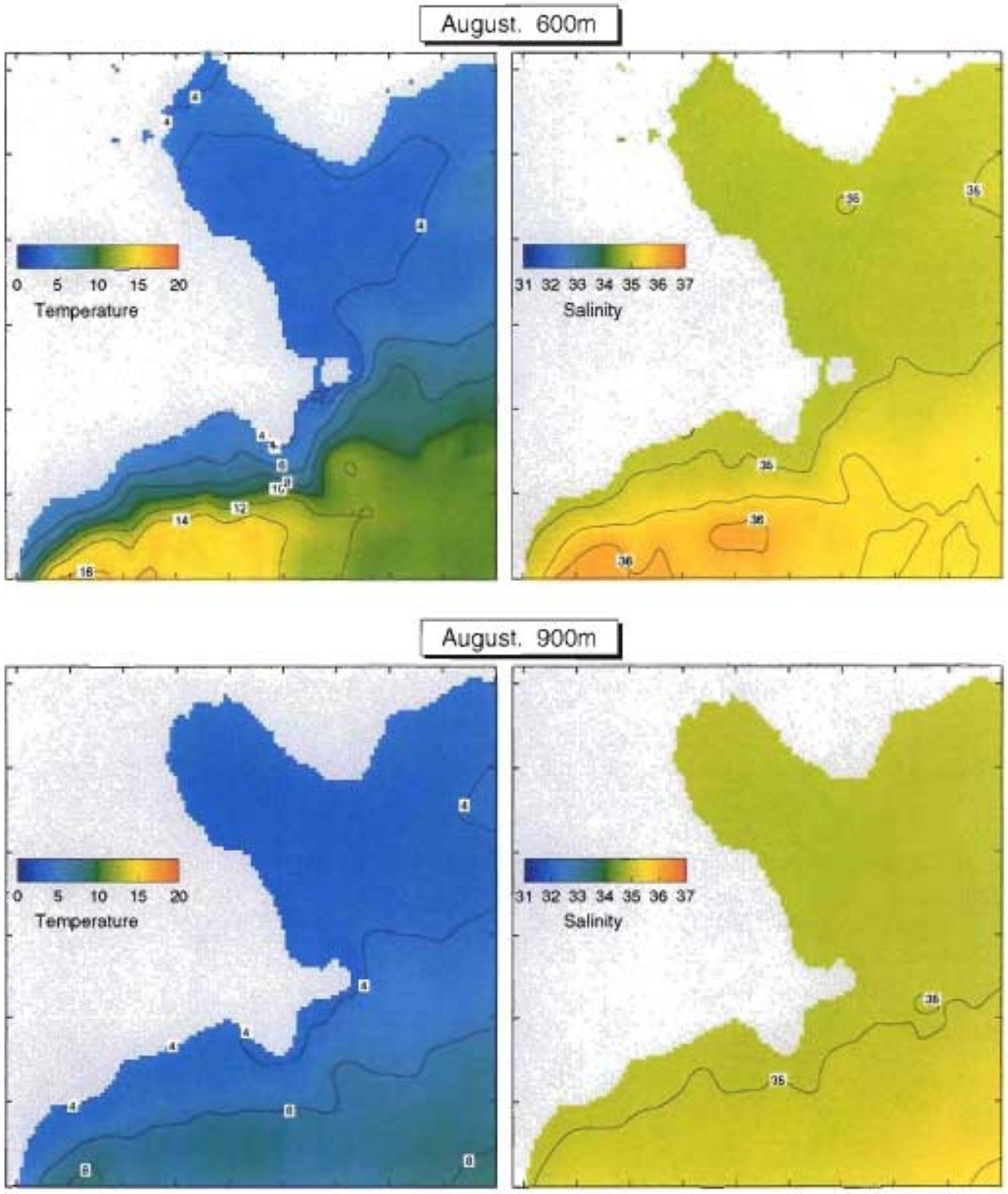

Figure 10d. Monthly mean in-situ temperature (°C) and salinity (psu) in August at 600 and 900 m.

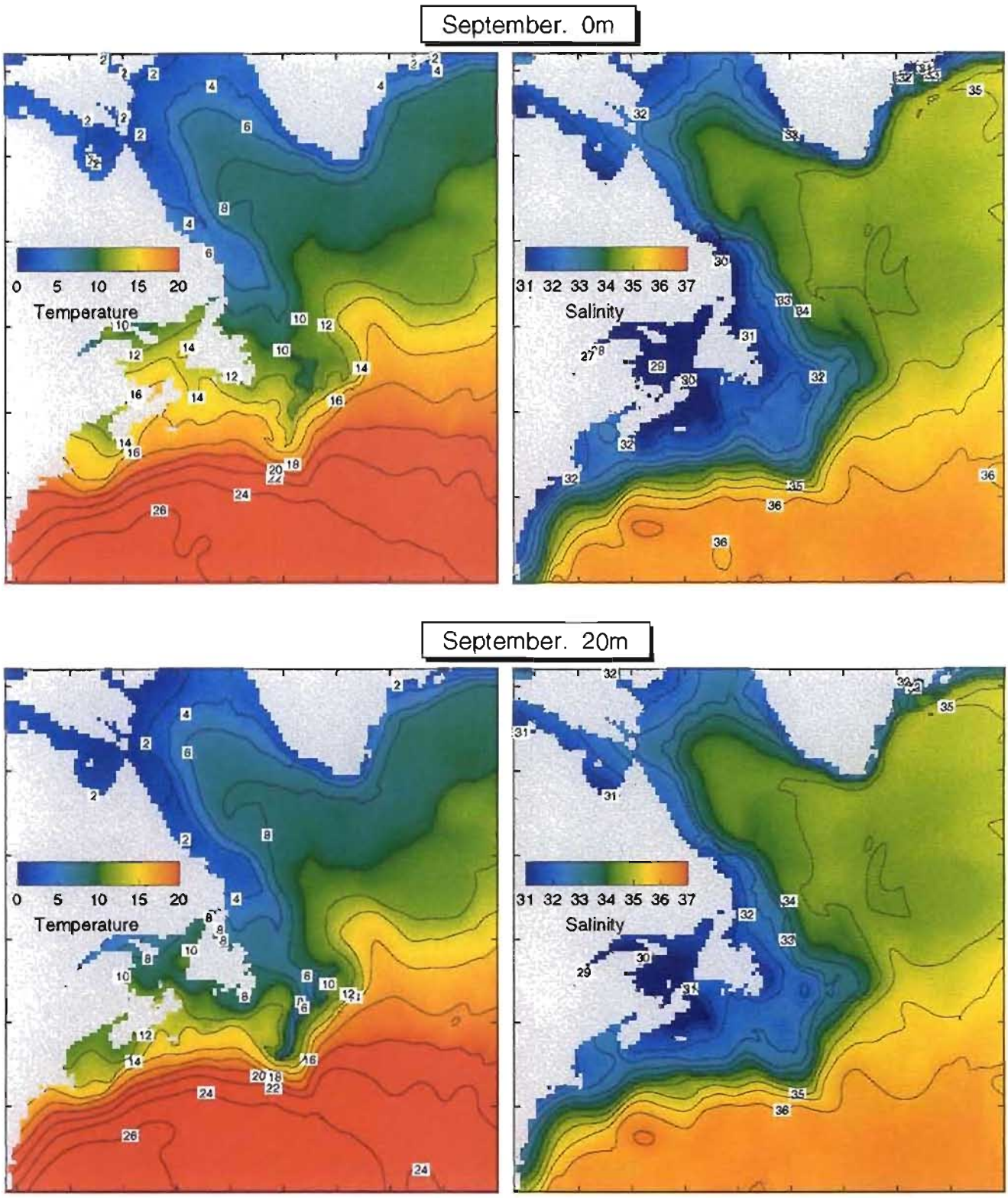

Figure 11a. Monthly mean in-situ temperature (^{o}C) and salinity (psu) in September at 0 and 20 m.

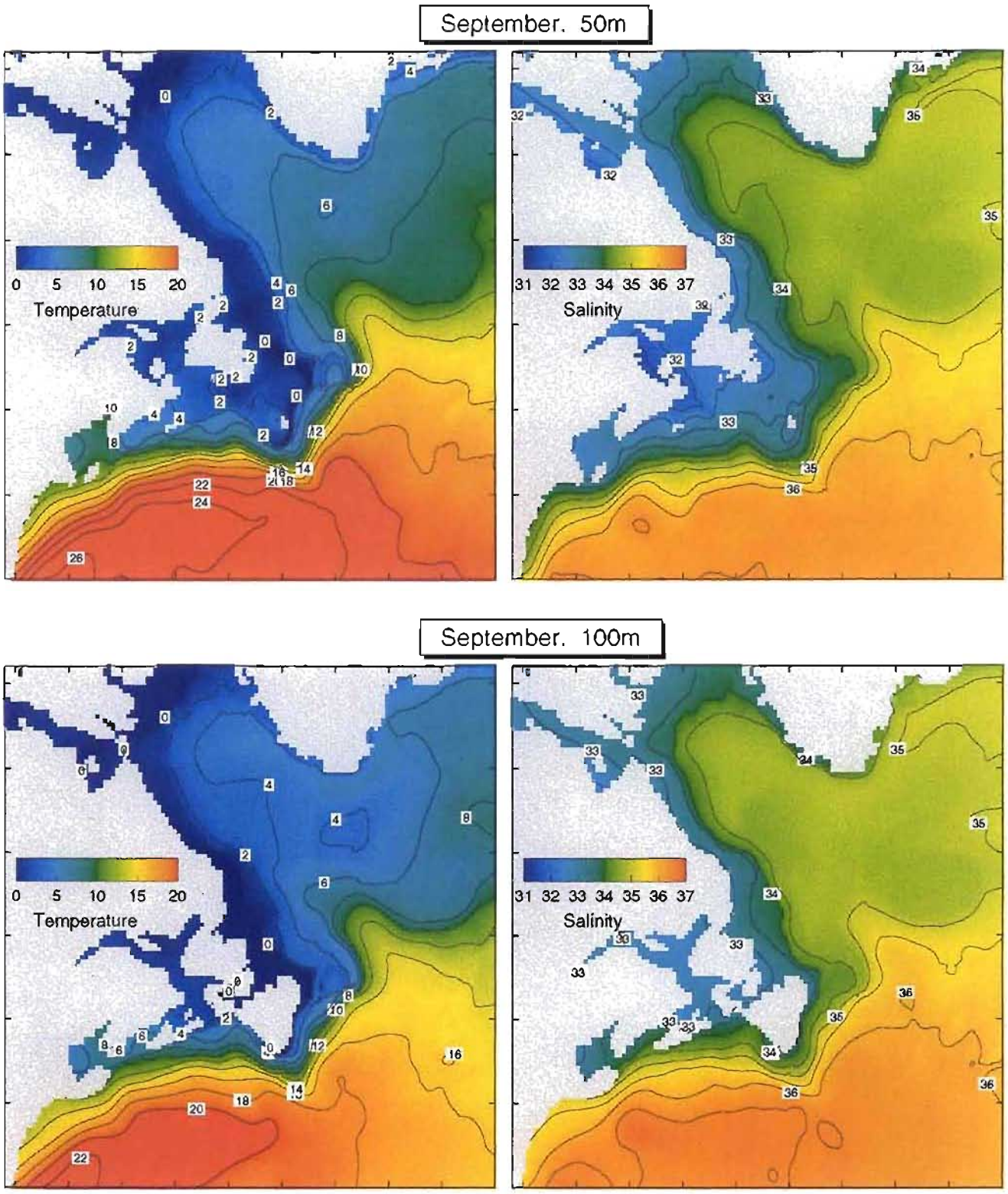

Figure 11b. Monthly mean in-situ temperature (°C) and salinity (psu) in September at 50 and 100 m.

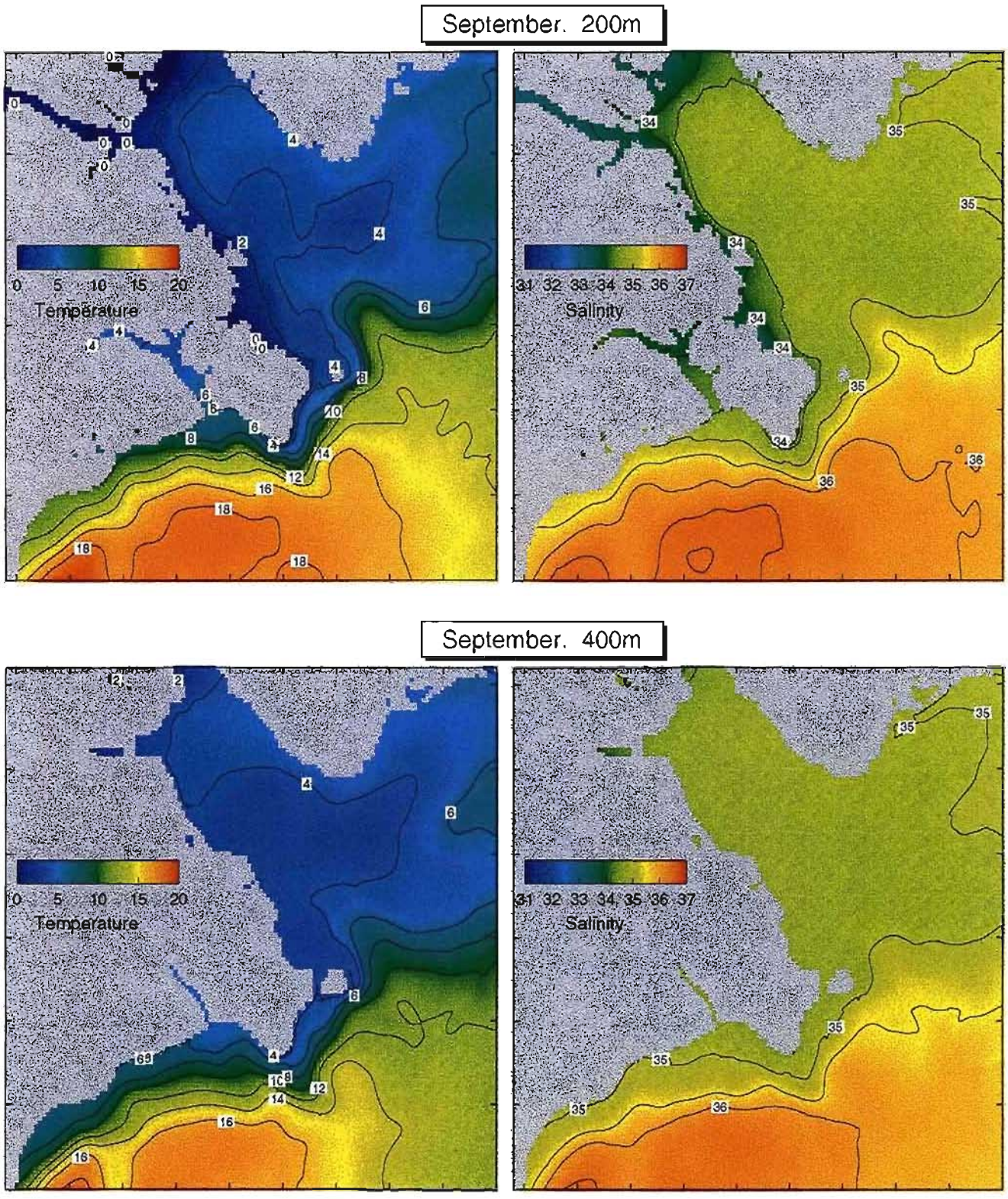

Figure 11c. Monthly mean in-situ temperature (°C) and salinity (psu) in September at 200 and 400 m.

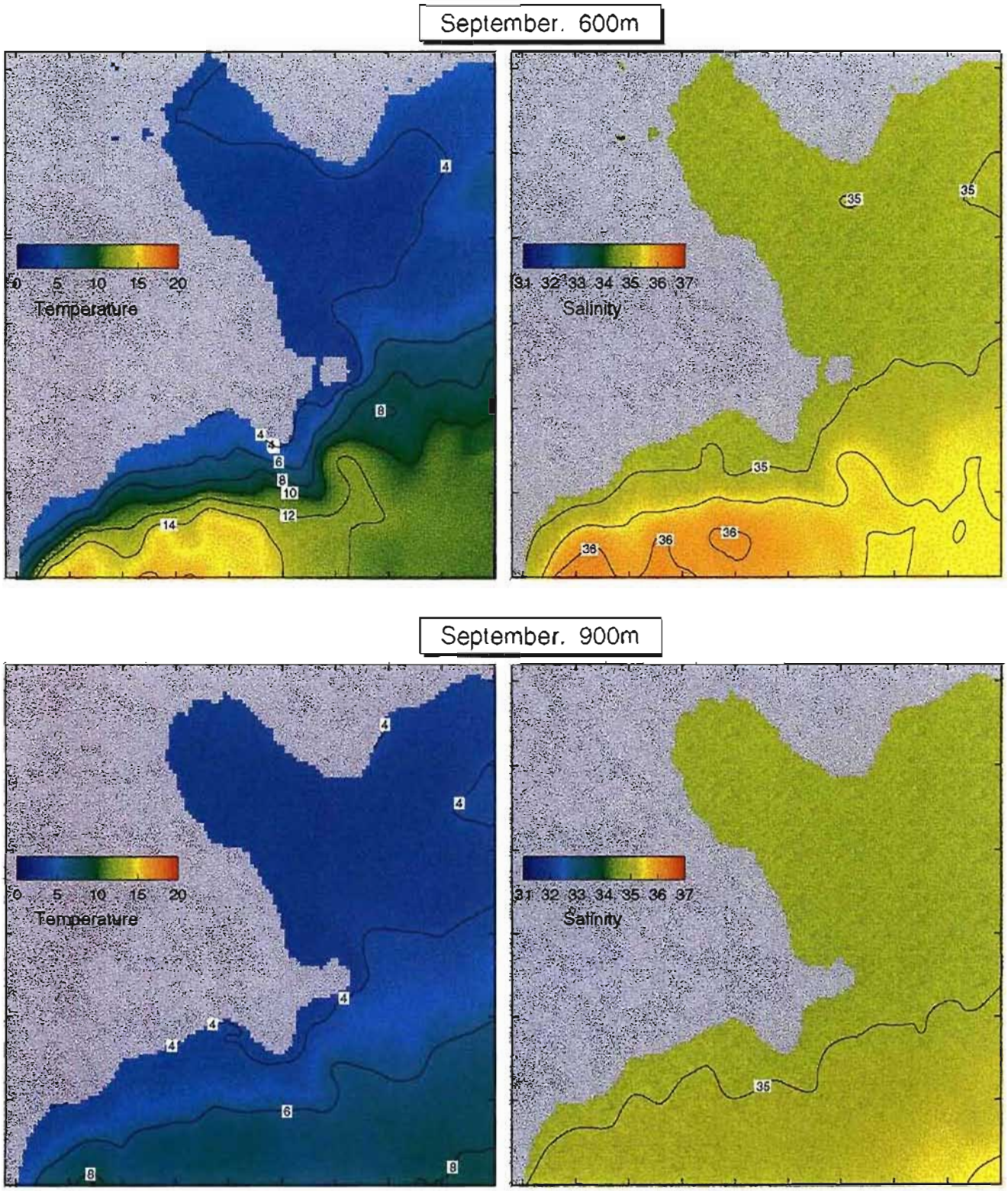

Figure 11d. Monthly mean in-situ temperature (°C) and salinity (psu) in September at 600 and 900 m.

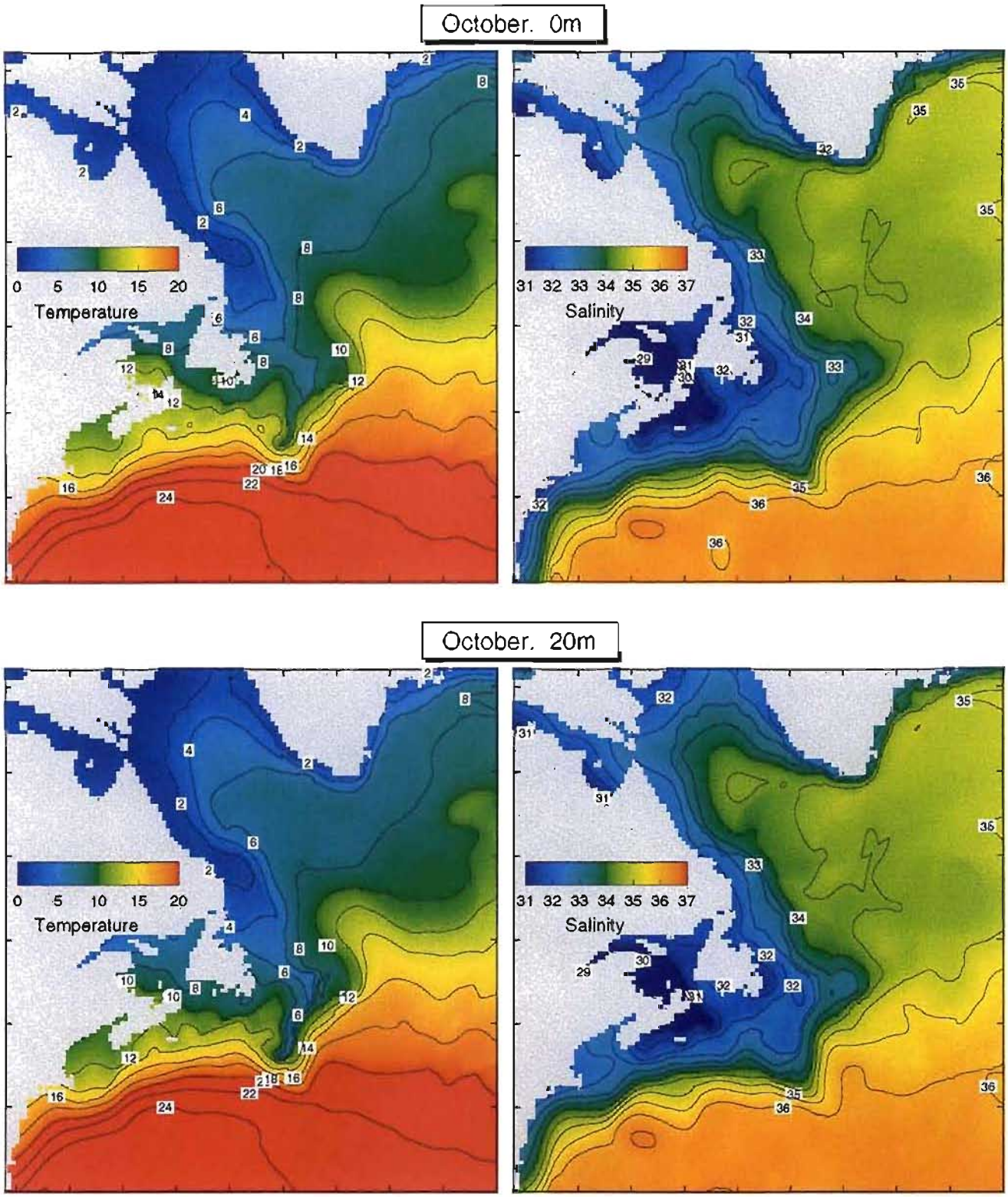

Figure 12a. Monthly mean in-situ temperature (°C) and salinity (psu) in October at 0 and 20 m.

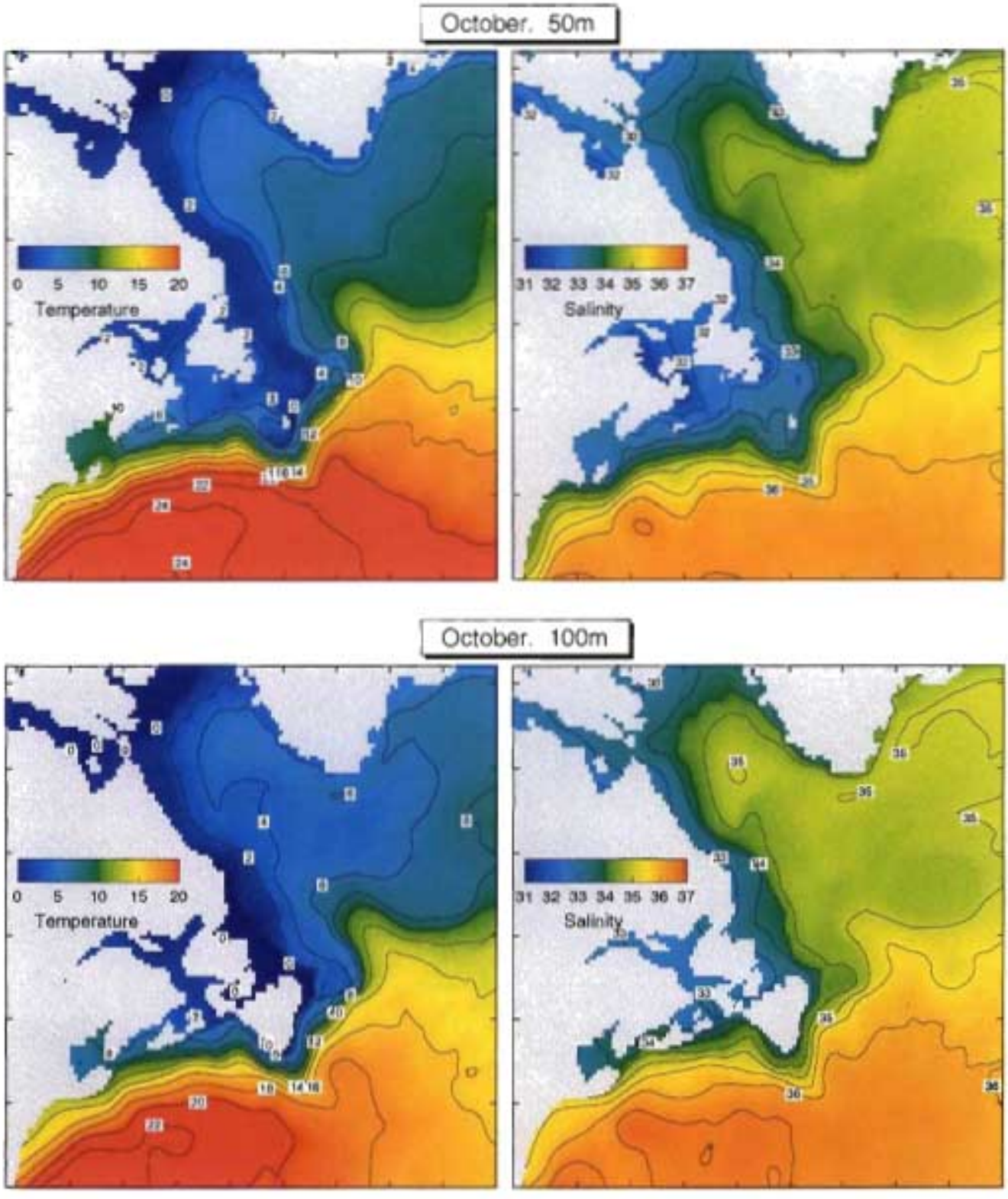

Figure 12b. Monthly mean in-situ temperature (°C) and salinity (psu) in October at 50 and 100 m.

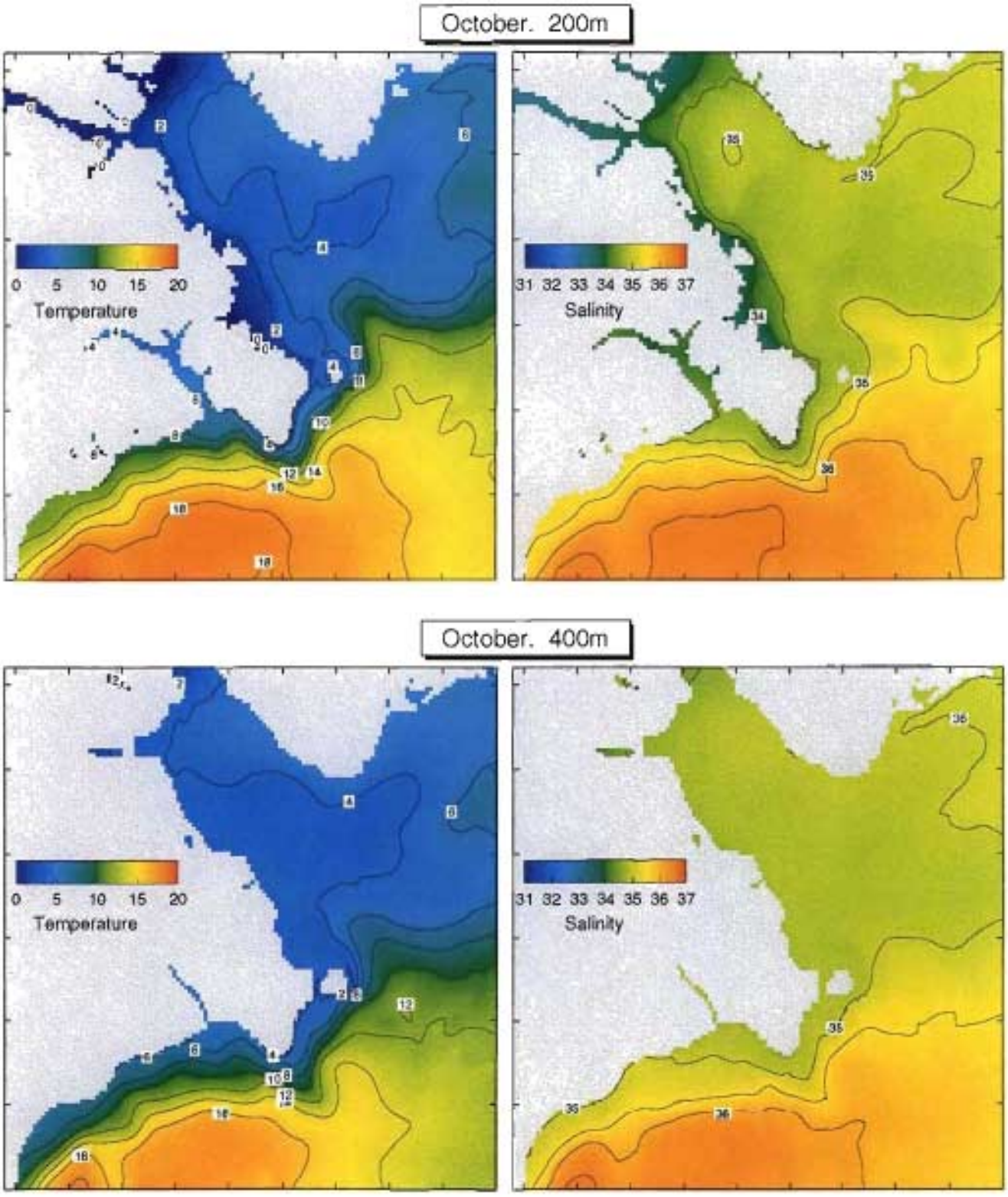

Figure 12c. Monthly mean in-situ temperature (°C) and salinity (psu) in October at 200 and 400 m.

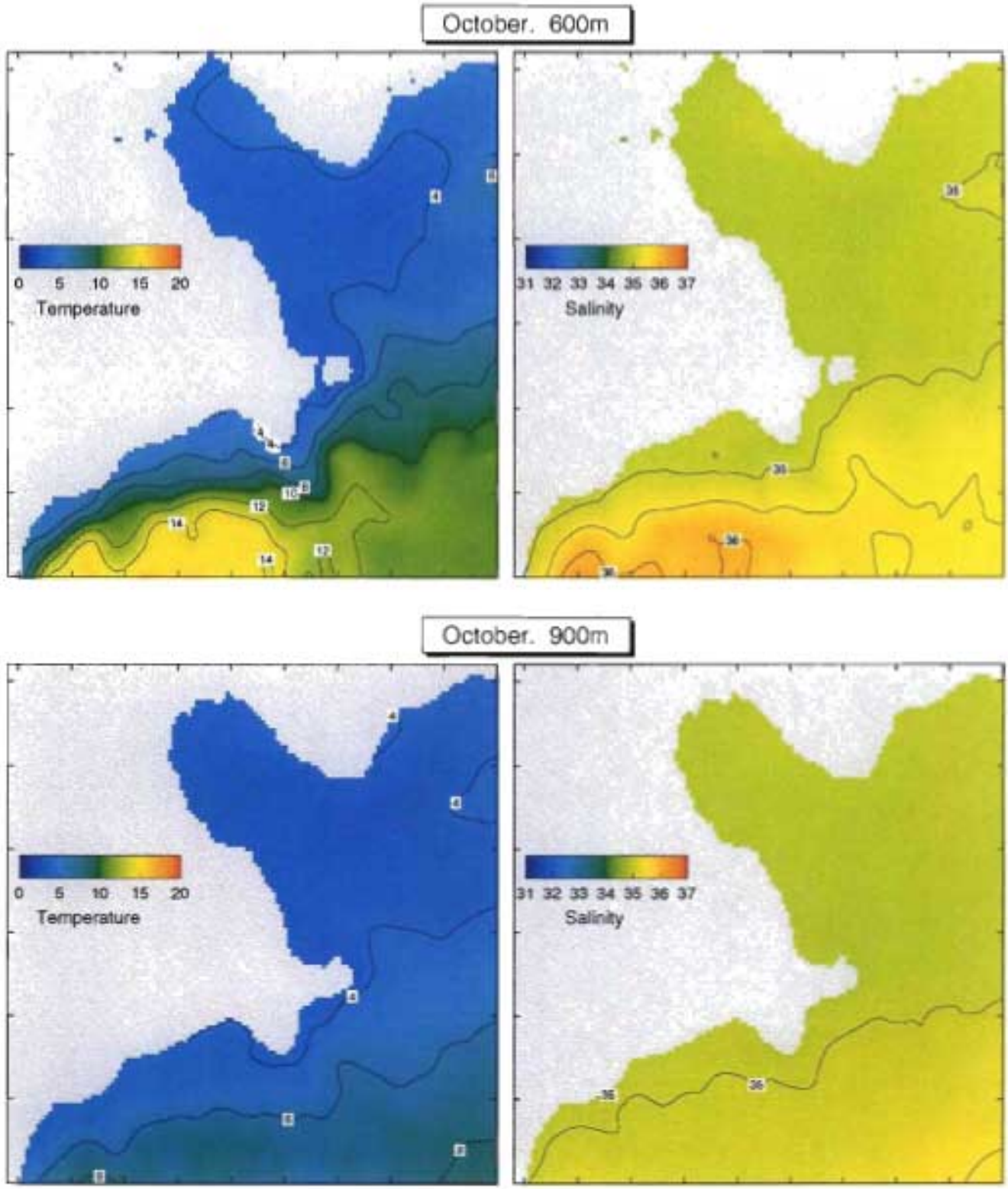

Figure 12d. Monthly mean in-situ temperature (°C) and salinity (psu) in October at 600 and 900 m.

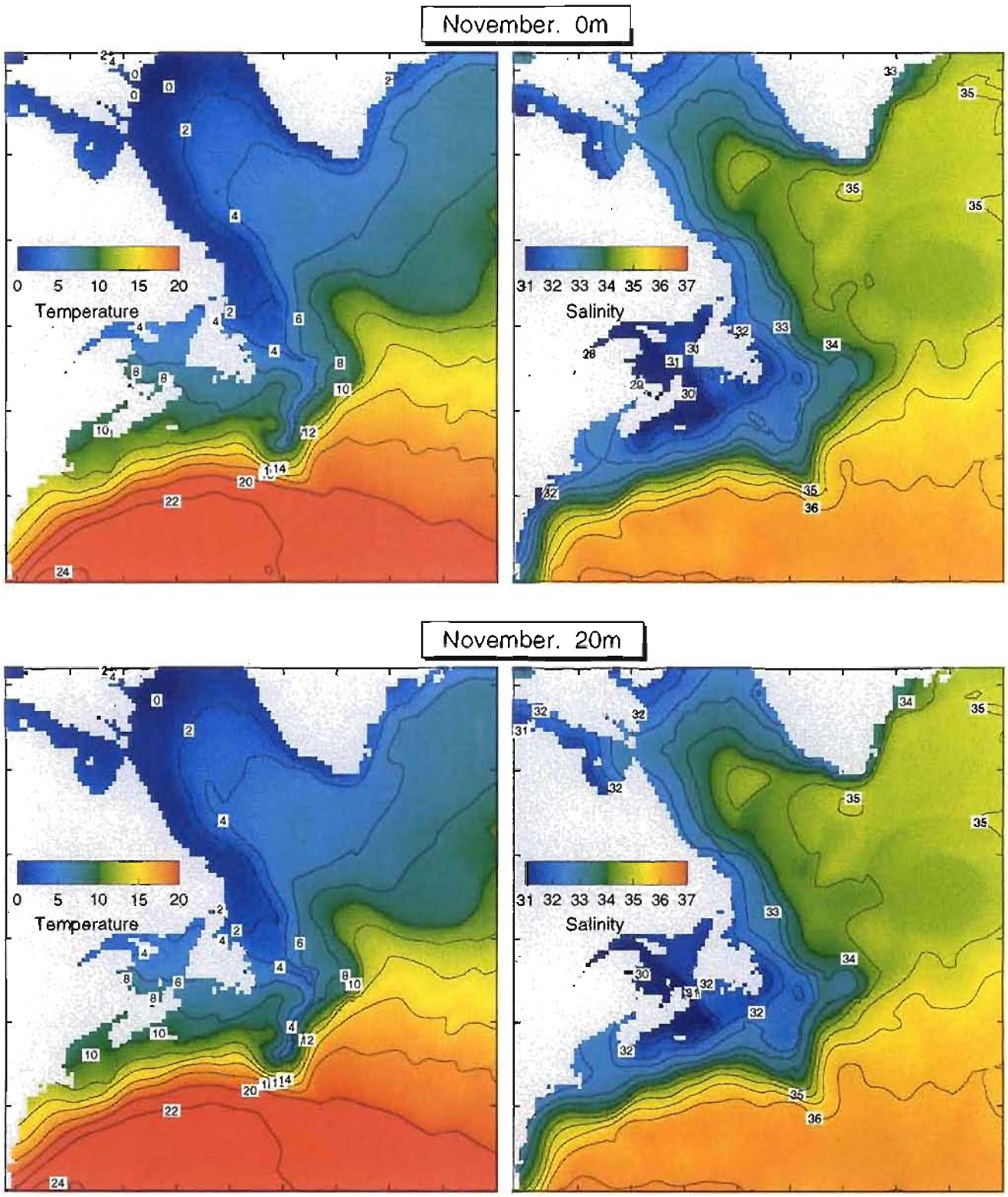

Figure 13a. Monthly mean in-situ temperature (°C) and salinity (psu) in November at 0 and 20 m.

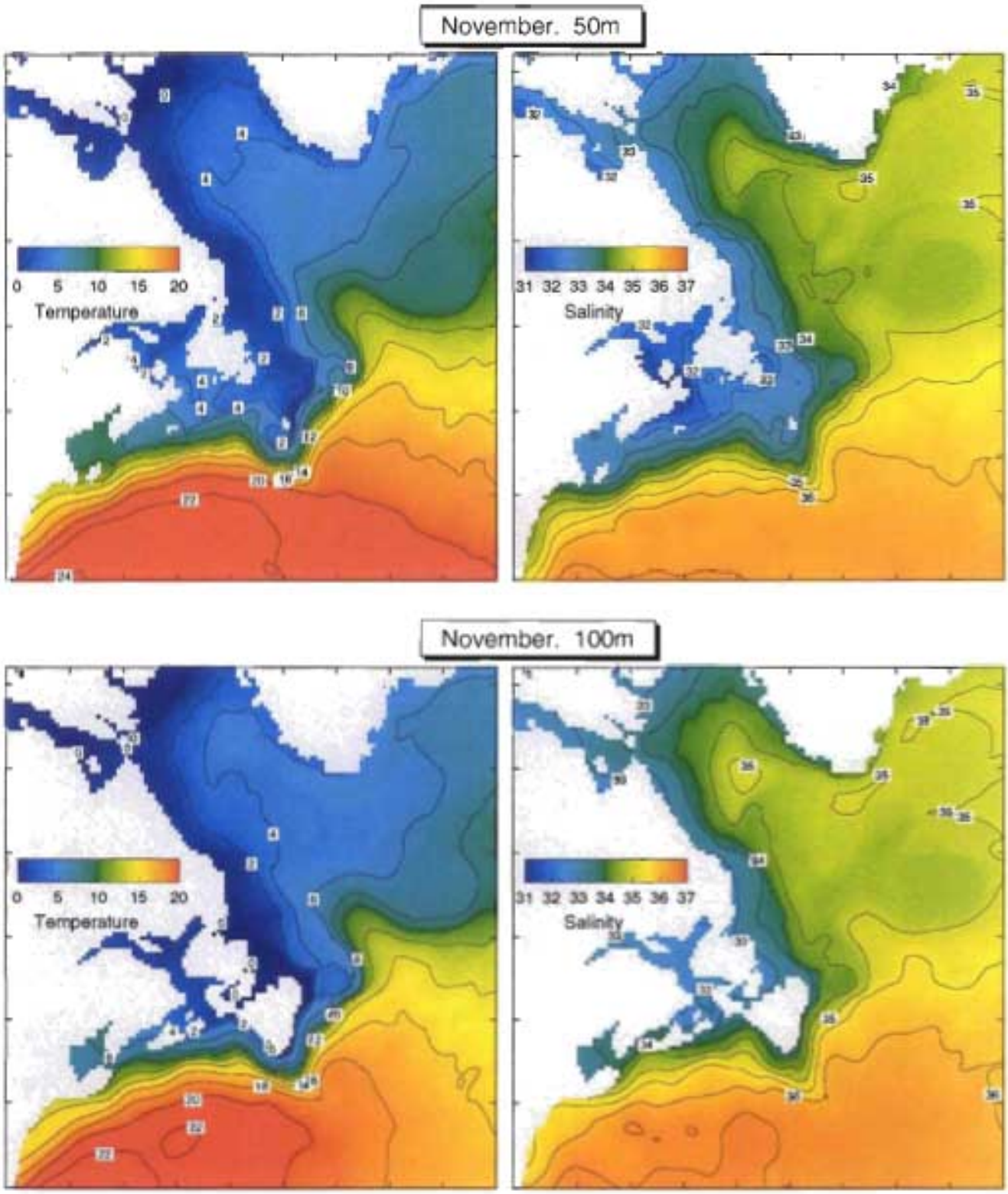

Figure 13b. Monthly mean in-situ temperature (°C) and salinity (psu) in November at 50 and 100 m.

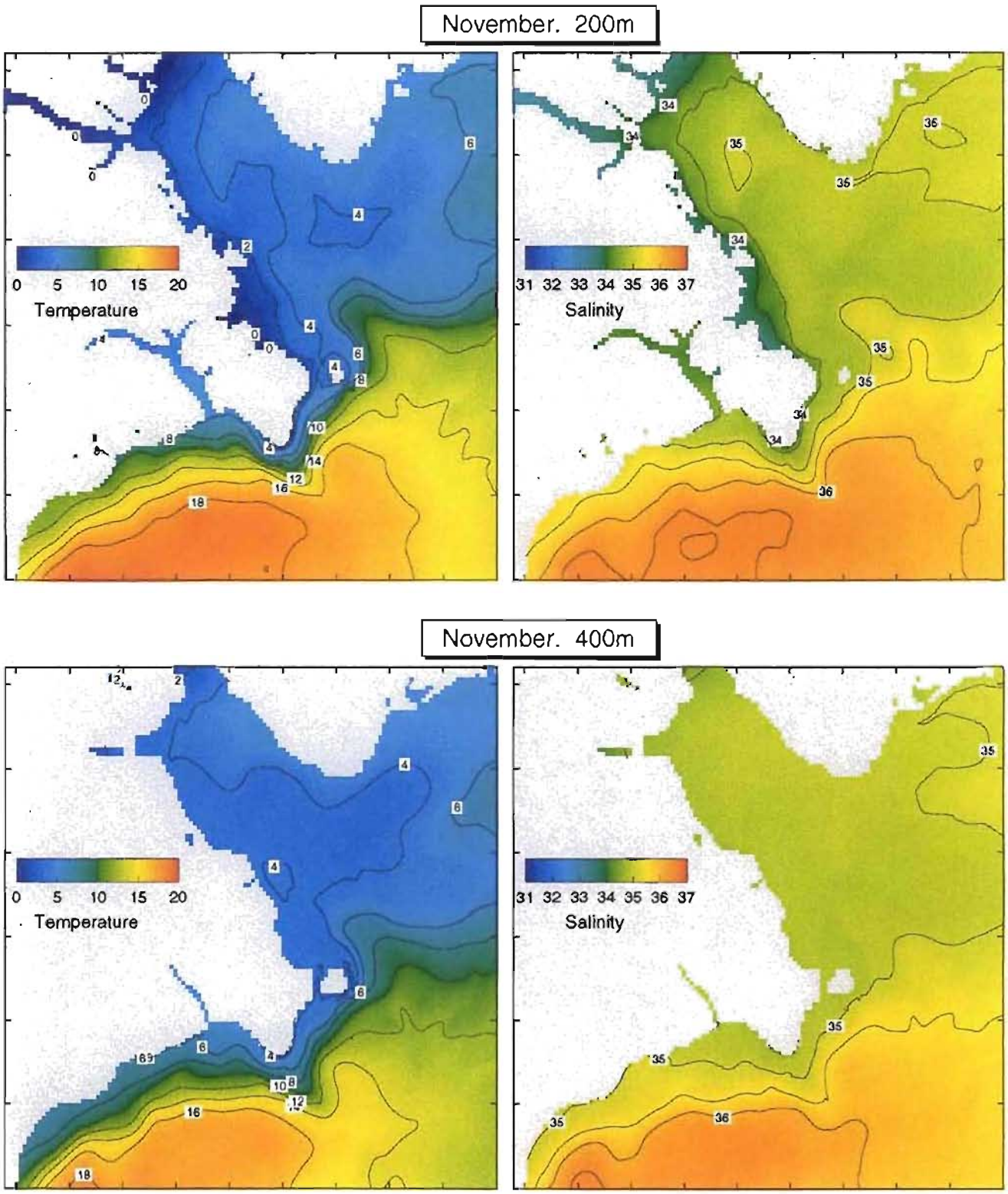

Figure 13c. Monthly mean in-situ temperature (°C) and salinity (psu) in November at 200 and 400 m.

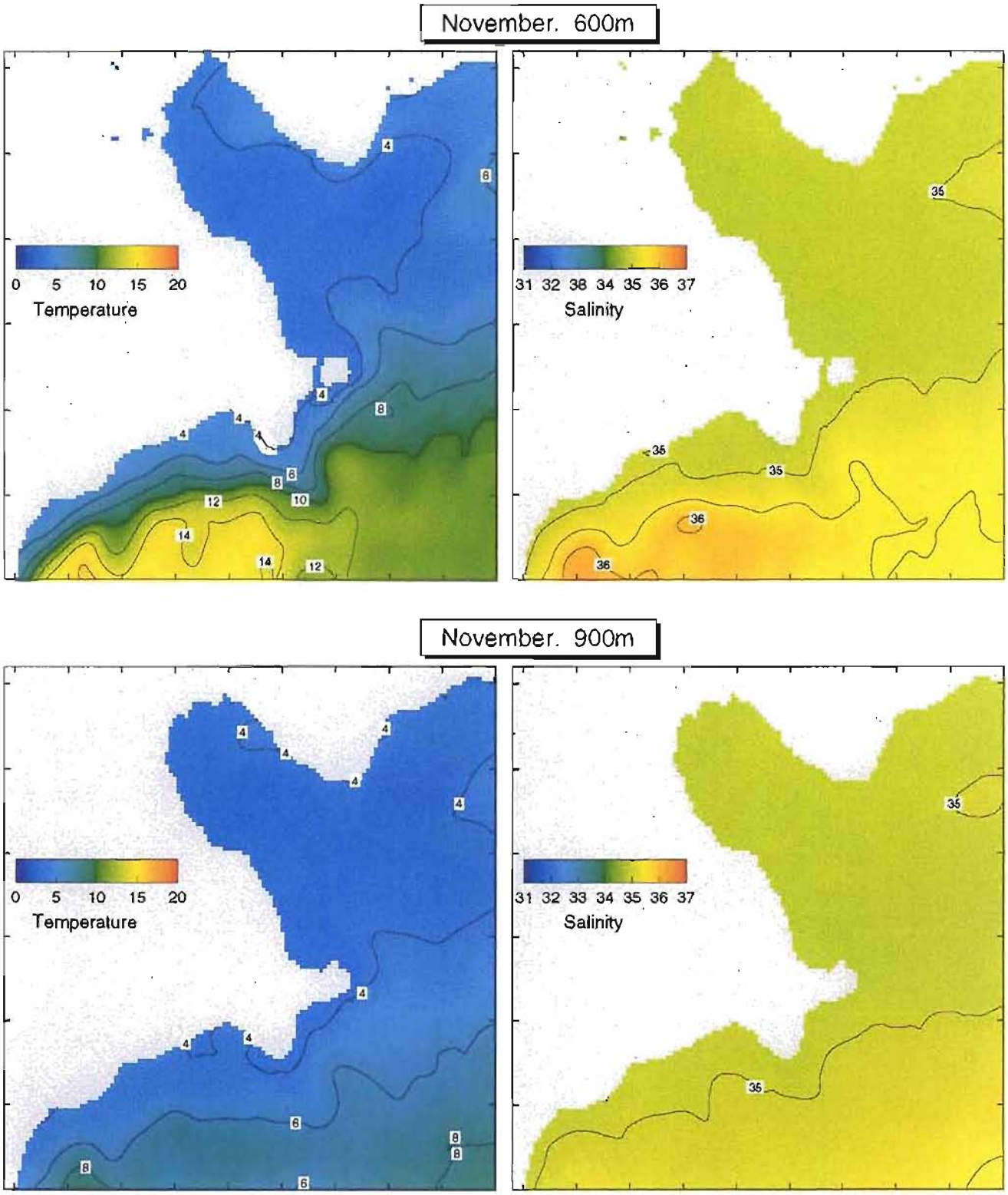

Figure 13d. Monthly mean in-situ temperature (°C) and salinity (psu) in November at 600 and 900 m.

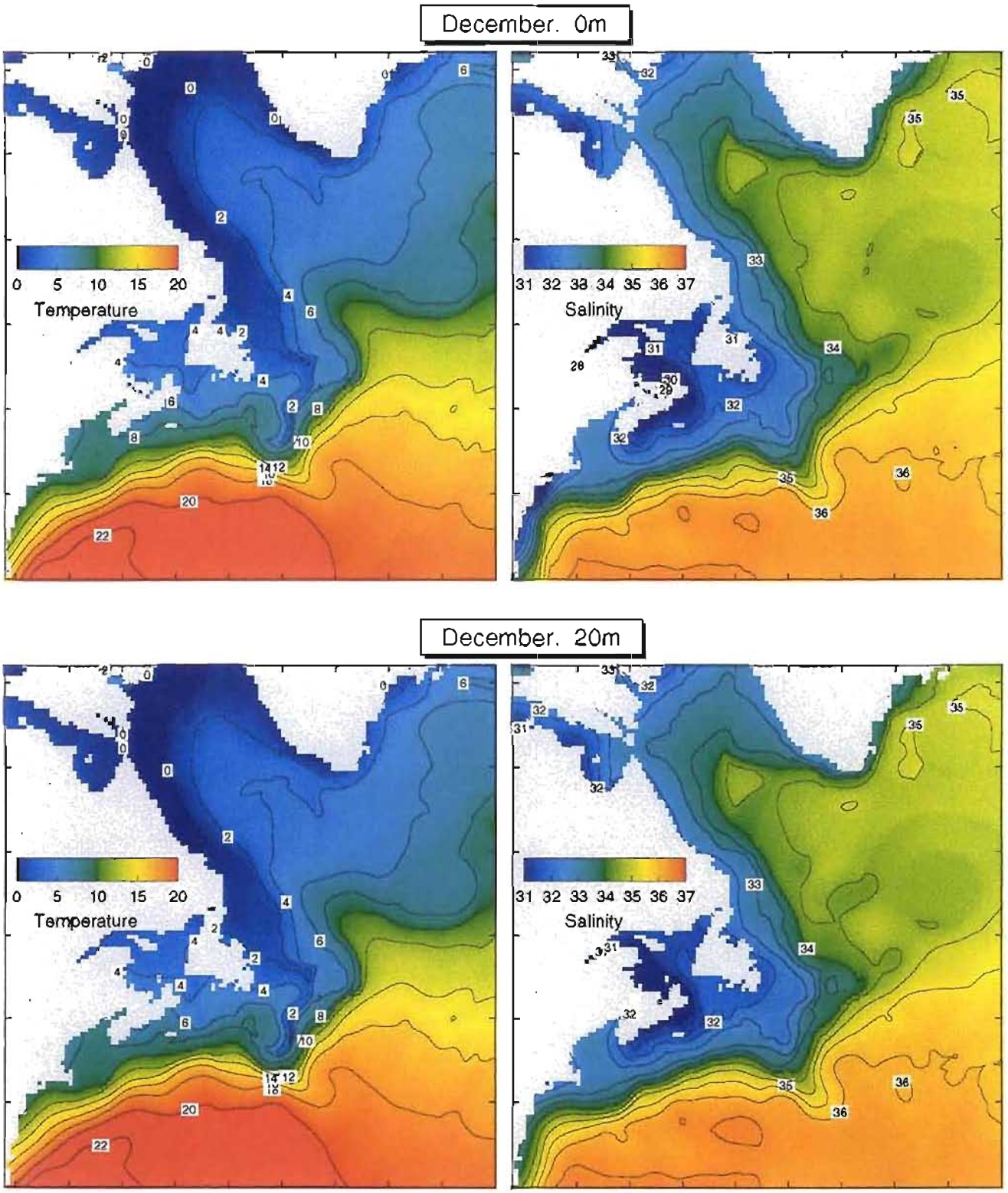

Figure 14a. Monthly mean in-situ temperature (°C) and salinity (psu) in December at 0 and 20 m.

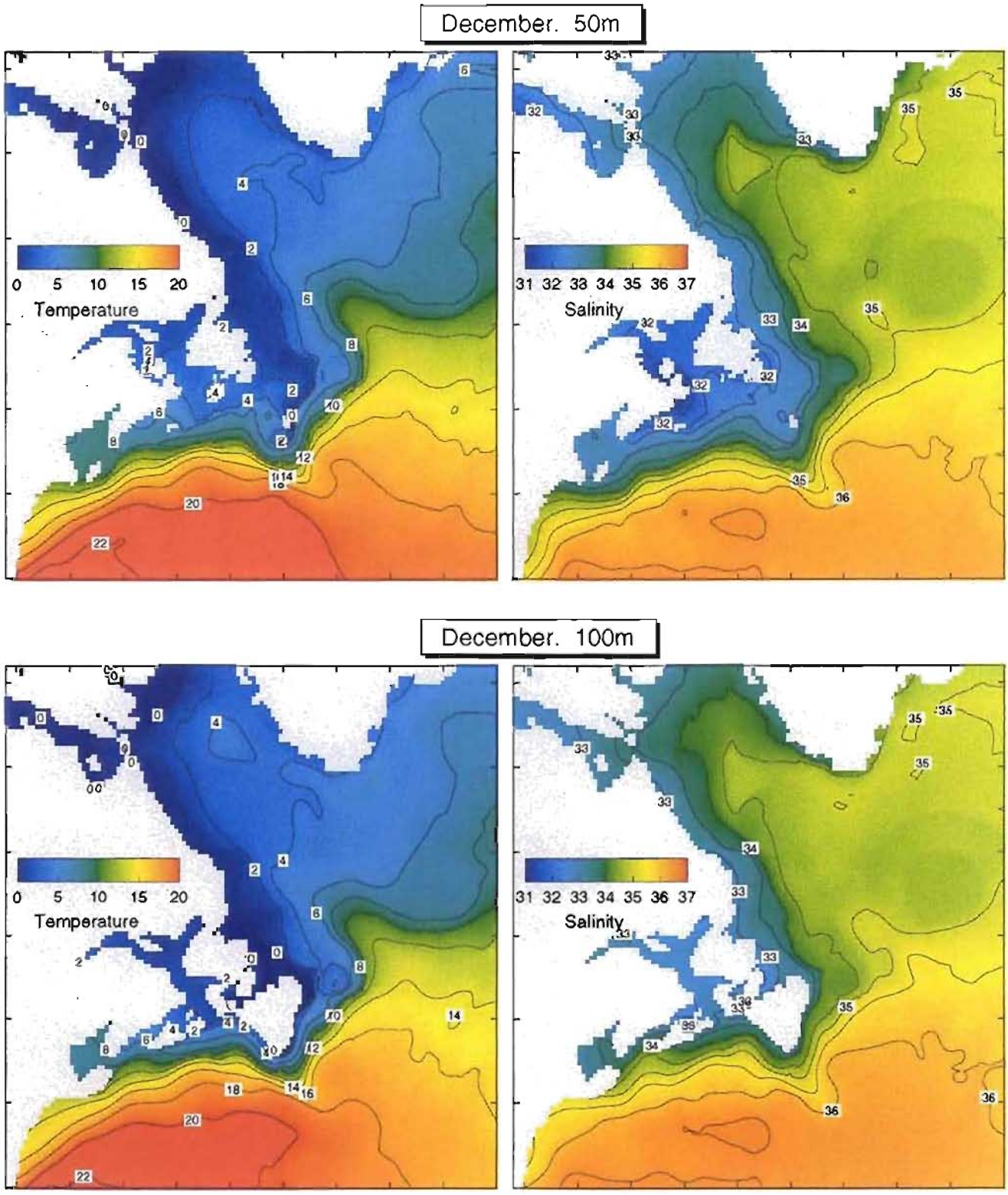

Figure 14b. Monthly mean in-situ temperature (°C) and salinity (psu) in December at 50 and 100 m.

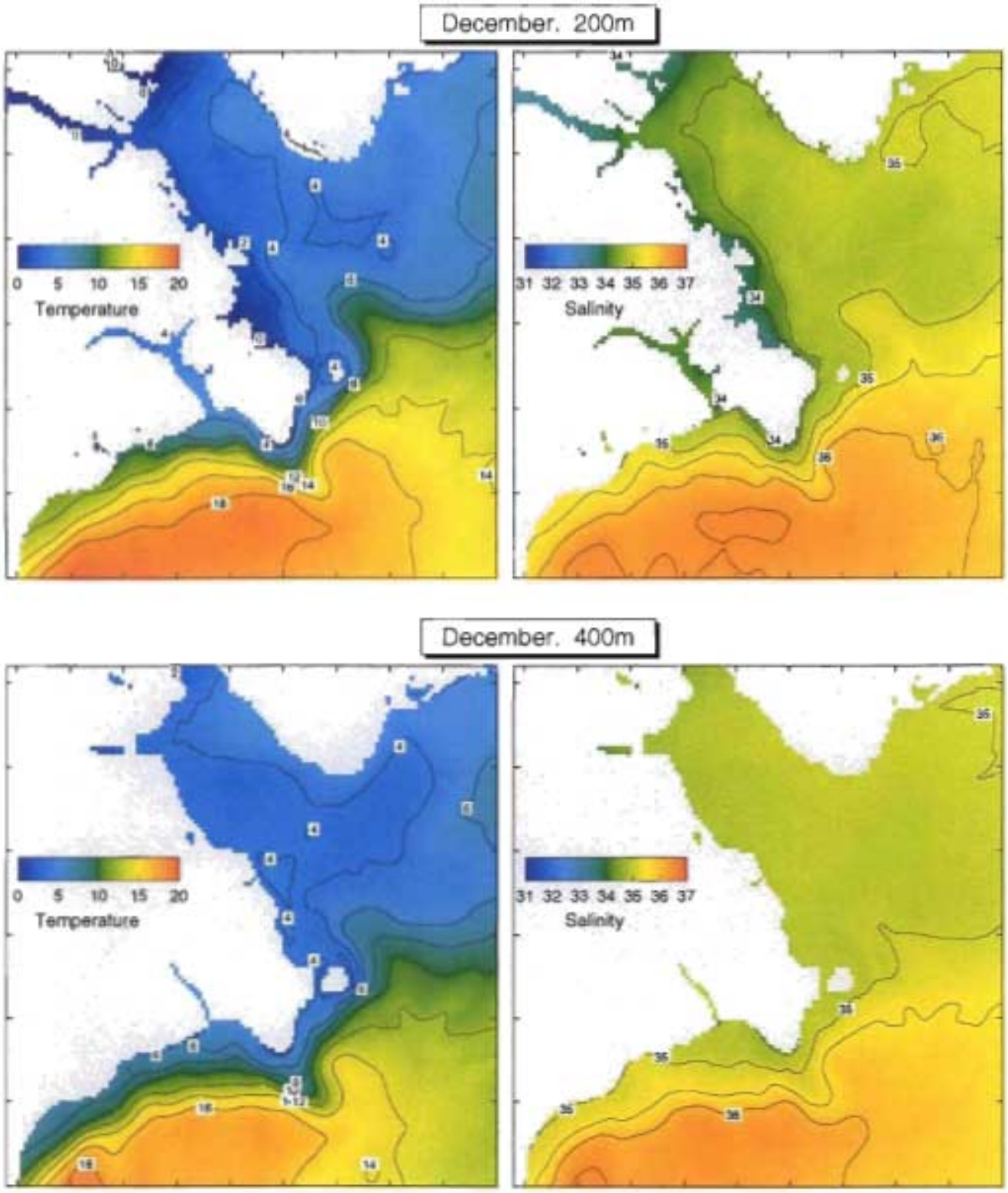

Figure 14c. Monthly mean in-situ temperature (°C) and salinity (psu) in December at 200 and 400 m.

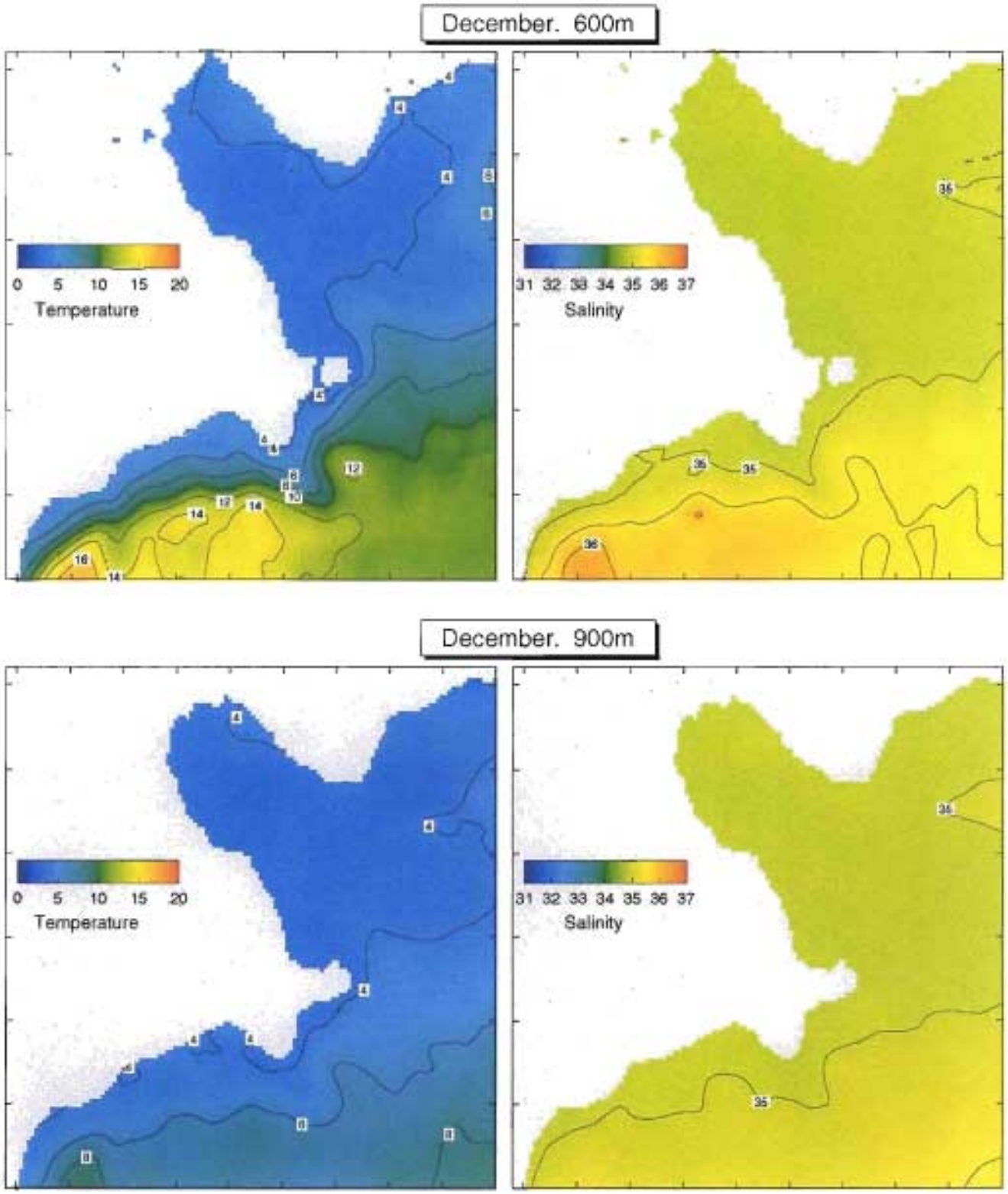

Figure 14d. Monthly mean in-situ temperature (°C) and salinity (psu) in December at 600 and 900 m.